Available online at www.sciencedirect.com

SCIENCE DIRECT®

Ecological Modelling 173 (2004) 31–94

ECOLOGICAL MODELLING

www.elsevier.com/locate/ecolmodel

A hierarchical approach for simulating northern forest dynamics

Don C. Bragg [a,*], David W. Roberts [b], Thomas R. Crow [c]

[a] *USDA Forest Service, Southern Research Station, UAM, P.O. Box 3516, Monticello, AR 71656-3516, USA*
[b] *Department of Forest, Range, and Wildlife Sciences, Utah State University, Logan, UT 84322-5320, USA*
[c] *USDA Forest Service, North Central Research Station, 1831 Highway 169 East, Grand Rapids, MN 55744-3399, USA*

Received 12 November 2002; received in revised form 21 July 2003; accepted 13 August 2003

Abstract

Complexity in ecological systems has challenged forest simulation modelers for years, resulting in a number of approaches with varying degrees of success. Arguments in favor of hierarchical modeling are made, especially for considering a complex environmental issue like widespread eastern hemlock regeneration failure. We present the philosophy and basic framework for the *NORTH*ern *W*oodland *D*ynamics *S*imulator (N*ORTHWDS*) *I*ntegrated *H*ierarchical *M*odel *S*ystem (*NIHMS*). NIHMS has an individual tree component (the N*ORTHWDS I*ndividual *R*esponse *M*odel (*NIRM*)), a mesoscale stand simulator (*NORTHWDS*), and a landscape model (N*ORTHWDS L*andscape *M*odel (*NLM*, presented in another paper)). *NIRM* predicts the behavior of a tree given the physical and biotic environment that constrains its performance, using process-response functions at a scale larger than the individual plant. The *NORTHWDS* model integrates both the structure of the individual tree model (including tree growth and mortality functions) with a series of ecosystem processes (e.g. competition, site biogeochemistry, small-scale disturbance, deer browsing) and even larger scale events (e.g. catastrophic windthrow) to predict long-term stand dynamics on a 5-year simulation cycle. The boundaries in time and space between the *NIRM*, *NORTHWDS*, and *NLM* models are not discrete, but overlap due to the multiscale expression of ecological and physiological processes. For example, the *NORTHWDS* model represents both the intersection between the *NIRM* and *NLM* models with additional unique mesoscale processes (e.g. intertree competition). At the highest level of *NIHMS*, *NLM* provides the environmental context for *NORTHWDS*, with all levels operating in an internally consistent and parsimonious manner.

Three case study scenarios are used to illustrate some of the potential applications of *NIRM*. *Scenario 1*: simulation of northern red oak survivorship, crown dynamics, diameter increment, and cumulative propagule production under different local stand densities; *Scenario 2*: the response of white ash along an available nitrogen gradient with respect to mortality, crown surface area, diameter growth, tree biomass, and propagule production; and *Scenario 3*: the survivorship and total propagule production of black spruce along a soil moisture gradient. Under Scenario 1, crown size decreased appreciably as local stand density increased from open-grown ($<1\ m^2$/ha) to closed canopy conditions (15–30 m^2/ha), triggering reduced annual increment, lower established propagule production, and increased small tree mortality. Similarly, nitrogen (for white ash) and moisture (for black spruce) gradients significantly affected crown size and growth potential, with many of the same consequences as noted for increased competition in northern red oak. These predictions were consistent with ecological expectations for all scenarios except the black spruce moisture gradient response, which arose because of scale-related issues and the complexity of gradients.

To evaluate *NORTHWDS* model behavior, a 36 ha synthetic stand resembling a hardwood-dominated forest from northern Wisconsin was simulated for 300 years using four windthrow disturbance scenarios (no windthrow, acute windthrow only, chronic windthrow only, and both types of windthrow). Acute (particularly severe but locally discrete and infrequent events) windthrow patterns were designed to generate many small, low intensity events, while chronic windthrow (pervasive yet low intensity

* Corresponding author. Tel.: +1-870-367-3464x18; fax: +1-870-367-1164.
E-mail address: dbragg@fs.fed.us (D.C. Bragg).

0304-3800/$ – see front matter
doi:10.1016/j.ecolmodel.2003.08.017

cyclic loss of trees) losses depended on species, stature, rooting depth, and tree exposure. These scenarios were compared by examining differences in structural (i.e. biomass, tree richness) and compositional attributes for a number of key species. *NORTHWDS* predicted the maturation of a pole-sized aspen stand and its eventual conversion to a predominantly sugar maple forest. Quantitatively, aboveground biomass levels comparable to field data were forecast (up to 250–300 Mg/ha, depending on the scenario). The predicted dominance of sugar maple was also consistent with other regional studies, and can be attributed to its shade and browsing tolerance.

Keywords: Forest dynamics; Hierarchy theory; Spatial modeling; *NIHMS*; *NIRM*; *NORTHWDS*

1. Introduction

Scientists have long strived to explain observable natural features through the deliberate analysis of established principles. The robustness of the theoretical foundations in many fields has produced great advances in knowledge, but this is by no means a universal attribute of all disciplines (Platt, 1964). The inconsistency and unevenness in advancing knowledge are not always a matter of inadequate scientific technique, but sometimes a function of complexity and scale-dependency. As an example, the response of terrestrial and aquatic ecosystems to management can be very difficult to anticipate due to their open boundaries, the links between their biophysical elements (e.g. soils, vegetation, fauna), and their inherent complexity (Simon, 1962; O'Neill et al., 1986; Roberts, 1987; Allen and Hoekstra, 1992). Our understanding of the relationships between spatial pattern and process has improved markedly during the last century through the examination of local, landscape, regional, and even global ecosystems. Yet, only recently have the biological sciences considered the inherent hierarchy of natural systems.

Hierarchical organization, resolution, and scale are general system concepts that are inexorably intertwined (O'Neill et al., 1986; Allen and Hoekstra, 1992). Imagine, for instance, the challenge of modeling the growth of an individual branch within a forest. This branch is only one of many in the crown of a tree that is part of a stand, which in turn is embedded in a larger landscape. Hence, the growth of the branch is not only a function its position within the canopy and exposed photosynthetic surface area, but by overall tree vigor, localized shading, site conditions, wind exposure and heat transfer (both sensible and latent), and the broader physical environment (e.g. weather patterns). A series of complex hierarchical relationships quickly become apparent. Further, the proper resolution for considering these relationships varies with the question, organizational level, and spatial scale of interest.

The axioms around which a general theory of hierarchical systems has developed provide a starting point for understanding these relationships. Feibleman (1954), for example, presented a list of "uniformities" among integrative levels that have been widely adapted into the current literature (Table 1). Consider the implications of a higher level providing direction for the lower level (e.g. regional climate limiting the potential vegetation at a given site). It is impossible to re-

Table 1
Axioms describing the relationship among levels within hierarchical systems, adapted from Feibleman (1954)

1.	Each level organizes the levels below it, plus each level embodies unique emergent properties. Because of the latter, it is impossible to reduce the higher level to the lower.
2.	Organizational complexity increases upward.
3.	In any organization, processes at the higher levels act in conformity with the laws of lower levels (i.e. higher levels depend upon lower levels).
4.	Lower levels are guided or directed by higher levels (i.e. downward causation).
5.	A corollary to axioms 3 and 4 could be stated as: the mechanisms of a nested hierarchy lie in the lower levels while the purpose of an organization exists at the higher levels.
6.	Events at any given level affect organization at other levels. For example, a disturbance introduced at any one level reverberates at all levels below it.
7.	The rate of change increases with descending organizational levels.
8.	A signal attenuates upward as it moves through a hierarchical organization.
9.	If axioms 1, 2, 7, and 8 are accepted, then an organization at any level is a distortion of other levels.
10.	Smaller resident populations exist at higher levels compared to lower levels.

duce the higher level to the lower because each has its own unique characteristics and scale-dependent qualities. Thus, the whole and the parts are equally real and valid objects of intellectual pursuit. Feibleman (1954) also recognized that the relationship among the levels in Table 1 may not always be described in terms of nested hierarchies, but sometimes better represented by a network or branching (the theory of branching). A food chain is an example of a non-nested system since the higher levels of the chain do not physically contain the lower ones (Allen and Hoekstra, 1992).

We believe that when hierarchical organization, resolution, and scale are considered as inseparable components, these concepts can be strategically linked to the development of model systems with considerable predictive value. Overton (1972), Goodall (1974), and Robinson and Ek (2000) considered hierarchical approaches vital to model development and this effort builds on their work. Our objective is to use the constructs presented by Feibleman (1954) and many others (e.g. Auger, 1986; O'Neill et al., 1989; Klijn and Udo de Haes, 1994; Simon, 1962; Overton, 1972; Pattee, 1973; Goodall, 1974; Jantsch, 1979; O'Neill et al., 1986; Allen and Hoekstra, 1992; Cullinan et al., 1997) who have explored hierarchical theory as the basis for understanding complex systems. This paper first describes a conceptual framework for a hierarchical model of temperate forest dynamics, and then proceeds to introduce two levels of this integrated system.

2. Hierarchy and forest modeling

W.S. Overton was amongst the first individuals to recognize the inherently hierarchical nature of ecosystems and consider methods of emulating this complexity (Overton, 1972; Overton et al., 1973). Overton (1975) further refined these concepts into what became probably the first deliberately hierarchical computer forest model (*REFLEX*), which outlined the structure and philosophy of many contemporary simulators. O'Neill et al. (1986) echoed many of Overton's beliefs that a hierarchical model system was the most effective way to address ecological complexity, especially when an integrated understanding of pattern and process was desired. In recent years, a number of hierarchically structured models have been developed (e.g. Luan et al., 1996; Wu and David, 2002; Mäkelä, 2003), in part because computational ability has increased greatly since the first such models were designed.

Modeling ecological systems is analogous to the number system concepts introduced by Weinberg (1975) and expounded on by O'Neill et al. (1986). The simulation of a small-number system (e.g. individual tree response) or large-number system (e.g. landscapes) is relatively straightforward. For example, predicting landscape change using a deterministic transition state model (e.g. Shugart et al., 1973) is often as productive as more complex biogeophysical process models (e.g. Running and Coughlan, 1988), because the model components can be approximated by average tendencies (O'Neill and King, 1998). However, middle-number systems, classically represented by an ecosystem (O'Neill et al., 1986; Shugart et al., 1992), are much less tractable because it is virtually impossible to reduce its level of complexity to a finite number of elements or to statistically convert an ecosystem into similar, stochastically behaving subunits (O'Neill and King, 1998). Hence, one of the greatest challenges to mechanistic ecological modeling is to meaningfully connect the organizational levels.

2.1. Defining a hierarchical model

How is a hierarchical model best defined? Obviously, the level of interest must be influenced by those above and below the focal scale, with specific interactions between them. O'Neill et al. (1986) envisioned process rates as the key identifier of different hierarchical levels. Thus, a hierarchical model would be one that operates at different rates based on the scale of consideration using readily "decomposable" and identifiable constructs (Wu and David, 2002). Unfortunately, establishing the "holons" (as defined by O'Neill et al., 1986) and assigning them a rate of operation related to their scale does not necessarily reflect all the relevant dynamics. Even though many authors have depicted the relationship between scale and process rate as an increasing function (Fig. 1), the true magnitude of the behavior depends on the process being considered. For example, the greater extent of a landscape would imply that its ability to change would be slower than for an ecosystem, yet catastrophic disturbances can alter landscapes in minutes or hours. Similarly, the biochemical responses of a single-cell organism occur at a very fine temporal scale, but its

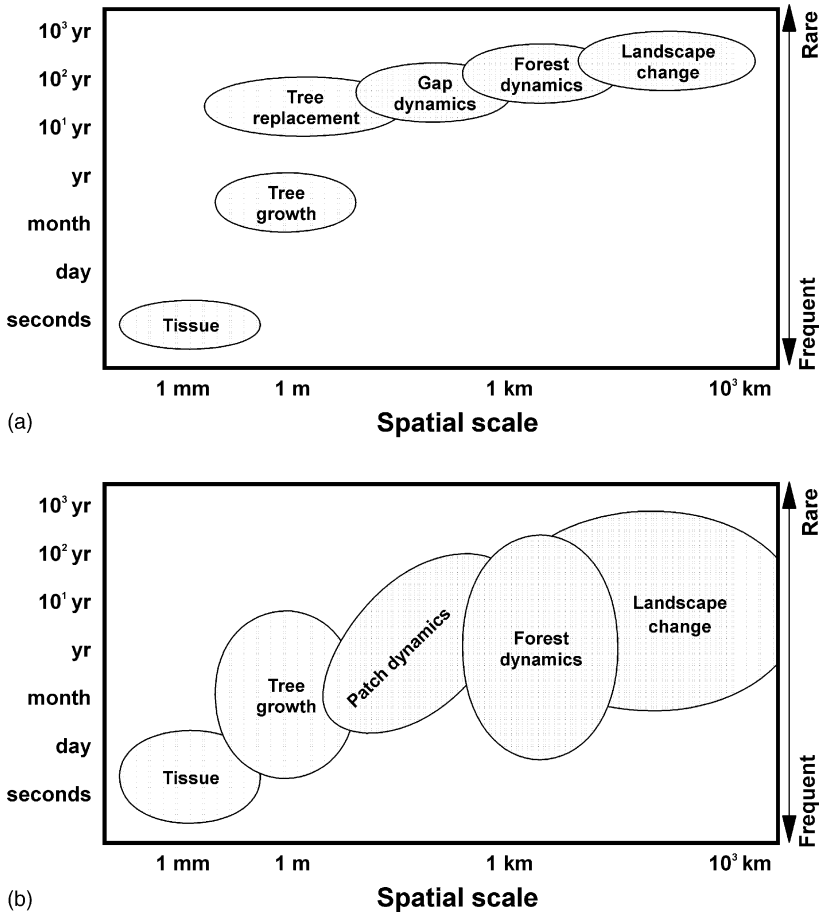

Fig. 1. Traditional representations (a) of the relationship between temporal and spatial scales are usually narrowly linked, with a strong correlation between the two (adapted from Urban et al., 1987). A more complex version of this model blurs the discreteness of some scales more (b), with transitional behaviors like "tree replacement" and "gap dynamics" blended into the more comprehensive "patch dynamics" category. A broader ranges of possible outcomes can also be expressed, especially across temporal scales, to reflect the inherent variability of natural events.

evolutionary changes are far slower. These examples highlight why it is important not to assign a hierarchical level solely as a function of a relatively uninformative label, but to consider the process and scale involved (Allen, 1998).

Robinson and Ek (2000, p. 1837) adopted a broad definition of a hierarchical model as "... any model that involves more than one instance of fitting or application ... simultaneously, sequentially, or independently." This perspective encompasses virtually every model system in existence, and while essentially correct, does not recognize the emergence of new approaches to ecological systems that are deliberately (rather than accidentally or unintentionally) hierarchical. For our purposes, we shall define a hierarchical model as an integrated, systematic approach to approximating ecological behavior across organizational levels, with internal feedback and external response mechanisms that can influence the predicted outcomes at different scales.

2.2. From individual trees to landscape structure—identifying what is important

Foresters and ecologists are very comfortable with individual trees or stands as an identifiable ecological

unit that can be recognized and appreciated by human sensibilities. Therefore, a tree was the logical first step for early computer simulators (e.g. Botkin et al., 1972; Ek and Monserud, 1974). With varying degrees of success, small groups ("gaps") of trees were used to predict individual tree and ecosystem responsiveness or even landscape processes (e.g. Shugart and West, 1977; Pastor and Post, 1986; Botkin, 1993; Urban et al., 1993). Individual-based models still receive considerable attention. For example, process models have been developed to predict tree carbon allocation from tissue response (e.g. Isebrands et al., 1990), while others apply them as the kernel of large-scale simulation (e.g. Pacala et al., 1996).

But how many large-scale processes can be predicted from an aggregated understanding of tissue or individual tree behavior? For instance, would reductionism adequately explain an emergent phenomena like succession? Intuition suggests that there are important processes operating at scales imperceptible to a single organism, a feature Roberts (1987) highlighted in his dynamical systems approach to ecosystems. Roberts believed that the traditional concept of vegetation existing solely as a function of its environment was a limiting view that failed to account for the dynamic interactions between biotic and abiotic components. A relational perspective steeped in set theory provided a more intuitive perspective on the vegetation and environment in which neither the vegetation nor the environment are independent of the other. The environment can dictate which species are possible at what potential abundance, but does not determine what are found or their frequency. However, the complex interactions of individuals, populations, and even communities with their physical environment are usually much less identifiable and hence more poorly understood.

Even an ecosystem perspective can only account for a fraction of what is observed. Knowing the vegetation in one (or a few) "gaps" only hints of what will be encountered in the encompassing stand, forest, landscape, region, biome, etc. Consider an isolated pocket of Engelmann spruce (*Picea engelmannii* Parry ex Engelm.) and subalpine fir (*Abies lasiocarpa* (Hook.) Nutt.) near timberline in the Rocky Mountains or a small black ash (*Fraxinus nigra* Marsh.) wetland embedded in a northern hardwood-dominated moraine. Neither system could be properly understood outside of the context in which they are contained, as these contrasting landscapes help to regulate the internal dynamics of these communities. The relevant compositional, structural, and functional gradients emerge not only from a specific ecosystem, but as a reflection of larger scale pattern and process (much of which occurred in the distant past). Just as a forest is more than a simple aggregation of trees, a landscape is more than an amalgamation of stands (see Wu and David, 2002).

Given these accounts, what is the most relevant scale to model an ecological question? Obviously, the solution depends on what is being asked. Many levels can contribute to the answer, but direction and purpose of the study should be clearly established before model delineation can occur. Perspective is not a trivial feature in ecological analysis, especially when it biases the interpretation of observed phenomena (O'Neill et al., 1986). Perhaps one is interested only in the growth of sugar maple (*Acer saccharum* Marsh.) under different stand densities. This easily identifiable objective can be decomposed to its critical elements (species, phenomena, environmental context) and then fit to the appropriate model system. But what if the level of consideration is not as obvious, or a simple modeling approach is not relevant? Some of the most frequent failings in science arise when we try to answer this question without considering the full range of possibilities (e.g. Platt, 1964; Chamberlin, 1965) or do not recognize that multiple factors (and, hence, scales) actually control the phenomena. Hierarchical models have been proposed as a means to efficiently address these issues (O'Neill et al., 1986).

2.3. Deer browsing and hemlock: an example of hierarchy in a natural system

Recognition of multiple scales and, therefore, multiple rates of change is the first and perhaps most critical step in the development of a hierarchical explanation to the phenomena through simulation modeling. The following example uses the eastern hemlock (*Tsuga canadensis* (L.) Carr.) regeneration problem in the northern Lake States (Michigan, Minnesota, and Wisconsin, USA) as an example of a resource issue best considered at several scales.

Conventional wisdom has held that browsing by white-tailed deer (*Odocoileus virginianus* Zimm.) is the primary reason for widespread regeneration fail-

ure of eastern hemlock (e.g. Bramble and Goddard, 1953; Beals et al., 1960; Waller and Alverson, 1997). However, some researchers have suggested other possible explanations for poor hemlock regeneration. For instance, Mladenoff and Stearns (1993) believed environmental changes like unfavorable germination conditions, reduced hemlock overstories, altered disturbance regimes, or climate change prominently contribute to eastern hemlock decline. Eastern hemlock regeneration problems are a function of all of these, and can be partially observed at each scale. Deer browsing and microsite inadequacies contribute to fine-scale establishment problems, while decreased mature hemlock abundance and increased deer densities have contributed to mesoscale failures, and regional land use and climatic changes produce less favorable establishment conditions with macroscale repercussions on eastern hemlock success.

Thus, it follows that simulation of eastern hemlock regeneration success should incorporate these controlling processes to successfully anticipate the dynamics of this species at micro-, meso-, and macroscales. Some have attempted to simulate the impacts of deer browsing on hemlock with moderate success (Frelich and Lorimer, 1985; Mladenoff and Stearns, 1993), but these examples have been limited by the narrow scale of the models used. There is a risk that an outcome may be forecast that does not match observations in the field. For example, deer browsing can be locally controlled by proper fencing. Does the exclusion of this herbivore then guarantee hemlock success? If there are no seed-producing eastern hemlocks in the vicinity, then the next generation will not establish. Similarly, if microsite conditions are unsuitable (e.g. deep leaf litter with no exposed mineral soil or decomposed wood), then germination will almost certainly fail. Eastern hemlock may also not establish if climate conditions have changed so markedly as to inhibit germination (either too warm, cold, droughty, moist, etc.). To be most valid, a model should include the appropriate organization to anticipate all of these possibilities.

2.4. Advantages to creating a new model system

We have developed a new, fully integrated hierarchical model designed to consider issues at multiple scales. The primary justification for creating a new system was a practical response to the evolution of ecological science and theory, as new visions of model organization and dynamics continue to arise. Without these advances, simulation modeling would do little more than statistically fit data to measurable variables and tell us very little about how the world operates. Though it can be argued that more ecologically consistent models rarely fit data as well as purely empirical constructs (Fleming, 1996), their true value lies not in increased precision but a better understanding of complex phenomena (Roberts, 1987; Zeide, 1991). However, we also believe that such a system is capable of accurately predicting practical attributes like timber yield, biomass production, or species composition, even under a changing environment.

A deliberately hierarchical model system that can be decomposed into internally consistent yet specifically identifiable and scalable components should be a notable improvement over more rigid designs. All too often models developed for a specific application space (e.g. a carbon-based biochemical model of photosynthesis) have been adapted to predict dynamics at scales far from what they were originally intended. This misapplication almost inevitably decouples their design from the relevant scale, usually consuming resources unnecessarily and distracting from the important features of that scale. For example, how does one transfigure almost instantaneous measures of stomatal conductance to annual growth of a forested landscape? Obviously, this event matters, but translating this process from its appropriate scale (leaf) to a much larger one (landscape) to ask such a broad question is highly inefficient unless greatly simplified (e.g. Beerling and Woodward, 2001).

3. N*ORTHWDS* *I*ntegrated *H*ierarchical *M*odel *S*ystem (*NIHMS*)

Every model is at least initially designed for a specific application space constrained by the scale of the question. For example, some simulators are tuned to fine-scale issues (e.g. predicting carbon allocation within *Populus* cuttings; Isebrands et al., 1990) while others are designed for much larger scales (e.g. evaluating the influence of hypothetical fire regimes on mountainous landscapes; Roberts, 1996a). A few have been adapted from one scale of interpretation to another, usually from a bottom-up approach (i.e. aggre-

gated from small to large scales like gaps to landscapes). In theory, an integrated model system is capable of emulating ecological dynamics across a range of scales because the environmental context is provided in an internally consistent manner. In other words, the sub-systems of the model are defined exactly the same when treated separately as when united into an integrated model.

The *NIHMS* evolved following the development of the *NORTH*ern *W*oodland *D*ynamics *S*imulator (*NORTHWDS*) ecosystem model (Bragg, 1999). *NORTHWDS* was designed to mechanistically simulate vegetation behavior across multiple scales while incorporating the dominant patterns and processes of the forests of the northern Lake States. Integrating *NORTHWDS* into a hierarchical model system allows for a consistent and multiscale design to address ecological questions at the most appropriate scale(s).

NIHMS consists of models capable of operating individually at different scales (Fig. 2). The N*ORTHWDS I*ndividual *R*esponse *M*odel (*NIRM*) is an individual tree-based (microscale) model that determines the response of an individual tree to key environmental factors (the current version considers local stand density, relative tree size, site moisture and available N, and local heat sum). Individual tree behavior is predicted from survivorship trends, growth increment, propagule production response functions sensitive to predefined top-down environmental controls. The *NIRM* increment algorithms described in Section 4.2.2.1 are identical to those used in the next highest level (*NORTHWDS*) of *NIHMS*. Therefore, the responses arising from different contexts imposed upon a *NIRM* simulation should parallel an individual embedded in the *NORTHWDS* mesoscale model. *NORTHWDS* simulates a matrix of 30 m × 30 m pixels (called "stand elements"). Each stand element consists of a juvenile (trees <6 cm in diameter at breast height (DBH)) stand table, a list of up to 1000 mature (i.e. trees at least 6 cm DBH) live trees, and an accounting of other direct and derived attributes (e.g. coarse woody debris totals, litter volume, local stand density, leaf area index). A series of ecosystem processes (e.g. competition, nitrogen cycling, white-tailed deer browsing) are also simulated. These processes are not expressly emulated in either the lower or higher levels of *NIHMS*, thus helping to define the mesoscale. The N*ORTHWDS L*andscape *M*odel (*NLM*) will be described in a later paper, but retains key commonalities from *NORTHWDS* (e.g. disturbance regimes, cover types, ownership and timber management relationships). *NLM* differs from both *NIRM* and *NORTHWDS* in that the simulation period is not fixed in the model but can range from annual to decadal increments based on the process under consideration.

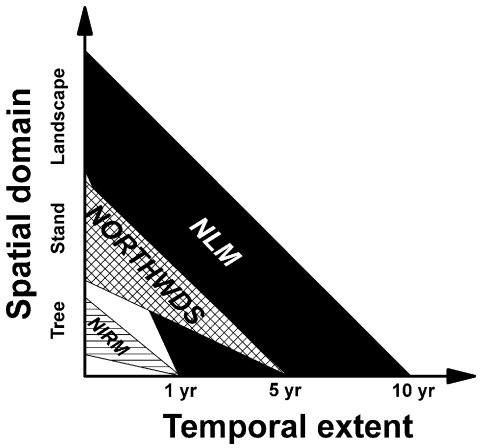

Fig. 2. Visualization of the scales of interest and organization of *NIHMS*. Note that while the *NIRM* and *NORTHWDS* models are restricted to specific 1 and 5 years temporal increments, *NLM* is adjustable from 1 to 10 years (hence its greater temporal extent). A greater distribution is possible for the relevant spatial scales because the entities all can range from small to large (e.g. a sapling to an overstory dominant).

Each model level in *NIHMS* represents an independent computer program linked to the others by code and assumption continuity so their implementations overlap between the levels of the hierarchy. *NORTHWDS* represents the union of the capabilities of *NIRM*, a set of ecosystem processes (e.g. competition), and larger scale landscape interactions (e.g. catastrophic disturbance). While the linkage between *NIRM* and *NORTHWDS* is strong and quite obvious, *NIRM*s relationship to *NLM* is not as apparent. Certainly, the stand-alone versions of *NIRM* and *NLM* occupy vastly different places in application space. For instance, the individual trees simulated by *NIRM* recognize only the fixed and finite environment in which they exist, while *NLM* incorporates individual trees as a virtually imperceptible component of its behavior. Nevertheless, the linkage does exist and is best expressed in the behavior of the integrated model, especially at the mesoscale.

Unlike *NIRM* and *NLM*, the mesoscale *NORTHWDS* model cannot be effectively decoupled from the other scales if realistic emulation of natural communities is desired. To do so would run counter to the advantages in hierarchical models (O'Neill et al., 1986; Allen and Hoekstra, 1992; Wu and David, 2002).

The real strength of this hierarchical design is the consistency in which the levels operate: the same core functions (e.g. tree growth submodels) driving *NIRM* are found in *NORTHWDS*, and the same landscape behaviors affecting vegetation in *NORTHWDS* exist in *NLM*. There are other distinct advantages to operating an integrated hierarchical model system. For instance, Goodall (1974) touted the benefits of conducting fine-scale sensitivity analysis on model sub-systems before aggregating them into the larger hierarchy. Under this approach, not only can the relative response of the integrated model be assessed, but even subcomponents can be evaluated.

4. The N*ORTHWDS* *I*ndividual *R*esponse *M*odel (*NIRM*)

4.1. Introduction to NIRM

Individual-based models have been used to study physiological dynamics like carbon allocation, linking environmental conditions to specific tree responses, or even as the kernel of larger scale gap or forest models (e.g. "big leaf models"). Most process-based tree simulators focus on tissue-level biophysical responses to environmental conditions that are aggregated to produce individual tree responses. For example, Isebrands et al. (1990) developed *ECOPHYS* to explore carbon allocation patterns and other dynamics within an individual *Populus* cutting. In *ECOPHYS*, growth responds to short-term (hourly) changes in environmental conditions like insolation and temperature as well as morphological variability, phenology, and intra-organismal carbon competition. This type of detailed physiological response model can provide useful information for the understanding of internal carbon dynamics of small cuttings, but they are usually too unwieldy to be scaled upward.

Many attempts (e.g. Woodward, 1993) to apply individual tree models across multiple scales have proved of limited value because most of these process models were originally designed for a narrow, small-scale application space. Perhaps the biggest challenge to scaling individual tree models is the recognition of the appropriate application space and the need to accommodate this in the development of the model. An individual tree "process" model does not have to reflect sub-organismal processes like photosynthesis, carbon allocation, or respiration, but may also include tree response to higher-level environmental conditions such as site quality, competition, or defoliation. Creating a model sensitive to ecosystem processes from the perspective of an individual plant (as opposed to a tissue or gap) should prove at least as useful in many applications as traditional physiological process models. This section highlights the capabilities of the individual tree component (*NIRM*) of a hierarchical model system (*NIHMS*).

4.2. Methods

4.2.1. Individual tree model

NIRM is a subset of routines within *NIHMS* directly related to the performance of an individual tree. The environmental context (e.g. stand density, moisture conditions, site quality) is not determined for every cycle using the mechanisms within *NIHMS*—rather, they are established as a set of initial conditions that may (or may not) vary over time. The basic constraints imposed by the growth, regeneration, and mortality routines of the mesoscale are still enforced, so that realized growth, for example, is a function of the optimal increment possible for a tree given its species and DBH and an environmental favorability scalar (Bragg, 1999). An environmental input file is read in by *NIRM* that lists the following variables by year: local stand basal area (m^2/ha), stand quadratic mean diameter (cm), drainage index score, available nitrogen (kg/ha), January average temperature (°F), July average temperature (°F), and percent gypsy moth defoliation (0–100%). These variables can be held constant over the simulation or varied annually.

NIRM can simulate up to 32,000 individuals for a maximum of 1000 years. A total of 24 native tree species are included in this version of *NIRM* (Table 2). Each tree is grown for a year, and has its diameter increment (cm), height (m), biomass (kg), crown surface area (m^2), relative vigor, probability of sur-

Table 2
Common and species names and identifier codes used in *NIHMS*

Common name	Species[a]	Alpha code	*NIHMS* code	FIA code[b]
Balsam fir	*Abies balsamea* (L.) Mill.	ABIBAL	1	012
Red maple	*Acer rubrum* L.	ACERUB	10	316
Sugar maple	*Acer saccharum* Marsh.	ACESAC	11	318
Yellow birch	*Betula alleghaniensis* Britton	BETALL	12	371
Paper birch	*Betula papyrifera* Marsh.	BETPAP	13	375
White ash	*Fraxinus americana* L.	FRAAME	14	541
Black ash	*Fraxinus nigra* Marsh.	FRANIG	15	543
Eastern larch	*Larix laricina* (Du Roi) K. Koch	LARLAR	2	071
Eastern hophornbeam	*Ostrya virginiana* (Mill.) K. Koch	OSTVIR	16	701
White spruce	*Picea glauca* (Moench) Voss	PICGLA	3	094
Black spruce	*Picea mariana* (Mill.) B.S.P.	PICMAR	4	095
Jack pine	*Pinus banksiana* Lamb.	PINBAN	5	105
Red pine	*Pinus resinosa* Ait.	PINRES	6	125
Eastern white pine	*Pinus strobus* L.	PINSTR	7	129
Balsam poplar	*Populus balsamifera* L.	POPBAL	17	741
Bigtooth aspen	*Populus grandidentata* Michx.	POPGRA	18	743
Quaking aspen	*Populus tremuloides* Michx.	POPTRE	19	746
Pin cherry	*Prunus pensylvanica* L.F.	PRUPEN	20	761
Black cherry	*Prunus serotina* Ehrh.	PRUSER	21	762
Northern red oak	*Quercus rubra* L.	QUERUB	22	833
Northern white-cedar	*Thuja occidentalis* L.	THUOCC	8	241
American basswood	*Tilia americana* L.	TILAME	23	951
Eastern hemlock	*Tsuga canadensis* (L.) Carr.	TSUCAN	9	261
American elm	*Ulmus americana* L.	ULMAME	24	972

[a] Nomenclature from Harlow et al. (1979).
[b] Numeric codes used by the USFS Forest Inventory and Analysis Program (Hansen et al., 1992).

vival, and propagule production determined using the same algorithms found in the mesoscale *NORTHWDS* model (calculated for annual rather than 5-year time steps). A key aspect differentiating *NIRM* from the other hierarchical levels in *NIHMS* is that it monitors a single tree within the predetermined physical environment until that individual dies, and then it resets the environment and proceeds with the next tree until the entire set has been completed. With the notable exception of the moment of mortality, all trees behave the same. The flexibility to examine a given environmental variable (or set of variables) is found in the alteration of the environmental context file, which allows the user to set basic variables (e.g. stand density, site quality) over the simulation period. Hence, a tree can be exposed to a constant or varying environment, and *NIRM* adjusts its growth and mortality accordingly. *NIRM* also records the dimensions and growth performance of longest-lived individual for later analysis.

4.2.2. NIRM model design and assumptions

4.2.2.1. Tree growth. Tree growth performance in *NIRM* uses a design that moderates optimal diameter increment based on environmental favorability similar to the approach in the gap models (e.g. Botkin et al., 1972; Shugart and West, 1977; Pastor and Post, 1986). Optimal growth equations (Bragg, 2001a) for the species in *NIRM* were derived from a large public inventory (see Hansen et al., 1992) and represent a conservative estimate of maximum tree growth potential based on species and tree size. This potential relative increment (PRI) methodology produced a set of nonlinear regression equations using thousands of trees from the Lake States (Bragg, 2001a):

$$\mathrm{PRI} = b_1 D_{\max}^{b_2} b_3^{D_{\max}} \quad (1)$$

where b_1, b_2, and b_3 are species-specific coefficients and $D_{\max}$ is the maximum increment within a given

Table 3
Variable definitions and their units (or possible range) incorporated in *NIHMS*

Variable	Definition (units or possible range)
η	Exponent of annual tree survival rate equation (unitless)
ρ	Relative site quality (unitless)
ω	$\omega = 0$ if cover type code = 14, 1 otherwise
ADJ_{DBH}	Relative size adjustment for crown density (unitless)
ADJ_{DI}	Site moisture adjustment for crown density (unitless)
ADP	Annual detrital production
AG_{bio}	Calculated aboveground live biomass (Mg)
ΔB	Annual biomass change
b_1–b_n	Species-specific coefficients
BA	Basal area (m^2)
BA_R	Relative basal area (unitless)
BA_{SE}	Basal area in stand element (m^2)
BIV	Local deer browsing intensity value (0–1)
BIV_{SE}	Stand element deer browsing intensity value (0–1)
BIV_{25}	Stand element deer browsing average of 25-cell neighborhood (0–1)
BIV_{361}	Stand element deer browsing average of 361-cell neighborhood (0–1)
BP_i	Deer browse palatability of species i (0–1)
BS_i	Deer browse sensitivity of species i (0–1)
C	Annual biomass consumption
c_1–c_n	Species-group coefficients
CB_{SE}	Crown biomass per stand element (Mg)
CD	Crown density (unitless)
CI	Competition index (0–1)
CLAY	Fraction of clay in upper 30 cm of soil profile
CLR	Crown length ratio (0–1)
CSA	Crown surface area (m^2)
CSA_{max}	Maximum crown surface area by species (m^2)
CSA_R	Realized crown surface area (m^2)
CTC	Cover type code (unitless)
CV	Cubic volume of bole (m^3)
CV_R	Relative cubic volume of bole (unitless)
CW	Crown width (m)
CWD_{bio}	Coarse woody debris biomass (Mg)
DBH_{max}	Species-specific maximum diameter (cm)
DBH	Current diameter at breast height (cm)
DI	Drainage index (0–1)
D_{max}	Maximum DBH growth by PRI diameter classes (cm)
DS	Site drainage score (0–100)
DS*	Precipitation modified drainage score (0–100)
D_{wt}	Sapling size weight (0–1)
EP_{sexual}	Sexually formed established propagules (count)
$EP_{asexual}$	Vegetative established propagules (count)
EP_{max}	Maximum number of established propagules by species (count)
FR_{SE}	Fine root biomass per stand element (Mg)

Table 3 (*Continued*)

Variable	Definition (units or possible range)
G	Combined IRM environmental favorability scalar (0–1)
GDD	Current number of growing degree-days (count)
GDD_{max}	Species-specific maximum growing degree-days (count)
GDD_{min}	Species-specific minimum growing degree-days (count)
GDD_{rel}	Relative growing degree-days (0–1)
HRL_{HSUM}	Hard regeneration limit determined by heat sum (0–1)
HRL_{LIGHT}	Hard regeneration limit determined by forest floor light availability (0–1)
HRL_{SQ}	Hard regeneration limit determined by site quality (0–1)
HSCI	Herb/shrub competition index (0–1)
HSI	Heat sum index (0–1)
HT	Calculated tree height (m)
I	Entity designator
I_a	Annual tree increment (cm)
IV_i	Importance value of species i
JM	Combined juvenile mortality fraction (0–1)
JM_{DEER}	Juvenile mortality fraction attributable to deer browsing (0–1)
JM_{HS}	Juvenile mortality fraction attributable to herb and shrub competition (0–1)
JM_{LIGHT}	Juvenile mortality fraction attributable to forest floor light availability (0–1)
JUV_{UP}	Fraction of juveniles moving into mature size classes (0–1)
k	IRM index designators
K'	Unweighted derived decomposition coefficient
K''	Weight (final) derived decomposition coefficient
K_{DS}	Decomposition coefficient as a function of drainage score
K_i	Initial decomposition coefficient by organic compartment
K_{LIGHT}	Decomposition coefficient as a function of forest floor light availability
K_{pH}	Decomposition coefficient as a function of soil pH
K_{surp}	Decomposition coefficient as a function of surplus N
K_{TEMP}	Decomposition coefficient as a function of heat sum
L	Crown length (m)
LAI	Leaf area index (m^2)
LBA	Local basal area (m^2)
L_{BT}	Branch and twig litter production (kg)
LIGHT	Forest floor available light (0 = none, 1 = full sun)
$MAXGDD_i$	Maximum growing degree-days for species i
$MINGDD_i$	Minimum growing degree-days for species i
MR	Calculated mortality rate (unitless)
n	Number of items
N_{atm}	Available N contributed by atmospheric deposition (kg)

Table 3 (*Continued*)

Variable	Definition (units or possible range)
N_{avail}	Annual plant available N (kg)
N_{DENITR}	Available N lost to denitrification (kg)
N_{FIX}	Available N contributed by fixation (kg)
N_{Gs}	Gross surplus available N (kg)
N_{LEACH}	Available N lost to leaching (kg)
N_{min}	Available N contributed by mineralization (kg)
N_{surp}	Net surplus available N (kg)
NI	Nitrogen index (0–1)
OM_i	Organic matter mass by compartment i (kg)
P	Remeasurement interval adjustment for PRI derivation
pH	Soil acidity
pH_L	Litter acidity
pH_{ppt}	Precipitation acidity
PPTmult	Precipitation multiplier (0–1)
PRI	Potential relative increment (unitless)
QMD	Quadratic mean diameter (cm)
R	Crown radius (m)
r_i	Unique random number for cycle i
SAND	Fraction of sand in upper 30 cm of soil profile
SI	Site index (m at base age = 50 years)
SI_{max}	Maximum species-specific site index (m at base age = 50 years)
SILT	Fraction of silt in upper 30 cm of soil profile
SLW	Specific leaf weight
SP	Stored propagules (count)
SP_{max}	Maximum number of stored propagules (count)
SR	Cyclic tree survival rate (unitless)
ST	Shade tolerance of species (unitless)
t	Current number of cycles
TDF	Temperature decay factor
$T_{Jan.}$	Mean January monthly temperature (°F)
$T^*_{Jan.}$	Adjusted mean January monthly temperature (°F)
T_{July}	Mean July monthly temperature (°F)
T^*_{July}	Adjusted mean July monthly temperature (°F)
VEGMAX	Maximum number of vegetative propagules by species (count)
$VPCA_i$	Vertical projected crown area for species i
WH_{DBH}	Chronic windthrow hazard due to tree size
WH_{DI}	Chronic windthrow hazard due to drainage score
WHR	Total chronic windthrow hazard rating (0–1)
WH_{RD}	Chronic windthrow hazard due to root restriction
WH_{SD}	Chronic windthrow hazard due to stand density
WH_{SPP}	Chronic windthrow hazard due to species
WH_{TP}	Chronic windthrow hazard due to topographic position
w_1, w_2, w_3, w_4	Equation weights for growth modifier and site index equations

DBH class (see Table 3 for variable descriptions and Table 4 for example coefficient values). To arrive at predicted periodic diameter increment (I_a), current DBH is multiplied by PRI and an environmental favorability scalar (G):

$$I_a = \text{DBH} \times \text{PRI} \times G \tag{2}$$

where G represents the fraction of optimal growth possible given the biotic and abiotic controls imposed by the location of the tree for each species. In the current version of *NIRM*, four indices define this environmental favorability: a competition index (CI); a drainage index (DI); an available nitrogen index (NI); and a heat sum index (HSI). These indices are combined using an integrated rate methodology (IRM) equation (Wu et al., 1994):

$$G = \frac{\sum_{k=1}^{4} w_k}{(w_1/\text{CI}) + (w_2/\text{DI}) + (w_3/\text{NI}) + (w_4/\text{HSI})} \tag{3}$$

where w_k are index-specific weights (all currently = 1). Because each index is scaled from (0, 1], the environmental favorability scalar G ranges from (0, 1], where a final value of 1 would translate into optimal conditions (Fig. 3). For example, a very dry site (i.e. low DI) causes that part of the denominator to become quite large, resulting in a lower growth rate. The weights allow for one or more factors to receive a level of emphasis and can be adjusted by species, although the present designs assume the same value for every species. Since each modifier is dynamic, growth rates depend not only on species constants but also on what is happening to local environmental conditions.

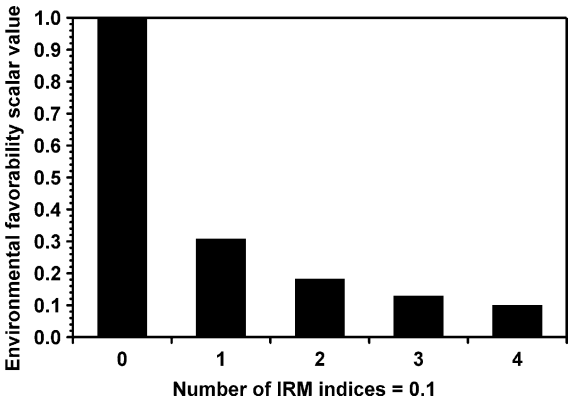

Fig. 3. Effect of environmental indices on IRM growth model (Eq. (3)) scalar response. When all four indices are optimal (=1), then $G = 1$. When one index is reduced to 0.1, $G = 0.308$; when two are lowered to 0.2, $G = 0.182$; when three are reduced, $G = 0.129$; and when all indices = 0.1, $G = 0.1$.

Table 4
Coefficients for the three species highlighted used in the *NIRM* model evaluation

Parameter	White ash	Black spruce	Northern red oak
FIA species code	541	95	833
Maximum DBH (cm)	245.8	50.1	299.1
Shade tolerance score (0–10)	5.0	6.4	5.2
b_1 (PRI coefficient)	1.120796	2.699954	2.241167
b_2 (PRI coefficient)	−0.131123	−0.786279	−0.506656
b_3 (PRI coefficient)	0.970378	0.976055	0.983046
b_4 (crown width coefficient)	4.067896	1.500497	1.796710
b_5 (crown width coefficient)	0.126510	0.013990	0.546875
b_6 (crown width coefficient)	1.055638	1.662184	0.758820
b_7 (crown width coefficient)	−0.087031	−0.017577	−0.077570
b_8 (height coefficient)	8.1782	20.0380	3.8011
b_9 (height coefficient)	0.27316	0.18981	0.39213
b_{10} (height coefficient)	1.7250	1.2909	2.9053
b_{11} (height coefficient)	0.38694	0.17836	0.55634
b_{12} (height coefficient)	0.10847	0.10159	0.09593
b_{13} (crown length coefficient)	4.49	5.54	4.20
b_{14} (crown length coefficient)	0.0029	0.0072	0.0016
b_{15} (crown length coefficient)	1.21	4.20	2.76
b_{16} (crown length coefficient)	0.065	0.053	0.025
b_{17} (competition index exponent)	1.4	1.5	1.4
b_{18} (drainage index coefficient)	−1.548184	−0.887348	−0.306177
b_{19} (drainage index coefficient)	0.100214	0.054866	0.046374
b_{20} (drainage index coefficient)	−0.001095	−0.000265	−0.000342
b_{21} (drainage index coefficient)	0.0000022	−0.0000020	−0.0000013
b_{22} (EP production coefficient)	1.00	1.00	1.00
b_{23} (SP decay constant)	0.000	−0.050	0.000
b_{24} (mortality coefficient)	0.99	0.99	0.99
b_{25} (mortality coefficient)	1.3150	1.6990	0.5639
b_{26} (mortality coefficient)	1393.00	53.78	29.09
b_{27} (mortality coefficient)	2.484	1.219	1.137
b_{28} (mortality coefficient)	0.03413	0.68280	0.01004
b_{29} (mortality coefficient)	4.9700	0.9598	3.8340
b_{30} (mortality coefficient)	0.8110	0.2250	0.3177
b_{31} (biomass coefficient)	0.1634	0.1137	0.1335
b_{32} (biomass coefficient)	2.3480	2.3160	2.4220
Maximum species site index (m at 50 years)	26	22	23
Low N tolerance group	1	3	2
Maximum no. of EPs	200	40	200
Maximum no. of SPs	0	750	0
Minimum species GDD	2414	600	2400
Maximum species GDD	10947	3800	9600

Site index (SI) is determined in a manner similar to Eq. (3), with the notable exclusion of the CI:

$$\mathrm{SI} = \frac{\sum_{k=2}^{4} w_k}{(w_2/\mathrm{DI}) + (w_3/\mathrm{NI}) + (w_4/\mathrm{HSI})}\mathrm{SI}_{\max} \qquad (4)$$

where maximum SI ($\mathrm{SI}_{\max}$) was taken from the literature (e.g. Hahn and Carmean, 1982) as a benchmark of productivity. Both the drainage and nitrogen indices have dynamic properties about them, so SI is not assumed to be a site constant.

Competition index (CI). Competition index is a function of tree crown area (CSA, m^2), calculated as a parabolic surface (Dale, 1962; Larocque and Marshall, 1994):

$$\mathrm{CSA} = \frac{4\pi L}{3R^2}\left[\left(R^2 + \frac{R^4}{4L^2}\right)^{1.5} - \left(\frac{R^4}{4L^2}\right)^{1.5}\right] \quad (5)$$

where the crown radius R (in m, from Bragg, 2001b) equals:

$$R = \tfrac{1}{2}(b_4 + b_5\mathrm{DBH}^{b_6} + b_7\mathrm{LBA}) \quad (6)$$

and crown length L:

$$L = \mathrm{HT} \times \mathrm{CLR} \quad (7)$$

assuming a tree height (HT, in m) (adapted from Ek et al., 1984) of:

$$\mathrm{HT} = \tfrac{1}{3.28}[4.5 + b_8(1 - \exp(-b_9\mathrm{DBH}))^{b_{10}}\mathrm{SI}^{b_{11}}\mathrm{LBA}^{b_{12}}] \quad (8)$$

This equation was selected over other models for two main reasons. First, Eq. (8) was developed for the major Lake States species using regional inventory data. Second, this model includes a measure of site quality (in this case, site index at base age 50 years), allowing for differentiation in height based on site characteristics. However, since *NORTHWDS* assumes a dynamic site, site quality must be determined every cycle. Crown length ratio (CLR) (from Holdaway, 1986) is:

$$\mathrm{CLR} = \frac{[(b_{13}/(1 + b_{14}\mathrm{LBA})) + b_{15}(1 - \exp(-b_{16}\mathrm{DBH}))] - 0.45}{10} \quad (9)$$

where LBA is local basal area (m^2/ha), SI is site index (height in m at base age = 50 years) and b_{13}–b_{16} are species-specific regression coefficients unique to each equation. Since both R and L have been shown to decrease under increasing local basal area (Holdaway, 1986; Bragg, 2001b), increased stand density reduces CSA. Additionally, CI is modified by crown foliar density (CD, ranging from 0 (no foliage) to 1 (densest foliage possible)), which has been established as a function of species shade tolerance (ST), local basal area (LBA), tree DBH, local quadratic mean diameter (QMD), site moisture favorability ($\mathrm{ADJ_{DI}}$), and tree size ($\mathrm{ADJ_{DBH}}$):

$$\mathrm{CD} = \exp\left[-\left(\frac{10 - \mathrm{ST}}{500}\right)\left(\mathrm{LBA}\frac{1.6}{\mathrm{DBH/QMD}}\right)\right] \times \mathrm{ADJ_{DI}} \times \mathrm{ADJ_{DBH}} \quad (10)$$

assuming

$$\mathrm{ADJ_{DI}} = 1 - (1 - \mathrm{DI})^{(15-\mathrm{ST})/5} \quad (11)$$

$$\mathrm{ADJ_{DBH}} = 1 - \left[1 - \exp\left(-\mathrm{DBH}\left(\frac{15 - \mathrm{ST}}{750}\right)\right)\right] \quad (12)$$

Shade tolerance scores were adapted from Graham (1954b) and range from 0 (very intolerant to shade) to 10 (very tolerant). Under this formulation, dense stands produce thinner crowns (Fig. 4a), shade tolerant species were assumed to have sparser crowns than intolerant ones under increasingly drier conditions (Fig. 4b), and small trees have relatively less foliage than large ones (Fig. 4c). Because of the behavior of crown length, width, and density, crown surface area reaches a species-specific maximum ($\mathrm{CSA_{max}}$) under open-grown conditions. The CI is calculated from:

$$\mathrm{CI} = \left(\frac{\mathrm{CSA_R}}{\mathrm{CSA_{max}}}\right)^{b_{17}} \quad (13)$$

where realized crown surface area ($\mathrm{CSA_R}$) = CSA × CD, $\mathrm{CSA_{max}}$ is the maximum predicted crown surface area for a tree of that diameter (when LBA = 0 and CD = 1), and b_{17} is a species-specific crown adjustment factor ($b_{17} > 0$). The exponent in Eq. (13) provides a non-linear response (Fig. 5) designed to reflect the cost of lower photosynthesis under competitive conditions. Therefore, a tree with a predicted CI of 0.5 and a b_{17} of 1.35 would grow about 40% as fast as one of the same size growing under optimal conditions.

Drainage index (DI). Measures of the effect of site moisture on tree growth are scarce, so a new design based on DI was developed. A drainage score (DS) is calculated for each site based on a modified version of the drainage class system developed by Hole (1978) and Schaetzl (1986). This system uses soil map unit information, texture class, and slope to produce a scoring from 0 (dry rock outcrop) to 100 (open water). In a process similar to the derivation of optimal growth rate, 10–20 cm trees were selected for their maximum increment over the range of DS values. The resulting distribution of points was assumed to indicate the species response to varying levels of moisture. After the set of optimal points was selected (similar to the PRI methodology described earlier), a

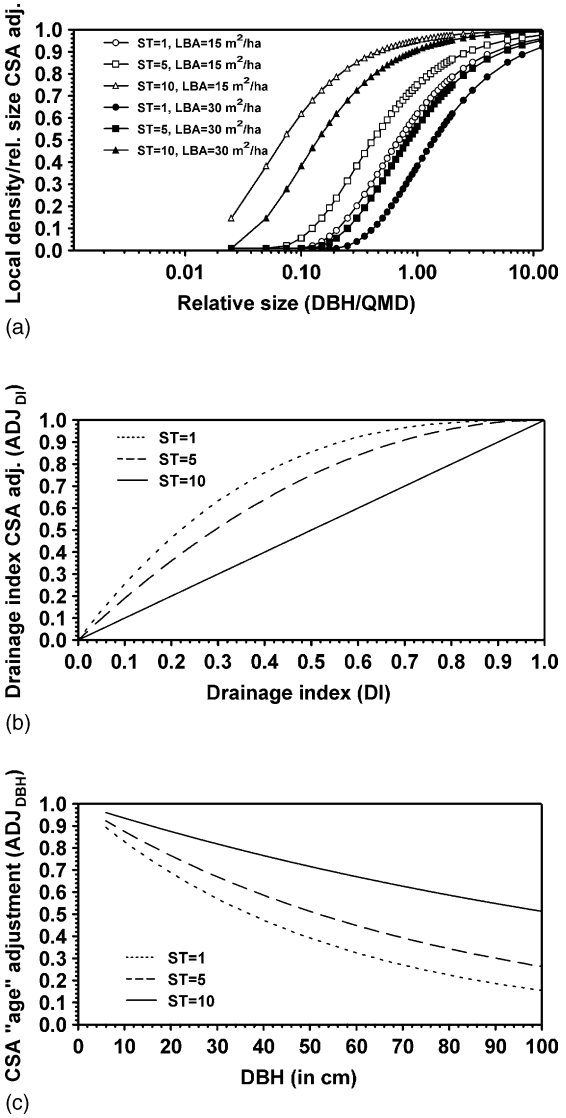

Fig. 4. Modifiers for crown surface area adjustment. Based on Eq. (10), *NIRM* predicts crown density as species-specific functions of shade tolerance, tree size, and drainage index. When open-grown, all species have a local density/relative size crown surface area (CSA) adjustment = 1, with decreasing crown area with increasing stand density and lesser shade tolerance (a). Shade tolerant species are more affected by decrease site moisture (b), while shade intolerant species are less sensitive. Using DBH as a surrogate for age, CSA decreases more with increasing DBH for shade intolerant species (c), although all trees displayed appreciable reductions in crown density as they got larger (older).

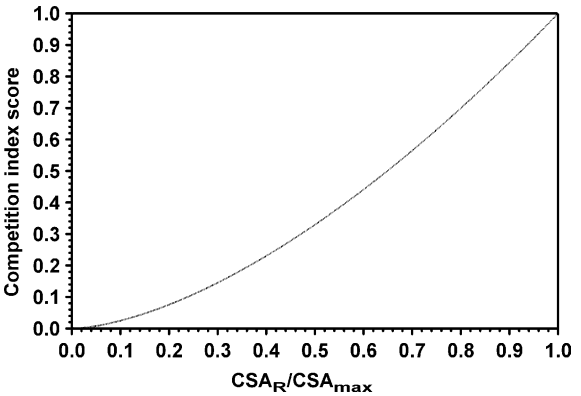

Fig. 5. An example of the competition index as determined by the ratio of realized crown surface area (CSA_R = CSA × CD) and optimal crown surface area (CSA_{max}).

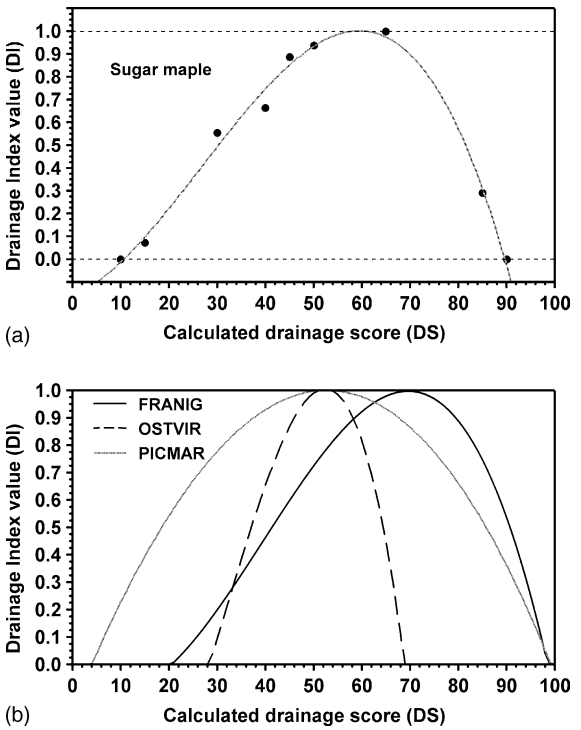

Fig. 6. Species response to moisture gradients (expressed as drainage index scores). Sugar maple (a) performs optimally in the middle portions of the moisture gradient, tapering off rapidly on both sides. Several response curves (b) are possible, depending on species autecology (see Table 2 for species codes).

third-order polynomial was fit to the data (Fig. 6a):

$$DI = b_{18} + b_{19}DS + b_{20}DS^2 + b_{21}DS^3 \quad (14)$$

where b_{18}–b_{21} are species-specific regression coefficients and DI is the DI score (from 0 to 1). This system conservatively estimates moisture-based growth response, but should provide a reasonable means to gauge species reaction to moisture gradients. Most taxa reach optimal growth from $45 \leq DS \leq 65$ with few occurring at $DS < 5$ or $DS > 95$, although the magnitude of moisture amplitude varied considerably. Some species covered virtually all of the moisture range, but others were noticeably more restricted in their response (e.g. white ash, eastern hophornbeam, balsam poplar, bigtooth aspen, pin cherry, and American basswood). A few taxa (e.g. eastern larch, black spruce, jack pine) grow fastest in intermediate conditions but are rarely seen in this range because of competitive exclusion. The growth responses were not always symmetrical, so that some species (e.g. black ash) more gradually responded to low moisture levels than high levels (Fig. 6b). DI is also used to adjust crown density to reflect that trees growing on sites that are either wetter or drier than ideal produce smaller crowns, and hence help to reduce growth and fecundity. In general, shade intolerant species are assumed to be less sensitive to sub-optimal site moisture than shade tolerant species (see previous section).

Nitrogen index (NI). Available nitrogen is well correlated with tree growth performance and has thus been incorporated in forest dynamics models (e.g. Aber et al., 1979; Pastor and Post, 1986). *NIRM* uses an adaptation of Aber et al.'s nitrogen availability growth response curves (Fig. 7):

$$NI = 1 - \exp\left(-\frac{N_{avail} - c_1}{c_2}\right) \quad (15)$$

where N_{avail} is the amount of available nitrogen (both NH_4^+ and NO_3^-) and c_1 and c_2 are group-specific low N tolerance coefficients (Table 5) based on the work of Mitchell and Chandler (1939), Aber et al. (1979), and Botkin (1993). N_{avail} represents a locally weighted average of N produced and lost through mineralization, atmospheric deposition, fixation, denitrification, and leaching. In *NIRM*, N_{avail} is pre-assigned for each cycle (*NORTHWDS* directly calculates N_{avail}, see Section 5.2.2.4).

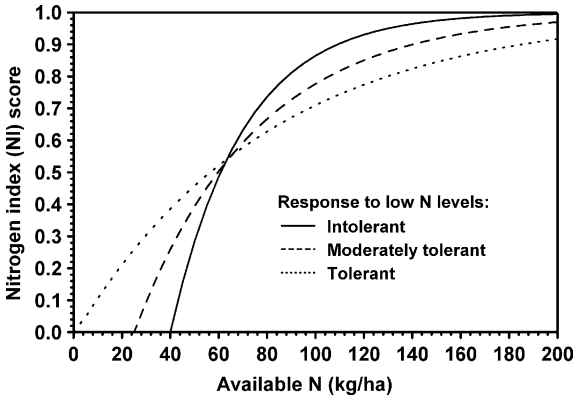

Fig. 7. Response curves of different species groups to available N levels, adapted from Aber et al. (1979). Species that are intolerant of low N levels (solid line) generally grow faster than low N tolerant species as N availability increases (Mitchell and Chandler, 1939; Aber et al., 1979).

Heat sum index (HSI). Thermal effects on species growth performance are poorly understood, but have been included in *NIRM* because of their logical influence on this biological process. Gap models assume that temperature ultimately limits the distribution of species, and that the central portions of the species range represents the most favorable climate. Growth rates taper off as heat sum increases or decreases past the optimum, with the maximum and minimum GDD values determined by the geographic limits of the species range. However, evidence suggests that heat sum is only one of many factors influencing the distribution of species and that a parabolic response curve may be a poor representation of the observed trends (Schenk, 1996). For example, Bonan and Sirois (1992) found that white spruce diameter growth was highest near the southern boundary of its range.

Table 5
Low N tolerance coefficients by species group

Coefficient	Group 1	Group 2	Group 3
c_1	40	25	1
c_2	30	50	80

Group 1 species codes: FRAAME, FRANIG, PICGLA, POPBAL, PRUPEN, THUOCC, TILAME, ULMAME.
Group 2 species codes: ACESAC, BETALL, LARLAR, OSTVIR, POPGRA, POPTRE, PRUSER, QUERUB.
Group 3 species codes: ABIBAL, ACERUB, BETPAP, PICMAR, PINBAN, PINRES, PINSTR, TSUCAN.

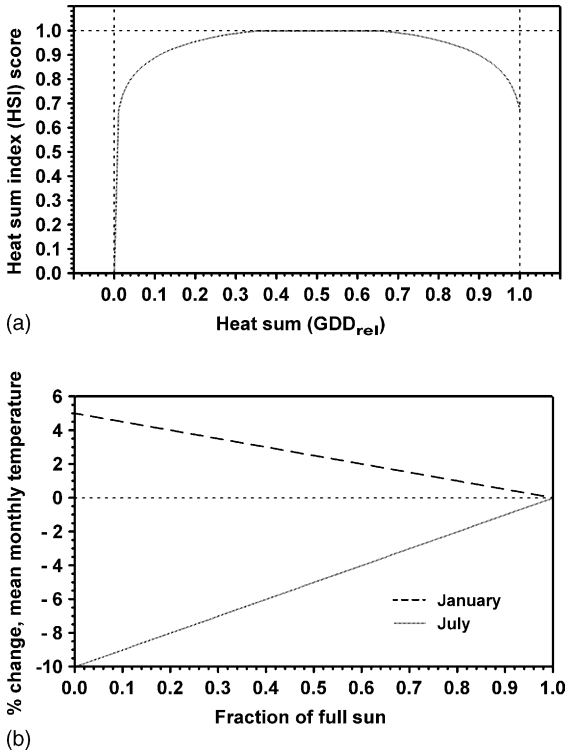

Fig. 8. Heat sum's influence (a) on tree growth rates. Seasonally-based influence of forest cover on monthly temperature (b) (which affects only juvenile establishment). Tree cover on a site reduces extremes by shielding the area from too much sunlight or radiative cooling at night.

NIRM uses an adaptation of the approach designed by Botkin et al. (1972), who envisioned a parabolic relationship between heat sum and tree growth. However, the symmetry and optimal central tendency imposed by this assumption has been called into question (Prentice et al., 1991; Bugmann et al., 1996; Schenk, 1996). To address this weakness, a more flexible model based on the β-function (Minchin, 1987) was used (Fig. 8a):

$$\mathrm{HSI} = 1.2(\mathrm{GDD_{rel}})^{0.125}(1.01 - \mathrm{GDD_{rel}})^{0.125} \quad (16)$$

where HSI is a function of relative growing degree-days ($\mathrm{GDD_{rel}}$):

$$\mathrm{GDD_{rel}} = \frac{\mathrm{GDD} - \mathrm{GDD_{min}}}{\mathrm{GDD_{max}} - \mathrm{GDD_{min}}} \quad (17)$$

$\mathrm{GDD_{rel}}$ depends on local heat sum (GDD, based on a 40 °F threshold) as a proportion of species minimum ($\mathrm{GDD_{min}}$) and maximum values ($\mathrm{GDD_{max}}$). Local GDD was determined in a manner consistent with Botkin et al. (1972), using mean adjusted January ($T^*_{\mathrm{Jan.}}$) and July (T^*_{July}) monthly temperatures (in °F):

$$\mathrm{GDD} = \frac{365}{2\pi}(T^*_{\mathrm{July}} - T^*_{\mathrm{Jan.}}) - \frac{365}{2}\left(40 - \frac{T^*_{\mathrm{July}} + T^*_{\mathrm{Jan.}}}{2}\right) + \frac{365}{\pi}\frac{40 - [(T^*_{\mathrm{July}} + T^*_{\mathrm{Jan.}})/2]}{T^*_{\mathrm{July}} - T^*_{\mathrm{Jan.}}} \quad (18)$$

Mean January ($T_{\mathrm{Jan.}}$) and July (T_{July}) monthly temperatures are taken from local climatological records. Since temperature data are collected from relatively exposed areas, it was felt that an adjustment for conditions that may include dense canopies was justified. Thus, mean monthly temperatures were modified for thermal exposure in the following manner:

$$T^*_{\mathrm{Jan.}} = T_{\mathrm{Jan.}} + [0.05(1 - \mathrm{LIGHT})T_{\mathrm{Jan.}}],$$
$$T^*_{\mathrm{July}} = T_{\mathrm{July}} + [0.10(1 - \mathrm{LIGHT})T_{\mathrm{July}}] \quad (19)$$

where LIGHT is the fraction of full sun reaching the ground. Eq. (19) has the effect of moderating the temperature range experienced under a canopy up to 5% warmer in January and as much as 10% cooler in July (Fig. 8b).

4.2.2.2. Propagule production. Propagule production is also tied to crown size. *NIRM* and *NORTHWDS* produce two classes of propagules: established (EP) and stored (SP). Established propagules are those germinants (or sprouts) that have survived multiple growing seasons. This distinction allows for the models to skip the uncertain germination and establishment phases of regeneration while retaining the dynamics of small juvenile trees. Stored propagules are seeds or root reserves that have been accumulated (but not established) on site and can survive at least one 5-year cycle. Only a small subset of species store propagules via different mechanisms: pin cherry (buried seed pool), jack pine and black spruce (unopened cones on branches), and aspen (root reserves).

Total established propagules (EP) represent the sum of sexual (i.e. seed generated) and asexual (e.g. root

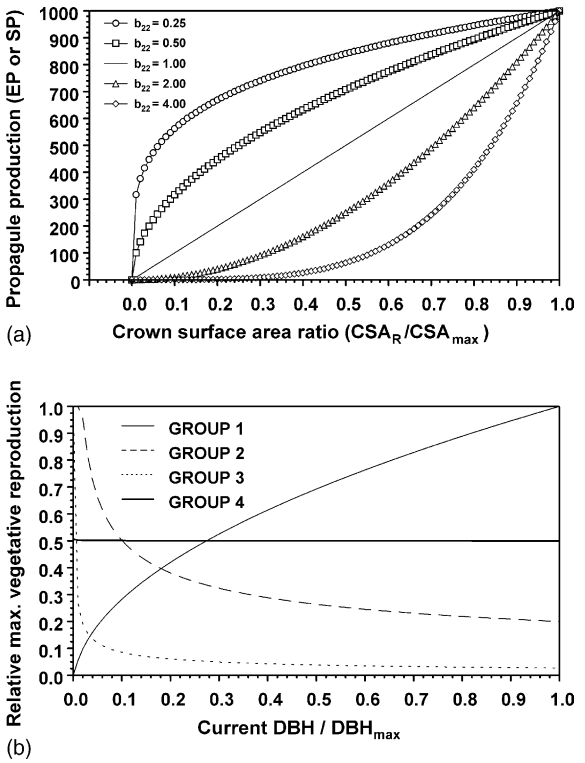

Fig. 9. Propagule (EP or SP) production as a function of relative crown surface area and species (a). Although currently = 1 for all species, different values of b_{22} could yield notably different response curves. Vegetative reproduction ($EP_{asexual}$) is calculated as a fraction of EP_{sexual} for the species groups (see Table 7) capable of this reproductive strategy (b). Notice how some species are better at asexual reproduction at small diameters, while others stay the same or continually improve.

or stump sprouts):

$$EP = EP_{sexual} + EP_{asexual} \quad (20)$$

Sexual EP production (EP_{sexual}) is a function of relative crown surface area (Fig. 9a):

$$EP_{sexual} = EP_{max}\left(\frac{CSA}{CSA_{max}}\right)^{b_{22}} \quad (21)$$

where EP_{max} and CSA_{max} are the maximum species-specific EP production and crown surface area, respectively, and b_{22} is a species-specific adjustment (currently = 1 for all species). Asexual EP production ($EP_{asexual}$) is available for a limited number of hardwoods in *NORTHWDS* only (since there are no disturbances in *NIRM*, there is no vegetative reproduction).

Through a variety of mechanisms several of the species modeled can "store" viable propagules for many years. Ecologically, the inclusion of stored propagules (SPs) permits the rapid recolonization of heavily disturbed sites by shade intolerant species. Classic examples of this include pin cherry (via long-term forest floor seed banks), some species of *Populus* (via root stores), and the serotinous cones of jack pine (Roe, 1963; Marks, 1974; Greene et al., 1999). Stored propagules are produced in a manner similar to EPs:

$$SP = SP_{max}\left(\frac{CSA}{CSA_{max}}\right)^{b_{23}} \quad (22)$$

where SP_{max} is a species-specific maximum number of SPs.

This design allows for different species propagule production based on their size, so that some species can start producing propagules early in life (small CSA_R:CSA_{max} or DBH:DBH_{max}) while others must be larger to begin propagule production. Associating sexual propagule production with crown size is an effective reflection of the biology of the process. Since large, healthy crowns produce more photosynthates, more effort can be invested in carbon-demanding reproductive structures like flowers, fruits, and seeds.

4.2.2.3. Individualistic tree mortality. Tree mortality in *NIRM* depends exclusively on death from reduced growth: senescence from exogenous disturbance event like wind, timber harvest, fire, or drought is not simulated. The association of mortality with reduced tree growth has been well documented (Buchman et al., 1983; Kobe et al., 1995) and appears in numerous other models of forest dynamics (e.g. Belcher et al., 1982; Wykoff et al., 1982; Hamilton, 1986; Pacala et al., 1996). Growth reductions could result from multiple causes, including competition, drought, defoliation, disease, nutrient deficiency, root loss, or some combination of these factors. A tree unable to add sufficient new tissues has a difficult time supporting its photosynthetic surface area, warding off disease, responding to herbivory, resisting other natural disturbances, or adding to its carbon stores, making it much more vulnerable to mortality. *NIRM* uses a mortality model developed by Buchman and others (Buchman, 1983; Buchman et al., 1983; Buchman and Lentz, 1984) that first

calculates tree survival rates (SR):

$$\mathrm{SR} = b_{24} - \frac{1}{1 + \exp(\eta)} \tag{23}$$

where

$$\eta = b_{25} + b_{26} I_{\mathrm{a}}^{b_{27}} + b_{28}(\mathrm{DBH} - 1)^{b_{29}} \times \exp[-b_{30}(\mathrm{DBH} - 1)] \tag{24}$$

I_{a} represents annual increment, and b_{24}–b_{30} are species-specific fitted regression coefficients (b_{24} coefficients for some species have been modified slightly from Buchman's original models). Mortality rate is then $1 - \mathrm{SR}^t$, where t is the number of years ($t = 1$ in *NIRM*, 5 in *NORTHWDS*) mortality is forecast. This model provides a complex mortality surface based on tree species, size, and growth rate. *NIRM* records the year of death of each simulated tree to a 10 years age class until the simulation is completed.

4.2.2.4. Aboveground biomass calculation. To calculate whole tree aboveground biomass, Ter-Mikaelian and Korzukhin's (1997) equation for oven-dry aboveground biomass ($\mathrm{AG_{bio}}$) was used:

$$\mathrm{AG_{bio}} = b_{31}\mathrm{DBH}^{b_{32}} \tag{25}$$

where b_{31} and b_{32} are species-specific coefficients. When Ter-Mikaelian and Korzukhin (1997) listed multiple sets of coefficients, those close to the northern Lake States across the greatest DBH range was chosen.

4.3. NIRM modeling approach

We use case studies to highlight the applicability of *NIRM*. Each case study contains one to several species of interest, a description of defining environmental conditions (including what is varied), and a discussion of the results of the experiment in both a modeling and ecological context. *NIRM* simulates an individual tree growing under a set of predetermined environmental conditions (e.g. local stand density, site drainage, N availability). These environmental conditions can vary on an annual basis, but must be set before simulation begins (no run-time adjustment can occur). Trees are simulated individually with no neighbor interactions. Trends were determined when the entire set of trees has been processed and sorted into different response categories. For example, survivorship patterns can be determined under different site conditions by examining the relative numbers reaching the age class distribution tracked by *NIRM*. A record is also kept of the performance of the longest-lived individual, which displays the behavior of tree components like DBH, height, crown area, vigor, probability of surviving to the next year, and propagule production. Since the only stochastic component of *NIRM* is when senescence occurs, the deterministic nature of the model means that every tree behaves the same over time. The replicates are used to identify mortality response patterns related to the environment defined for each tree, under the assumption that the analysis of aggregate behavior suggests model performance.

4.3.1. Case study 1: Relationship between stand density and tree attributes

Species considered:	
Northern red oak	
Defining (fixed) conditions:	
Simulation period = 400 years	Site index ($\mathrm{SI_{50}}$) = 18.6 m
Trees simulated = 5000	$\mathrm{N_{avail}}$ = 80 kg/ha
Beginning DBH = 6 cm	Drainage index (DI) = 60
Variables:	
Scenario 1.1:	
Stand density = 0.1 $\mathrm{m^2}$/ha	Quadratic mean diameter (QMD) = 0 cm
Scenario 1.2:	
Stand density = 15 $\mathrm{m^2}$/ha	QMD = 12 cm
Scenario 1.3:	
Stand density = 30 $\mathrm{m^2}$/ha	QMD = 12 cm

This case study is designed to show the relationship between local stand density (measured in terms of basal area) and individual tree performance as simulated by *NIRM*. The first scenario in this study considers northern red oaks under open-grown conditions (thus the QMD = 0 cm), while the density increases to 15 and 30 $\mathrm{m^2}$/ha in the second and third scenarios, respectively. Since competition is often held to be

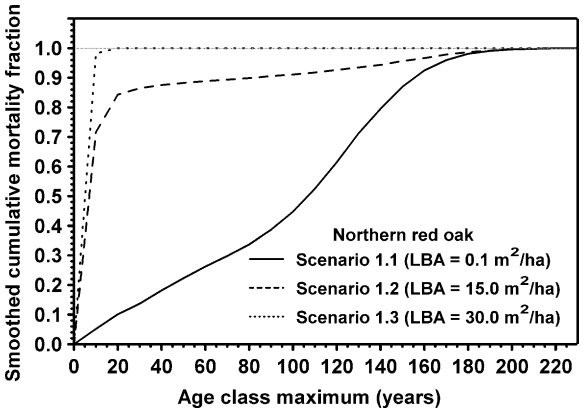

Fig. 10. Differences in northern red oak mortality rate under increasing levels of stand density. Data are from 5000 trees (starting at 6 cm DBH) under fixed local basal area and QMD values.

the most significant factor influencing forest dynamics (Pacala et al., 1996), on average the trees growing free from competition should be the biggest and most productive individuals over their lifespan, with greater survivorship, increment, and propagule production.

4.3.1.1. Survivorship. *NIRM* simulations indicated northern red oak has markedly greater survivorship under open-grown conditions (Fig. 10) when only productivity (not disturbance) is considered. The individuals growing in the absence of a competing overstory (Scenario 1.1) experienced a slow but steady rate of mortality for the first 100 years, and then mortality rates increased slightly until 150+ years, upon which the survivors persisted until the final tree perished at 227 years. Mortality occurred in every age class, although few young oaks died when there was no substantive canopy over them. However, the mortality submodel design (Eqs. (23) and (24)) assures that trees die even under optimal conditions.

In Scenarios 1.2 and 1.3, the 6 cm DBH subject trees beginning under a canopy experienced high mortality during the first 10–20 years of simulation. After 20 years, the intermediate stand density (Scenario 1.2) individuals transitioned from high to low mortality as the survivors passed from a suppressed understory condition to canopy dominants. Since the QMD and local density were held at fixed levels, once a subject tree extended above the competing vegetation, its mortality rate dropped appreciably. Very few trees managed to survive past the first couple decades of these competitive conditions, but a small number did manage to live past 150 years (the oldest tree died at 227 years). Increased stocking further inhibited northern red oak performance. Scenario 1.3 represented a very dense canopy that eliminated virtually all (over 98%) small northern red oaks by 10 years post-initiation, and the remaining fraction died before 20 years (the oldest tree only reached 18 years).

4.3.1.2. Crown surface area. Northern red oaks under the open-grown scenario developed the largest crown for the first 150 years, a difference that was especially prominent for trees <80 years (Fig. 11a). However, the tree experiencing intermediate competition (Scenario 1.2) was predicted to eventually overtake the open-grown oak and have a slightly larger crown. This pattern arose because once the subcanopy tree ascended to the canopy, it was able to receive sufficient light to grow relatively unencumbered. Between this freedom to develop a denser crown and the greater vertical elongation experienced by growing in a competitive environment, the northern red oak in Scenario 1.2 eventually produces a larger crown than a shorter tree in Scenario 1.1. Notice how the tree in Scenario 1.1 plateaus and then gradually declines in crown surface area after 80 years (Fig. 11a). This constraint to crown surface area results from limitations implemented by *NIRM* to restrict crown size as the tree gets larger (older). Although it has not yet begun to decline before the tree died, the oak in Scenario 1.2 also experienced a constraint on crown size.

4.3.1.3. Annual diameter increment. Diameter growth follows similar trends to crown surface area behavior, with the open-grown individual (Scenario 1.1) exceeding the intermediately suppressed tree (Scenario 1.2) for the first 60 years after model initiation (Fig. 11b). This is followed by somewhat better performance of the northern red oak in Scenario 1.2 for the rest of the simulation period. Once again, this transition occurs because the tree in Scenario 1.2 emerges from this unfavorable environment, rapidly adds leaf area, and experiences substantial growth for years afterward. Northern red oak responds well to release once canopy codominance has been reached, but may struggle when young and in an overstocked

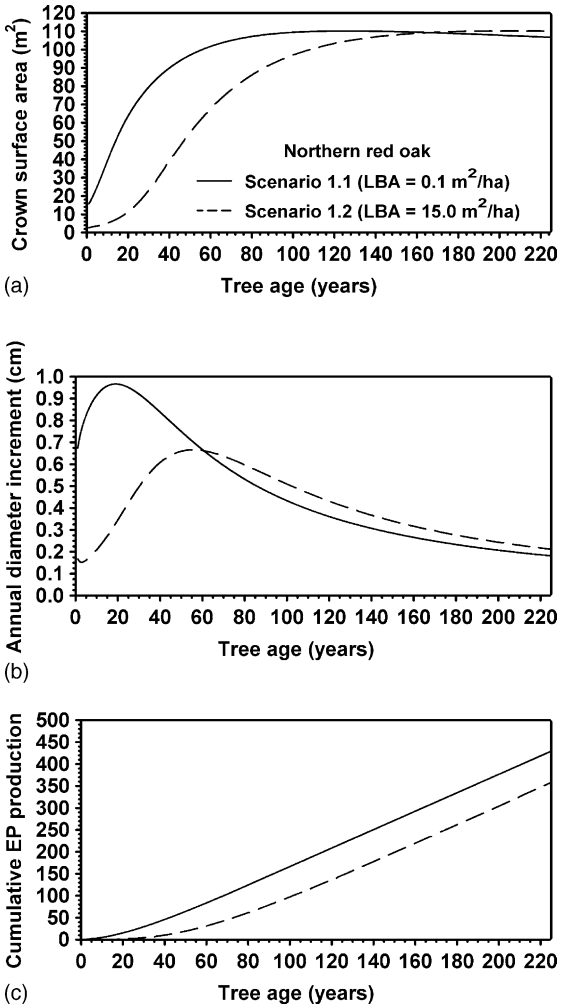

Fig. 11. Contrasting response of free-to-grow and intermediately suppressed northern red oaks (Scenario 1.3 responses were omitted because of extremely high mortality and truncated lifespans). Measures include crown surface area (a), annual realized diameter increment (b), and cumulative established propagule (EP) production (c).

stand (Graney, 1987). Much of the elevated increment noted in Scenario 1.2 arises because the growth model is diameter (not age) based, and the suppressed 60 years old oak is smaller in size and has an inherently higher increment potential than the larger free-to-grow oak would at that age. The slightly greater amount of crown surface area the tree in Scenario 1.2 develops also contributes to the additional growth.

4.3.1.4. Cumulative propagule production. Under open-grown conditions, northern red oak is predicted to produce a limited amount of established propagules (EPs) only a few years after model initiation because its crown size exceeded the propagation initiation threshold (Fig. 11c). Sander (1990) stated that crown size appeared to be the most influential characteristic affecting northern red oak acorn production, with more acorns coming from superior crowns. Regenerative capacity increases rapidly with increasing tree size, although the inherently low rate of acorn production and somewhat unfavorable site conditions help to limit EP production. Even with a seemingly low rate of establishment, over a 220+ years lifespan, a single tree is capable of producing greater that 400 EPs (these represent only a fraction of total acorn production). This may seem limited, but it is on a scale consistent with other observations (e.g. Sander, 1990).

Since *NIRM* directly associates fecundity with crown size, the open-grown northern red oak in Scenario 1.1 has an approximately 30 years advantage over the oak in Scenario 1.2 in EP production (Fig. 11c). The number of propagules produced during these first few decades comprise the majority of the difference in total establishment on this site. Note that establishment of propagules does not guarantee long-term sapling survivorship, so the difference in canopy recruitment success may be even more pronounced between the scenarios.

4.3.2. Case study 2: Sensitivity of white ash to different available N levels

Species considered:
White ash

Defining (fixed) conditions:

Simulation period = 400 years	Stand density = 15 m^2/ha
Trees simulated = 5000	QMD = 12 cm
Beginning DBH = 6 cm	DI = 60

Variables:

Scenario 2.1:	
N_{avail} = 50 kg/ha	SI_{50} = 13.6 m
Scenario 2.2:	
N_{avail} = 100 kg/ha	SI_{50} = 23.2 m

Scenario 2.3:	
$N_{avail} = 2000$ kg/ha	$SI_{50} = 24.3$ m

This case study highlights the sensitivity of a species to differing levels of available N. White ash was chosen because of its inherently high demand for N (Mitchell and Chandler, 1939; Aber et al., 1979).

4.3.2.1. Survivorship. Even though the available N gradient used in this case study appears substantial (50–200 kg/ha), the N response functions used in *NIRM* were not as influential on growth performance as local basal area (Case study 1). Since available N is only one of several factors determining site quality, its diminished impact is understandable. The gradient is sufficient to affect survivorship, however. *NIRM* predicts white ash found in the lowest site to experience greater initial mortality than the two better sites (Fig. 12). The long-term difference is survivorship is largely explained by increased mortality in younger (10–20 years old) classes, followed by a flattening of the response curve. The better sites actually experience slightly higher mortality rates for much of the simulation period, resulting in similar levels of survivorship between all treatments by ~200 years after initiation. The white ash on the poorest site even produced the longest-lived tree (305 years versus 280–285 years).

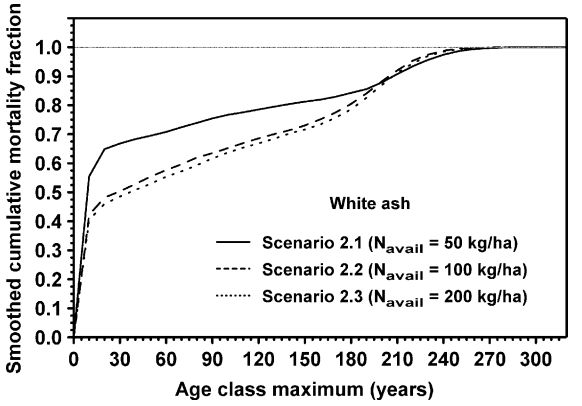

Fig. 12. Under different available nitrogen regimes, white ash mortality behavior showed some differentiation, with the highest mortality rate occurring at the lowest N_{avail} level (Scenario 2.1). Very little difference arose between the moderate (Scenario 2.2) and the highest (Scenario 2.3) N availabilities.

4.3.2.2. Crown surface area. *NIRM* predicts that sites with higher available N levels will produce trees with greater crown surface area (Fig. 13a). Both the medium and high available N scenarios were forecast to produce crowns of roughly 120 m^2 by 150 years of age, approximate 20% higher than comparably old white ash growing on the lowest site quality (Scenario 2.1). The very slight difference between Scenarios 2.2 and 2.3, while consistent, is not likely to be ecologically significant.

It is likely that an available N gradient in the natural environment would have also corresponded to changing levels of other growth-related factors. Individual tree response (and, hence, response of most of the factors considered in this case study) would have been accentuated if other gradients (e.g. moisture) were allowed to increase favorably with the increase in available N. However, since this is an exercise on model sensitivity to individual growth components, all other gradients were held constant.

4.3.2.2. Annual diameter increment. Growth rates peaked for Scenarios 2.2 and 2.3 slightly earlier than for the lowest available N level (Fig. 13b), and the magnitude of their difference was also noticeably greater (approximately 30% more). Net increment for the white ash in Scenario 2.1 somewhat exceeds the other treatments by about 100 years after model initiation, but this difference arises largely from the application of the increment models (see discussion in Case study 1). Even with this slight advantage for 180+ years, the white ash in Scenario 2.1 never fully catches up to the diameters of the trees on better sites, and remains a few cm smaller by the time it dies 20–25 years after the oldest trees in the other scenarios.

4.3.2.3. Aboveground live tree biomass and cumulative propagule production. Scenarios 2.2 and 2.3 produced noticeably larger white ash than Scenario 2.1 (Fig. 13c), consistent with observations that white ash biomass production is greater on more fertile sites (Schlesinger, 1990). This difference primarily originates from the greater woody biomass produced by the larger trees possible on better sites. Better sites will also tend to have more total leaf area, but this component is not as pronounced as the difference in woody biomass.

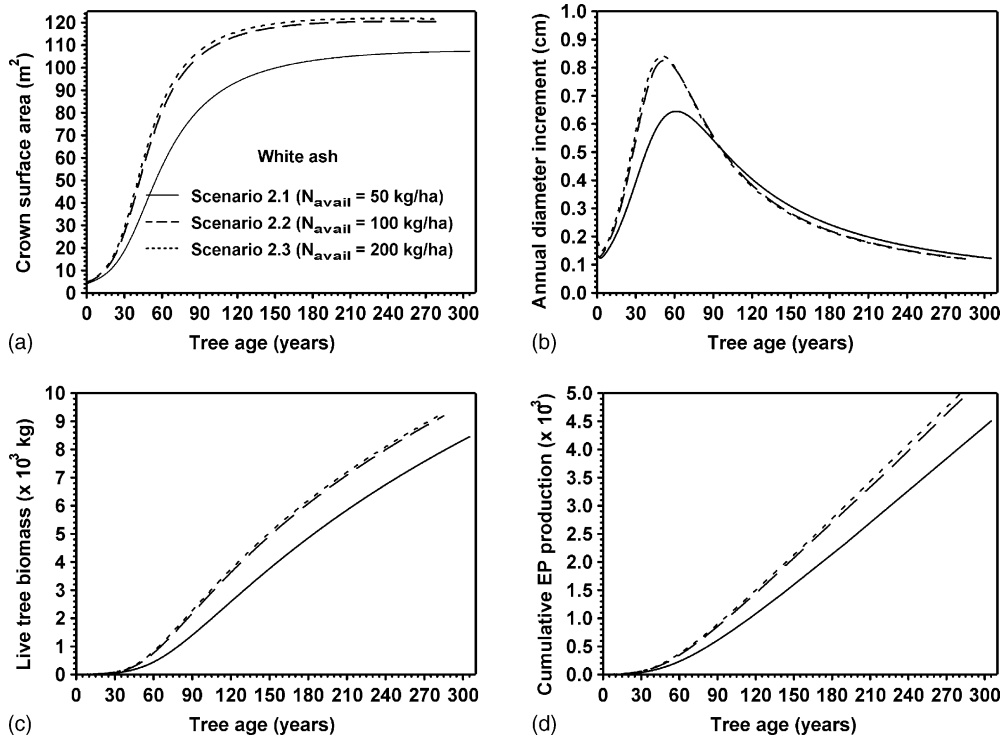

Fig. 13. Similar to the mortality patterns (Fig. 12), white ash was predicted to develop larger crowns (a), grow faster (b), produce larger individual aboveground live biomass (c), and more established propagules (d) with increasing available N (note how similar the behavior of the two highest N_{avail} levels are).

Likewise, better sites result in the production of more EPs (Fig. 13d) for most of the same reasons as increased biomass (more crown surface area = more propagules produced). The slightly higher amount of EPs produced in Scenario 2.3 over Scenario 2.2 may prove important, especially when translated over a larger area. For example, if another factor (e.g. deer browsing) were acting to limit white ash regeneration, then any additional stocking in the juvenile size classes may mean the difference between persistence or local disappearance.

4.3.3. Case study 3: Species performance along a moisture gradient

Species considered:	
Black spruce	
Defining (fixed) conditions:	
Simulation period = 400 years	Stand density = 15 m^2/ha
Trees simulated = 5000	QMD = 12 cm
Beginning DBH = 6 cm	N_{avail} = 80 kg/ha
Variables:	
Scenario 3.1:	
DI = 30	SI_{50} = 13 m
Scenario 3.2:	
DI = 60	SI_{50} = 16.8 m
Scenario 3.3:	
DI = 90	SI_{50} = 12.8 m

Some species display a bimodal abundance across complex environmental gradients like site quality. In many cases, individual tree performance is highest in the intermediate portions of this gradient, yet overall species presence is minimal. Black spruce is a classic example of this bimodality: in the northern Lake States, it can be found on very dry sites or, more commonly, on very wet locations, but its absence in the

mesic sites is pronounced. The mechanisms responsible for this occurrence pattern may include competitive displacement (Huston, 1979) or regeneration failure due to poor germination and/or establishment conditions. This case study considers the potential of black spruce to grow across a range of site moisture, given its establishment.

4.3.3.1. Survivorship. In *NIRM*, suboptimal moisture levels directly reduced growth via the DI modifier and indirectly through reductions in crown surface area (adjustments to Eq. (10)). Black spruce survivorship reacted strongly to changes in site moisture (Fig. 14a). The moisture response curves incorporated in *NIRM* have a peak typically based in the middle of the DI range (roughly DI = 50–60), with rapid declines in growth performance with increasing or decreasing soil moisture. Therefore, the reduction in black spruce mortality in Fig. 14a under Scenario 3.2 (DI = 60) when compared to drier (Scenario 3.1) or moister (Scenario 3.3) sites was expected. Little difference between the very dry and very wet DI scenarios arose, although a slight increase in mortality for a few decades appeared for the wet sites. The more vigorous black spruce tracked for Scenario 3.2 outlived (334 years) the individuals on drier (310 years) and wetter (279 years) sites. Differences in the average age at death were pronounced: 28.9 years for Scenario 3.1, 77.0 years for Scenario 3.2, and 27.8 years for Scenario 3.3.

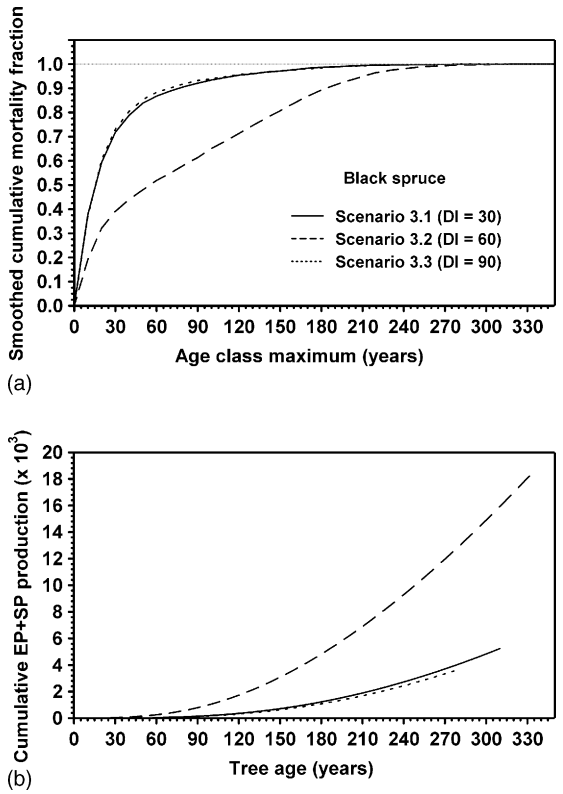

Fig. 14. Black spruce experiencing intermediate site moisture (Scenario 3.2) survived at an appreciably higher rate than those on drier (Scenario 3.1) or wetter (Scenario 3.3) sites (a). This faster growth and increased vigor produced several times more propagules that the poorer sites (b), although propagule production does not necessarily translate into regeneration success.

4.3.3.2. Propagule production. Since *NIRM* associates reproductive potential with photosynthetic surface area, trees with greater crown size are decidedly more capable of producing propagules. Thus, favorable moisture conditions confer a noticeable advantage in propagule production. Young black spruce under any soil moisture level contribute few propagules (black spruce produces both established (EP) and stored (SP)), but the scenario with the most favorable growth (Scenario 3.2) yielded several times the production of either alternative scenario (Fig. 14b). Of the total propagules reported in Fig. 14b, approximately one-third were established and two-thirds were stored propagules.

4.4. Discussion of NIRM results

4.4.1. Ecological consistency of NIRM predictions

Under most scenarios, the *NIRM* results reported in this paper are consistent with regional expectations for the species of interest (northern red oak, white ash, and black spruce). For example, northern red oak lacks the shade tolerance to persist in a closed forest unless gaps sufficiently open the canopy to provide the necessary release. Since stand density was held constant and assumed to be unchanging in the competitive scenarios, high mortality rates were anticipated (Sander, 1990; Schlesinger, 1990). The functions used in *NIRM* are designed to reduce growth response in a manner suggestive of compensating deficiencies (i.e. another resource becomes more limiting, thus reducing growth response). For instance, white ash was not predicted to continue unconstrained diameter growth response

with additional available N. Growth and survivorship predictions by *NIRM* were consistent with the controlled conditions they experience, and suggest that these behaviors should hold in larger scale simulation.

However, not all simulated responses can be directly explained and may actually appear to be contradictory, given the scale of simulation. As an example, when only the moisture gradient response of black spruce is isolated, *NIRM* predicted considerably greater species success in the mesic (as opposed to xeric or hydric) portions of black spruce's range. Black spruce's natural absence on mesic sites in the northern Lake States is more likely an autecological response conditioned by very poor propagule establishment success, followed by the inability to persist in these favorable environments given the competition from other species (Viereck and Johnston, 1990), conditions not incorporated in *NIRM*.

4.5. Context and utility of NIRM

NIRM is the first-level subset of a larger hierarchical model system. Given an environment that affects individual tree behavior, *NIRM* is capable of suggesting how an individual tree would respond in *NORTHWDS*. However, the structure of *NIRM* makes it an inappropriate level to consider how a forest or a landscape would respond to catastrophic disturbance, for example. A tree responds in one of two ways to such an event: it either survives the perturbation, or does not. Ecosystem or landscape responses to catastrophic disturbance are far more complicated, as their organization and dynamics have been altered dramatically. For instance, what species have suffered most under the disturbance? What propagules are available and capable of exploiting the altered resource environment? Are other disturbances likely to arise from the original event? Has nutrient cycling or soil moisture dynamics changed appreciably? These fundamental questions are beyond the scope of information the response of an individual tree model can provide.

NIRM can improve our understanding of how a tree responds to key aspects of its environment and, hence, allows for a fuller appreciation of the tree's behavior when incorporated in a larger context. *NIRM*'s utility extends beyond a sensitivity analysis role to include parameter estimation, assessment of stand density's role on tree growth, estimation of future tree size for updating inventories, and any other need that calls for the prediction of individual tree behavior given a known physical environment. The simple design of the model would also lend itself to additional modules designed to anticipate tree response to defoliation or other changes to external growing conditions. However, *NIRM* is not capable of addressing finer-scale issues like photosynthate production, internal carbon allocation, or root turnover found in physiological processes models (e.g. Rasse et al., 2001) because it lacks the resolution to frame those questions and does not contain the specific mechanisms (e.g. photosynthesis, stomatal conductance) that drive such processes.

Ultimately, the primary factors for evaluating model success should be the quality and utility of predictions, given a model's inherent assumptions (Zeide, 1991; Vanclay, 2003). Simulated responses should be consistent with expectations of natural systems throughout the range of environmental variability that is possible. One of the most valuable applications of *NIRM* lies in its ability to allow for local environmental manipulation and the evaluation of individual responses. This sensitivity analysis can then be used to adjust aspects of model behavior to achieve the desired pattern and process. Evaluating at this scale is more efficient and relevant than attempting to distinguish cause and effect on individual trees in the more complex *NORTHWDS* model.

NIRM is fundamentally different from most individual tree models in that it does not employ a reductionist or bottom-up aggregative approach for simulating tree growth or survivorship. Many such models consider key biological processes like photosynthesis, transpiration, respiration, or internal carbon allocation (e.g. Isebrands et al., 1990; Hoffman, 1995; Bossel, 1996), even though these processes may be difficult to adequately measure in a reliable fashion (Zeide, 2003). In some ways, *NIRM* is similar to the canonical model approach (Voit and Sands, 1996a,b) that subsumes the intricate biochemistry and tree physiology to a higher level of interest (e.g. long-term tree growth patterns). However, it differs in the level of detail related to specific driving mechanisms. Both finer- and coarser-scale processes that define the potential and constraints of tree behavior are represented as either assumed processes (e.g. growth or mortality as a function of diameter increment, which is driven by crown volume, which is associated with photosynthetic ca-

pacity, which depends on insolation, stomatal conductance, leaf moisture balance and nutrition, and so on) or established state variables (e.g. local stand density, relative tree size, site nutrient and moisture levels).

5. The *NORTH*ern *W*oodland *D*ynamics Simulator (*NORTHWDS*)

5.1. Introduction to NORTHWDS

Most dynamical forest simulators are still based on gap model principles developed up to 30 years ago, although advances in computer technology and geographic information systems have seen the advent of new model systems that represent notable departures from earlier designs (e.g. Pacala et al., 1993; Williams, 1996; Roberts, 1996a,b; Liu and Ashton, 1998; Kimmins et al., 1999). Even with the abundance of models developed in the last few decades, phenomena occurring at the mesoscale (a few ha to a few hundred ha) are especially challenging to emulate, in part because of scale and intermediate levels of complexity (see Shugart et al., 1992; O'Neill and King, 1998).

The stand-alone *NORTHWDS* represents the intermediate (mesoscale) tier of a larger hierarchical model system designed to predict vegetation change as a function of scale, process, and structure. *NORTHWDS* differs from many individual-based models in its integrative, hierarchical structure (as opposed to aggregative approaches). *NORTHWDS* produces an ecosystem-level projection by incorporating fine-scale components (an individual tree-based projection) with multiple ecosystem holons and a series of higher-level constraints and disturbances to form its general architecture. In this paper, we first present a detailed overview of the assumptions and design of *NORTHWDS*, followed by a sensitivity and responsiveness test using a series of simulations based on differences in windthrow regime.

5.2. NORTHWDS model design

5.2.1. NORTHWDS organizational context

The *NORTHWDS* model is the mesoscale component of *NIHMS* (Fig. 2), which also includes the *NIRM* microscale model and a macroscale model (*NLM*, in preparation). Fig. 15 provides a flowchart of the design of *NORTHWDS*. Although many *NORTHWDS* subsystems differ in their operation, the model contains most of the same steps and features as traditional forest models. Each compartment in Fig. 15 (and most of the fluxes) are described in greater detail later in this paper.

5.2.1.1. Grain and extent considerations. To help balance ecological mechanism with ecosystem pattern, *NORTHWDS* was designed to avoid conflicts between detail and parsimony. Physiological process models (e.g. Isebrands et al., 1990), while often preferred for understanding the interaction between a tree and its environment, are too ponderous and dependent on initial conditions for analysis beyond a handful of trees. On the other extreme, models developed for landscapes lack fine scale mechanism and rely heavily on pattern and trend analysis. The *NORTHWDS* mesoscale model was developed with its finest spatial resolution (grain) of a fixed 30 m × 30 m "stand element." Each stand element is comprised of a juvenile stand table containing species by diameter classes (Table 6) and a mature (≥6 cm DBH) tree list of up to 1000 individuals. The current version of *NORTHWDS* incorporates up to 24 native tree species (Table 2), representing the major forest taxa of the northern Lake States.

Depending on what ecological processes are being simulated, each stand element may operate as a discrete operational unit or can be aggregated into larger neighborhoods or patches. Under some circumstances, stand element aggregates are fixed in their size and shape, often using the nearest eight neighbors to provide local context. Other groups may be assembled from similar adjacent stand elements, and hence form patches that may be tens to hundreds (or more) of

Table 6
NORTHWDS juvenile size class descriptions (for all tree species)

Size class	Description	Code
1	Reserved for stored propagules	SP
2	Established propagule class 1 (no DBH)	EP1
3	Established propagule class 2 (>0–1 cm DBH)	EP2
4	Established propagule class 3 (>1–2 cm DBH)	EP3
5	Established propagule class 4 (>2–4 cm DBH)	EP4
6	Established propagule class 5 (>4–6 cm DBH)	EP5

>6 cm DBH trees are considered "mature" and added to the stand element tree list.

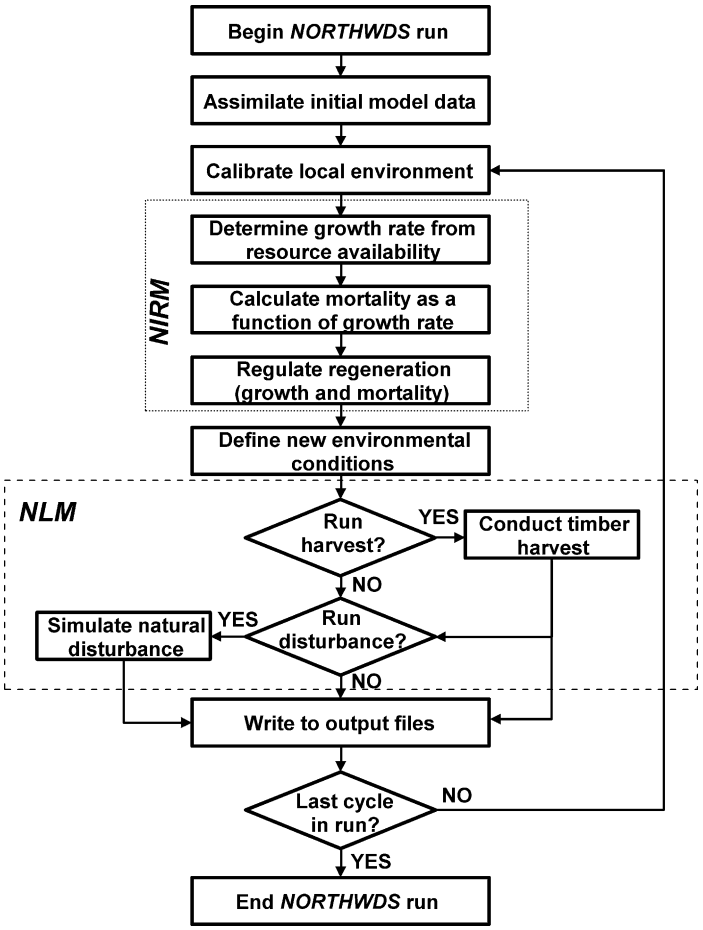

Fig. 15. Schematic of the basic model structure of *NORTHWDS*, including realms of overlap with *NIRM* and *NLM*.

stand elements in extent. Timber harvesting, for example, reflects a goal-driven strategy constrained by the composition and volume of managed forests using dynamically defined patches of harvest opportunity. Currently, *NORTHWDS* is constrained to a minimum grid extent of 20×20 stand elements (36 ha) and a maximum of 250×250 stand elements (5625 ha). While the minimum extent is fixed by the scaling of some processing (e.g. deer browsing), the theoretical application realm of *NORTHWDS* extends to the point where either the species or environmental space becomes invalid (e.g. new species appear).

5.2.1.2. NORTHWDS time step. A 5-year step termed a "cycle" marks the advance of time for *NORTHWDS*. This, too, represents a compromise between the desire to measure fine-scale temporal events with the limitations of data and resource availability. Hourly, daily, or even monthly increments exceed the resolution of the model structure assumed by *NORTHWDS*, while decadal or longer steps would miss important ecosystem attributes.

5.2.2. Calibrating the local environment

NORTHWDS calibrates local environmental variables in two steps: once at the beginning of a simulation run to build historical soil pH levels and maximum possible crown surface area by species, and repeatedly (every cycle) to calculate site quality and other growth-modifying conditions. This dynamic restructuring of the physical and biological environments assures that the relational nature of these levels reflects

the underlying interdependence of site-species interactions (sensu Roberts, 1987).

5.2.2.1. Soil pH reconstruction. *NORTHWDS* uses a weighted sum of the particle size distribution, litter pH, and precipitation pH to determine site soil pH, which plays an important role in *NORTHWDS* biogeochemistry and site quality determination (see later sections). *NORTHWDS* takes the average soil surface (top 30 cm) pH from the stand element biophysical attribute file, back-calculates 100 cycles of soil pH values using this measure (i.e. 100 cycles of the same pH as the default), and stores them in a registry for eventual pH determination using an inertial approach. *NORTHWDS* calculates the number of cycles (n) to average using the fraction of sand (SAND), silt (SILT), and clay (CLAY) of the surface soil:

$$n = (\text{SAND} \times 6) + (\text{SILT} \times 12) + (\text{CLAY} \times 24) \tag{26}$$

where n is expressed as an integer. The number of cycles (from a minimum of 6 (30 years) and maximum of 24 (120 years)) indicates the rate of change that would be expected for soil pH, given the mixture of soil particle sizes in that stand element. Stand element soil pH is determined by:

$$\text{current pH} = \frac{\sum_{i=t-n}^{t} \text{pH}_i + \text{pH}_\text{L} + \text{pH}_\text{ppt}}{n+2} \tag{27}$$

where the current pH value is the average of the previous registry of site pH's (pH_i) for n cycles, current litter pH (pH_L), and precipitation pH (pH_ppt). From Eqs. (26) and (27) it is apparent that the higher the clay content of the soil, the less responsive the site will be to changing pH, while the higher the sand content of the soil, the more rapid the change. Fig. 16 provides an example of the sensitivity of three different soils comprised entirely of sand, silt, or clay (though Eq. (26) does allow for soils of mixed particle sizes). Note how rapidly the sandy soil responds, while both the clay and silt soils have yet to asymptote at 100+ cycles (500+ years). This inertial approach results in a "plastic" response of the environment to vegetation (Roberts, 1987). For instance, long-term deposition of litter and precipitation gradually changes soil pH.

5.2.2.2. Site moisture dynamics. Moisture distinctly affects tree growth in forested ecosystems. As a rule

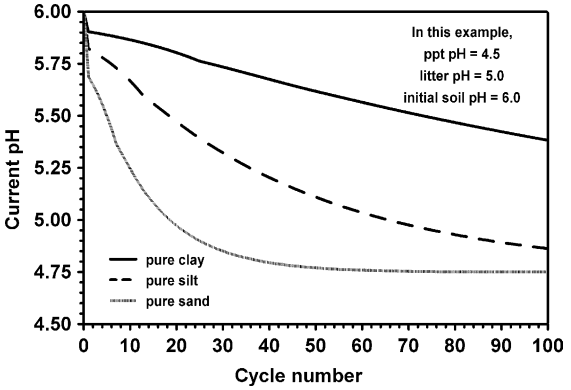

Fig. 16. Results of inertial soil pH modification by vegetation and precipitation. Each line represents a pure example (100%) of different particle size classes for demonstration purposes: various admixtures of these particle size classes are possible. Different initial soil and precipitation pH values would also result in different trajectories.

of thumb, the more moisture available on a site, the greater the productivity until high soil moisture limits the amount of oxygen available to the fine roots. Some species have a very broad moisture amplitude. Jack pine and black spruce, for example, are found on excessively drained outwash and very poorly drained organic soils. Many models emphasize some aspect of site moisture, especially drought (e.g. Running and Coughlan, 1988), while others have chosen to downplay this component (e.g. Pacala et al., 1993, 1996, also see Caspersen et al., 1999). Gap models accumulate water deficits by calculating the relative monthly difference between potential and actual evapotranspiration, and address high site moisture by comparing species-specific minimum depth to water table tolerance to the actual depth of the water table (Botkin, 1993). *NORTHWDS* operates on a 5-year time step, so monitoring daily, monthly, or even annual changes in site moisture is not possible, which limits the ability to simulate short-term drought.

Drainage index. A modified version of the drainage class system developed by Hole (1978) and Schaetzl (1986) was adapted for use as the moisture regime for *NORTHWDS*. The DI uses information on a soil map (e.g. suborder, great group, subgroup, texture class, and slope class) to rank a site from 0 (dry rock outcrop) to 99 (open water). In addition, a vegetation cover modifier sensitive to the *NORTHWDS*

herb/shrub cover index (Section 5.2.7) allows for a shift of up to ±6% of the total drainage score (DS) if the site goes from dense, closed forest to completely open (or vice versa). This modifier assumes that tree cover reduces site moisture through heightened evapotranspiration (Pearson, 1930; Sartz and Knighton, 1978). DS values can also be adjusted for changes to precipitation (see next section). Drainage index (see Eq. (14)) ranges from 0 (exceedingly poor site) to 1 (optimal conditions). This system conservatively estimates moisture-based growth response, but should provide a reasonable means to gauge species reaction to moisture gradients.

Precipitation influences. Changes in precipitation can also have significant ecological implications, especially if they represent long-term trends. While *NORTHWDS* lacks the temporal resolution to address short-term precipitation variation, it is capable of addressing long-term precipitation changes by adjusting the DS:

$$DS^* = \begin{cases} DS \times PPT_{mult} & \text{if } PPT_{mult} \geq 1 \\ \left[\left(\frac{DS}{100}\right)^{1/PPT_{mult}}\right] \times 100 & \text{if } 0 < PPT_{mult} < 1 \end{cases} \quad (28)$$

where DS^* is the modified drainage score and PPT_{mult} is a precipitation multiplier > 0 (default value $= 1$). Under wetter-than-average scenarios, all sites experience some increase in moisture (higher DS values), although the greatest increases occur in the wettest sites (Fig. 17). This reflects the nature of regional drainage patterns, in which the lowest (and, hence, wettest) areas receive both additional precipitation and upslope runoff. Under prolonged drought, all stand elements would experience a reduction in their DS score. Once again, the response is not equal, with the greatest drying occurring in the intermediate DS range. Wet areas would dry somewhat, but since they serve as collection points, their response to drought are somewhat buffered. Very dry sites would not desiccate much further because there was little initial moisture.

5.2.2.3. Temperature controls on growth. For *NORTHWDS*, we adapted some features of the gap model approach to heat sum while trying to avoid their limitations (Eqs. (16)–(19) and Fig. 8). The heat sum response range (Fig. 8a) given by Eq. (16) results in a diameter growth rate = 0 at the coldest end of the species botanical distribution, but not at the warmest limit as assumed by gap models. While some growth decline is experienced, species are still capable of adding considerable increment at their southern limits (*NORTHWDS* assumes up to two-thirds of the maximum). Also note the extensive area in which optimal growth is possible (from GDD_{rel} ~0.35 to ~0.65). Species are prevented from occurring outside of their current GDD range by hard regeneration limits (Section 5.2.6.2) that preclude the establishment of new seedlings under certain conditions.

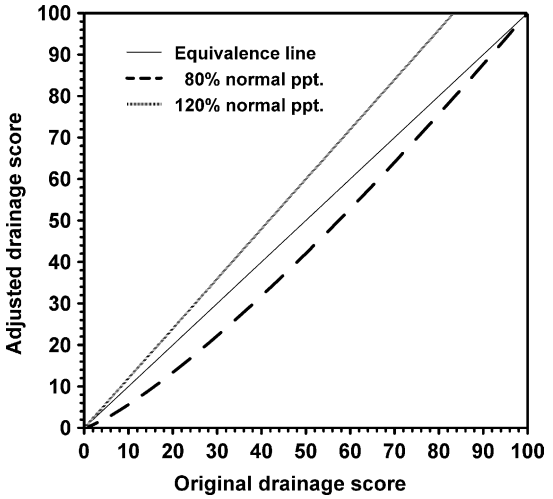

Fig. 17. Influence of varying (departures from long-term) 5-year average precipitation on site drainage index. Wet sites tend to get very wet under abnormally moist conditions, while intermediate sites experience the greatest drought.

5.2.2.4. Nitrogen index and biogeochemistry. Plant-available nitrogen (NH_4^+ and NO_3^-) has long been considered an important growth factor for trees (Mitchell and Chandler, 1939; Waring and Schlesinger, 1985). Other macro- and micronutrients play significant roles in the growth and development of forests, but the research into these components has generally not lent itself to ecosystem simulation. *NORTHWDS* currently tracks only N and assumes that other nutrients are correlated to N and site moisture.

The NI in *NORTHWDS* is the culmination of a series of pools, fluxes, and interactions (Fig. 18). An important feature apparent in Fig. 18 is the link between the vegetation (VEG) and the various compartments of

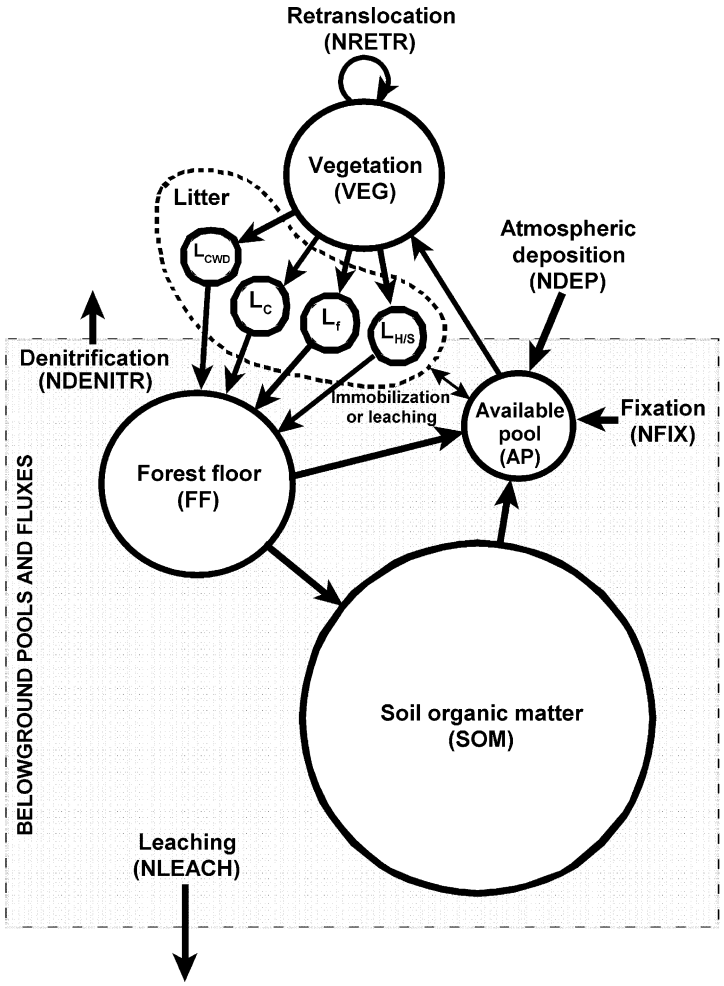

Fig. 18. Visualization of the pools and fluxes involved with biogeochemistry as modeled in *NORTHWDS* (each compartment is described in further detail in the text).

the physical environment. Detritus is produced by the vegetation (both above- and belowground), gets transferred to litter (*L*) and is decomposed, with the residual transferred to the forest floor (FF) for further decay. Finally, the material that remains is shifted into the soil organic matter pool (SOM), which represents the final organic stage of the detritus. At this stage, N is either stored, transferred to the available pool (mineralized), lost from the system (leached), or compartmentalized (immobilized). Other processes associated with N biogeochemistry in *NORTHWDS* include atmospheric deposition, denitrification, fixation, and leaching. The vegetation responds positively to available N, so that any process that increases plant-available forms of N should improve growth.

Vegetation impacts on biogeochemistry. Vegetation interacts with site biogeochemistry via several different pathways in *NORTHWDS*. First, it responds in growth to the availability of environmental N through the application of an NI. NI was previously determined in Eq. (15) and is a locally adjusted variable in *NORTHWDS*. Available N (N_{avail}) is calculated from:

$$N_{avail} = N_{min} + N_{atm} + N_{FIX} - N_{DENITR} - N_{LEACH} \quad (29)$$

or the sum of the mineralized N (N_{min}), N deposited from the atmosphere (N_{atm}), N fixed (N_{FIX}) in the soil and woody debris, and N lost to denitrification (N_{DENITR}) and leaching (N_{LEACH}).

As shown in Fig. 18, retranslocation of N (N_{RETR}) within the tree is also estimated. For the current version of *NORTHWDS*, N_{RETR} is constant (half of foliar N) within species regardless of environmental N levels and retranslocation occurs only in the fine litter compartment (i.e. leaves, reproductive structures, small twigs, and fine roots).

The vegetation recycles N, C, and other chemicals back to the environment through detritus deposition. *NORTHWDS* simulates litter production in four distinct categories: fine litter (L_f—defined earlier), coarse litter (L_C—large branches and roots, juvenile trees), coarse woody debris (CWD) (L_{CWD}—dead trees $\geq$10 cm DBH), and herbaceous/shrubby litter (L_{HS}—defined later). Each litter subcompartment behaves in a different manner depending on its decomposition rate. Fine litter degrades rapidly due its extensive surface area to volume ratio and relatively high N levels. The fine litter decomposition coefficient is based on a species-based weighted average collected from several references (e.g. Perala and Alban, 1982; Bockheim et al., 1991) designed to reflect differences in litter quality by species. Organic matter decomposition for each component was predicted as:

$$OM_{t+1} = OM_t \exp(-5K'') \quad (30)$$

where the amount of a particular organic compartment carried into the next 5-year cycle (OM_{t+1}) is a function of the initial quantity (OM_t) and a decomposition coefficient (K''). For the fine, coarse, and CWD litter compartments, K'' is species-specific, while it is fixed for the L_{HS}, FF, and SOM compartments.

K'' has also been designed to be sensitive to changes in the physical environment, responding to soil pH, forest floor available light, site wetness (DS), and "surplus" N. Soil pH affects K'' as follows:

$$K_{pH} = 0.10 + 0.90^{(pH-7.0)^2} \quad (31)$$

where pH is stand element soil acidity, which has the effect of decreasing decomposition as soil pH approaches either extreme (Fig. 19a).

Because increasing organic matter temperature accelerates bacterial decomposition (Waring and Schlesinger, 1985), an available light factor was included as a surrogate for temperature (assuming that as more light reaches the soil surface, ground temperature increases). Available light influences K in the following manner:

$$K_{LIGHT} = 0.2 + [1 - \exp(-7.0 \times LIGHT)]^{5.0} \quad (32)$$

With this adjustment, decomposition rates should rise quickly as the canopy opens to a maximum at zero overstory (Fig. 19b).

Increasing site moisture generally increases decomposition until fairly saturated, when excess water deprives decomposers of the oxygen needed. To simulate this response, K increases progressively until a high soil saturation point indicated by DS:

$$K_{DS} = 0.02156DS - 0.00024DS^2 + 0.0000079DS^3 - (7.706 \times 10^{-8})DS^4 \quad (33)$$

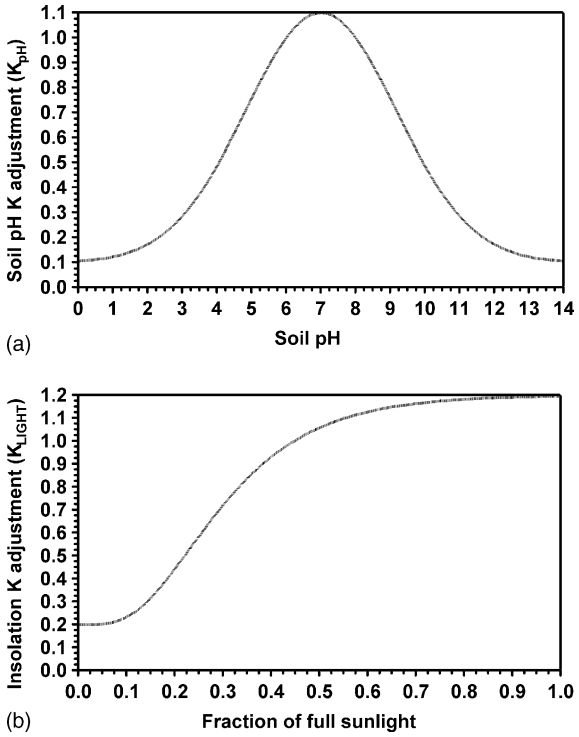

Fig. 19. Influence of soil pH and sunlight on organic matter decomposition coefficients. Soil pH (a) is assumed to produce a modal response to the decomposition coefficient, while insolation produces a gradually increasing response curve (b).

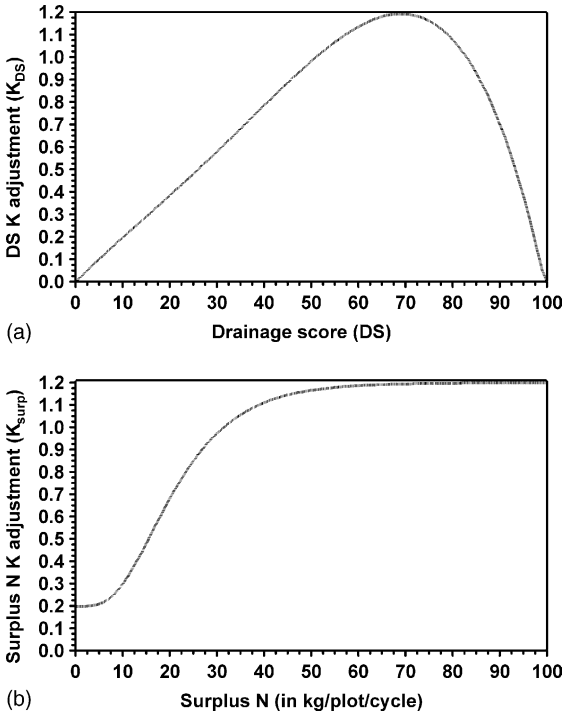

Fig. 20. Influence of soil moisture and available N on organic matter decomposition coefficients. Site drainage is assumed to impact decomposition coefficients following a skewed modal distribution (a), while surplus N follows an exponential response curve (b).

Very dry and very wet sites experience relatively slow decomposition (Fig. 20a).

An adjustment to the organic matter decomposition coefficient is also taken from the surplus available N. "Surplus" refers to N in excess of vegetation demand and ecosystem production calculated by *NORTHWDS*. When N is not in surplus, then $K_{surp} = 0.2$. Otherwise, K_{surp} assumes:

$$K_{surp} = 0.2 + [1 - \exp(-0.1 \times N_{surp})]^{5.0} \quad (34)$$

where surplus N (N_{surp}) is in kg/plot/cycle. Under this formulation (Fig. 20b), K_{surp} approaches an asymptote of ~1.2 at about 50–60 kg N_{surp}/plot/cycle to reflect saturation of the N-based decomposition potential of a site. Before it is used to adjust K, N_{surp} is decremented to reflect microbial consumption of excess N with:

$$N_{surp} = N_{Gs}^{0.85} \quad (35)$$

where N_{Gs} is the gross surplus N (in kg/plot/cycle). Under this assumption, microbes consume a large portion of the excess N on the site, although the fraction lost decreases slightly as N_{surp} increases. This helps to locally conserve site N since the N_{surp} not incorporated into living biomass (or other pools) is otherwise assumed to be lost via leaching.

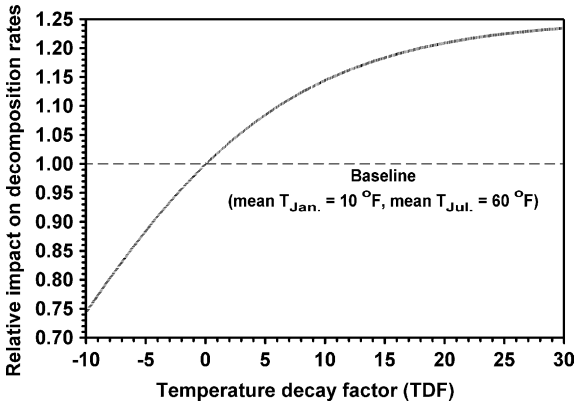

Fig. 21. Temperature-based response curve for decomposition rates. Deviations from the assumed mean January and July baseline temperatures either increases or decreases decomposition.

Heat sum also affects decomposition rates. Since decomposition depends on microbial activity and their associate biochemistry, additional warmth serves to accelerate the process (Waring and Schlesinger, 1985). To achieve this response (Fig. 21), a temperature-based decomposition factor (TDF) sets the rate of the process (using a base mean July temperature (T^*_{July}) = 60 °F (15.6 °C) and a base mean January temperature ($T^*_{Jan.}$) = 10 °F (−12.2 °C)):

$$TDF = 0.9(60 - T^*_{July}) + 0.1(10 - T^*_{Jan.}) \quad (36)$$

which is then converted into another decomposition rate modifier:

$$K_{TEMP} = \exp(0.1 \times TDF) \quad (37)$$

This modifier differs from K_{LIGHT} in that it reflects large-scale temperature regimes as opposed to localized impacts of canopy removals.

To calculate the initial decomposition coefficient (K'), each component (K_{pH}, K_{LIGHT}, K_{DS}, K_{surp}, and K_{TEMP}) enters the following equation:

$$K' = \frac{5}{(1/K_{pH}) + (1/K_{LIGHT}) + (1/K_{DS}) + (1/K_{surp}) + (1/K_{TEMP})} \quad (38)$$

Under certain conditions (e.g. elevated temperatures), the value of K' may exceed 1. The final decomposition component (K'') is determined for each organic pool using:

$$K'' = K(1 + K'w) \tag{39}$$

where K is the initial species-weighted decomposition coefficient or a universal value for forest floor or soil organic matter pools and w is a dampening weight added to reduce the effects of changes in the environmental parameters (pH, light, DI, N_{surp}, and temperature) on the given compartments. Dampening weight values for fine litter, coarse litter, and CWD equal 1 (maximal impact) because they are on the most biologically active surface. The forest floor and soil organic matter compartments received lower weights of 0.5000 and 0.0312, respectively, because of their shift from easily decomposable litter materials (carbohydrates, proteins, and pectins) to highly resistant constituents of the soil organic matter (waxes, resins, and lignins) (Pritchett and Fisher, 1987). The net effect of Eq. (39) would at least double decomposition rates for an ideal environment (i.e. favorable pH, full light, ample moisture, surplus N, warm).

Other N fluxes. Atmospheric deposition, fixation, denitrification, and leaching complement N dynamics contributed by retranslocation, litter production and decomposition, and mineralization (Fig. 18). While mineralization provides the largest of the N fluxes in *NORTHWDS* biogeochemistry, the contributions from other processes are not trivial. For example, wet and dry atmospheric N deposition contributes a small and geographically variable input (on the order of a few kg/ha per year), but accumulated over centuries this can prove significant.

Regionally, N deposition probably ranges from 6 to 10 kg/ha per year, depending on prevailing wind patterns and localized point sources. An area in central Ontario, Canada not far from the study region has been reported to receive around 7 kg/ha per year through this flux (Mitchell et al., 1992). While this is lower than that reported for areas in New England (USA) (Bormann et al., 1977; Mitchell et al., 1992; Bormann and Likens, 1994), this is not surprising as the upper Lake States are more isolated from the industrial and automotive sources of N. Currently, *NORTHWDS* assumes atmospheric deposition of N is assumed to be a constant 7 kg/ha per year.

With the exception of atmospheric deposition, all biogeochemical processes in *NORTHWDS* represent some interaction between the vegetation and the environment, either directly (e.g. retranslocation) or indirectly (e.g. fixation). Bormann et al. (1977) followed a mass-balance approach to estimate total N fixation in Hubbard Brook northern hardwoods at approximately 14 kg/ha per year. Roskoski (1980) measured N fixation for northern hardwood forests in the northeastern United States using acetylene reduction procedures and estimated its flux in woody litter and debris ranged from 1 to 3 kg/ha per year. Her results suggested that N fixation was correlated to CWD loads, which tend to peak for stands immediately after harvest (from logging residue) or in old-growth. *NORTHWDS* estimates total N fixation (N_{FIX}) as the sum fixed in CWD and that generated in the soil:

$$N_{FIX} = 6.0(1 + HSCI) + 0.8CWD_{bio} \tag{40}$$

where CWD_{bio} is in Mg per stand element and HSCI is an indirect measure of crown closure (see Section 5.2.7). *NORTHWDS* assumes that open skies (full sun) are more favorable for N fixers (both symbionts and free-living organisms). Under most conditions, Eq. (40) results in N_{FIX} values ranging from 6 to 15 kg/ha per year, depending on canopy openness.

Denitrification represents a loss of N resulting from microbial conversion of plant-available forms into gaseous N. In a study of several soils in Michigan, Groffman and Tiedje (1989a,b) correlated denitrification loss with particle size distribution and soil moisture. Their results indicate that fine-textured soils had a high rate of denitrification and while very sandy soils experienced virtually no denitrification. Groffman and Tiedje (1989b) also found a positive correlation between drainage and denitrification, as wetter soils experience more activity than drier ones (see also Groffman et al., 1992). Since there is a strong correlation between particle size distribution and soil moisture, Groffman and Tiedje (1989b) improved prediction of denitrification (N_{DENITR}, in kg/ha per year) with a model (adapted for *NORTHWDS*) that includes both the sand fraction (SAND) and drainage score:

$$N_{DENITR} = 11.81 + 0.35DS - 0.4SAND \tag{41}$$

Under Eq. (41), as DS increases so does N_{DENITR}, while the opposite occurs with increasing sand content. Because of DS's sensitivity to canopy cover, N_{DENITR} can vary both spatially (from one soil map unit to the next) and temporally (with forest maturation).

Another potential loss of N from each *NORTHWDS* stand element is leaching. Because of its chemistry, plant-available N is either quickly assimilated by the biota or lost via denitrification or leaching. Rather than developing a specific submodel to calculate leaching, a mass-balance approach determined its magnitude. Leaching (N_{LEACH}) thus accounts for the mass of N not garnished by any other component of the N cycle. In a rapidly growing forest, demand for plant-available N should be sufficient to make this resource limiting and therefore largely conserved. *NORTHWDS* allows N_{LEACH} to vary from every cycle depending on short-term changes in stocking and litter decomposition. As noted earlier, surplus N levels affects microbial acquisition of available N, so N_{LEACH} is also sensitive to the absolute quantity of N_{avail}.

5.2.3. *NORTHWDS* growth functions

5.2.3.1. NORTHWDS growth functions. While weaknesses can be found in any growth model (see Zeide, 1993 and Bragg, 2001a, for critical reviews), our goal was to develop a model that was reliable across a range of site qualities, was responsive to shifting biophysical conditions, and is computationally efficient. To achieve this, *NORTHWDS* adjusts potential increment with modifiers to predict actual cyclic growth. The design used by *NORTHWDS* to forecast growth is identical to that in *NIRM* (Section 4.2.2.1), and will not be repeated in detail in this section.

5.2.3.2. Deriving a competition index. Light is a primary driving factor affecting species growth. Thus, the greater the photosynthetic surface area, the greater the diameter increment (Guttenberg, 1953; Zeide, 1989; Deleuze et al., 1996; Raulier et al., 1996). Rather than applying complex individual-tree crown shading and position approaches (e.g. Ek and Monserud, 1974; Pacala et al., 1993, 1996; Luan et al., 1996), a more generalized design was adopted for *NORTHWDS*. Since the spatial resolution of *NORTHWDS* does not extend to individual trees, the impact of competition on diameter growth was linked to the influence of stand density on three variables (crown length, crown width, and crown density). The basal area from a nine pixel local neighborhood is proportioned (Fig. 22) to generate stand density affecting the focal stand element, including an asymmetrical weighting designed to reflect diurnal photosynthetic trends. Thus, stand elements to the south were deemed considerably more influential than those to the north (the sun is always in the southern half of the sky in this part of the northern hemisphere) while easterly pixels were slightly more influential than westerly ones (due to more favorable site moisture and temperature conditions for photosynthesis). This biased local basal area approach permits the limited simulation of light-based edge effects on tree growth.

0.01	0.02	0.01
0.03	0.60	0.04
0.04	0.20	0.05

Fig. 22. Spatial distribution of weights associated with local basal area impacts on crown size. The center (focal) pixel (the stand element of interest) receives the highest weight (0.60), while those on the north side (top of page) of the focal pixel receive the least. This design allows for the inclusion of edge effects in this portion of the northern hemisphere.

Crown width (Eq. (6)), length (Eq. (7)), and foliar density (Eq. (10)) are the primary measures used to generate crown surface area, as all are inversely related to stand density (Holdaway, 1986; Bragg, 2001b). To adjust cycle-to-cycle sensitivity of crown length, width, and foliar density to changes in stand density, local basal area was averaged from current and previous cycle values. This should mitigate a rapid change in local density, as it would be unrealistic for a crown suddenly isolated to develop open-grown characteristics in a single cycle.

5.2.4. Individualistic tree mortality in NORTHWDS

NORTHWDS estimates both self-thinning (individualistic) and disturbance-mediated mortality. Individualistic mortality is determined using a model (Eqs. (23) and (24)) developed by Buchman and co-workers (Buchman, 1983; Buchman et al., 1983; Buchman and Lentz, 1984) for the *STEMS* model (Belcher et al., 1982) from inventory data collected across the upper Lake States. This model assumes that mortality is a species-specific function of tree size and growth rate. To implement mortality in *NORTHWDS*, a stochastic algorithm (sensu Hawkes, 2000) was used to identify mortality candidates—i.e. a random number is drawn for every tree within each stand element and if the number is lower than the calculated mortality rate, the tree was killed. Otherwise, the tree remains with the living. The inclusion of growth rate is an important step in mortality modeling since growth is strongly correlated with long-term survivorship (Buchman et al., 1983; Waring, 1987; Kobe et al., 1995).

Unlike some individual-based models, *NORTHWDS* does not regulate mortality with a slow growth stress queue. However, since long-term inventories were the basis for the Buchman models, most of the cumulative effects of slow growth should be incorporated in the mortality predictions. Intuitively, this model meets expectations of mortality patterns by species and size class. Buchman et al. (1983) noted that some species suffered their highest mortality when small and slow growing (e.g. red pine or sugar maple). Other taxa (e.g. jack pine or quaking aspen) produced a bimodal response with the highest mortality for low vigor trees at either diameter extreme while those of intermediate size (but the same growth rate) survived significantly better.

Stochastic mortality events like lightning strikes are not expressly simulated unless included within the individualistic mortality model or incorporated in a larger natural disturbances such as windthrow (discussed later). Mortality also occurs in the juvenile stand table, but is based on a unique set of criteria described in the section on juvenile tree dynamics.

5.2.5. Stand density, volume, biomass, and productivity estimation

5.2.5.1. Stand density, wood, and CWD biomass. *NORTHWDS* generates biomass and volume estimates on the mature size classes (height, crown length, crown width, and crown surface area calculations were discussed earlier). Basal area (BA, in m^2/ha) is calculated using the following formula:

$$\mathrm{BA} = 0.00007854\mathrm{DBH}^2 \tag{42}$$

Another measure included in *NORTHWDS* is quadratic mean diameter (QMD), adapted from the formulation in Clutter et al. (1983):

$$\mathrm{QMD} = \sqrt{\frac{\mathrm{BA}/n}{0.00007854}} \tag{43}$$

where n is the number of trees per hectare. *NORTHWDS* also calculates stand density index (SDI) using the general form proposed by Long and Daniel (1990):

$$\mathrm{SDI} = \sum_{i=1}^{n} \left(\frac{\mathrm{DBH}_i}{10}\right)^{1.6} \tag{44}$$

where DBH_i is in inches. Eq. (44) allows for the determination of SDI for both even- and uneven-aged stands since it calculates SDI for each tree rather than relying upon the distribution-sensitive quadratic mean diameter (Long and Daniel, 1990). Live aboveground volume estimates come in two forms (cubic meters and board feet) adapted from Raile et al. (1982) who derived cubic volume (CV) from inventory data collected in Michigan with the following function:

$$\mathrm{CV} = b_{33}\mathrm{SI}^{b_{34}}[1 - \exp(b_{35}\mathrm{DBH})]^{b_{36}} \tag{45}$$

where b_{33}–b_{36} are species-specific coefficients. The inclusion of a site index (SI) factor in this equation allows better quality sites to produce taller trees with greater volumes than on poor sites. For more production-oriented volume, Raile et al. (1982) adapted Eq. (45) for board foot volume based on the International 1/4-in. rule. From Eq. (45), coarse woody debris oven dry biomass ($\mathrm{CWD_{bio}}$) is estimated by multiplying predicted CV for trees $\geq$7.5 cm DBH by the weight of an oven-dried volume of species i (OD_i, in Mg/m^3):

$$\mathrm{CWD_{bio}} = \sum_{i=1}^{24} \mathrm{CV}_i \times \mathrm{OD}_i \tag{46}$$

OD_i values were adapted from Panshin and de Zeeuw (1970), Smith (1985), and Tsoumis (1991).

5.2.5.2. Whole tree above- and belowground biomass. *NORTHWDS* uses the same formulation (Eq. (25)) as *NIRM* to calculate total aboveground live biomass for trees ≥6 cm DBH. Coefficients were adapted for understory trees (those <6 cm DBH) from Smith and Brand (1983) for Eq. (25). Leaf production (crown biomass only) for each stand element (CB_{SE}) is the product of summed individual tree vertical-projected crown areas ($VPCA_i$) and specific leaf weight (SLW_i):

$$CB_{SE} = \sum_{i=1}^{24} VPCA_i \times SLW_i \quad (47)$$

assuming

$$VPCA_i = \pi \left(\frac{CW_i}{2} \right)^2 \quad (48)$$

where crown width (CW) of the individual trees was determined using Eq. (6). Consider vertical projected crown area as the sum of the leaf area of all trees on a given stand element if the leaf area was distributed evenly along a disk. Cumulative VPCA compared to stand element size (VPCA/900) is almost always >1 because the projection of VPCA using this equation forces a three-dimensional volume of foliage onto a two-dimensional surface. Multi-storied stands may have partial layers underneath a closed canopy, also resulting in a cumulative VPCA of >1. For each species *i*, VPCA is converted to leaf area index (LAI, in m^2/m^2) with:

$$LAI = 4 \times \sqrt{\left(\sum_{i}^{24} VPCA_i \right)} \quad (49)$$

Other forests will probably have different values for VPCA, but this design works well for the upper Lake States region. Once LAI has been estimated, it is possible to convert this factor to leaf biomass by multiplying specific leaf weight (SLW, or the species-specific oven dry weight of a square meter of leaf tissue, estimated from Jurik, 1986 and Ledig and Korbobo, 1983). Leaf surface area is calculated for juvenile trees in a manner similar to mature stems and leaf and root production are estimated from this. To calculate cyclic leaf production, *NORTHWDS* uses an average of the current and previous cycle biomass to ameliorate rapid shifts in stand biomass.

Calculating belowground biomass is more difficult since very few studies of mature root systems have been done. *NORTHWDS* considers belowground biomass as the sum of the fine and large roots, each of which is calculated separately. Fine root production is derived as a function of leaf production and turnover. Given crown biomass, fine root biomass (FR_{SE}) can be inferred from both crown biomass and relative site quality (ρ, where $\rho = SI_{actual}/SI_{max}$):

$$FR_{SE} = CB_{SE} \times b_{37}((100\rho)^{0.6})(0.98^{100\rho}) \quad (50)$$

where b_{37} is a species-specific coefficient. This relationship arose from the following assumptions: fine root biomass is positively correlated with leaf biomass and responds to site quality (more fine roots on poorer sites) (see Waring and Schlesinger, 1985). When they senesce, both crown and fine root biomass are added to the fast decaying fine litter pool.

5.2.5.2. Litter production. *NORTHWDS* partitions litter into three main components: fine, coarse, and herb/shrub litter. Fine litter is comprised of dead leaves, fine roots, and reproductive structures and is primarily a function of the leaf and fine root turnover, which depends on leaf and fine root longevity. Deciduous species (all hardwoods and eastern larch) lose their foliage every year, while most conifers hold their needles from 2 to 10 years (Harlow et al., 1979). Estimates of average foliar turnover rates were made for each species (based on leaf longevities reported in Harlow et al., 1979) and recalibrated for the cyclic time step of *NORTHWDS*. Since fine root production is correlated to leaf production, fine root litter production was also assumed to be related to leaf production (fine root litter is predicted the same way as leaf litter, i.e. as a function of the annual turnover of fine roots). Reproductive litter production is estimated from the number of propagules produced by the tree so that the more favorable the conditions are for propagules, the greater the amount of reproductive litter formed.

Coarse litter yield was calculated by summing three components: branches and twigs, coarse roots, and juvenile stem wood. Branch and twig litter production (L_{BT}) is estimated from stand element basal area (BA_{SE}):

$$L_{BT} = 0.39 BA_{SE}^{0.25} \quad (51)$$

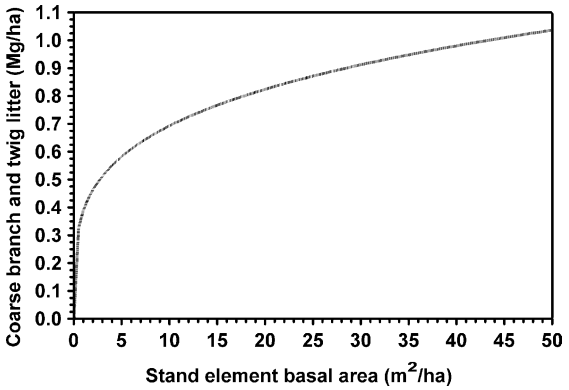

Fig. 23. Annual coarse branch and twig litter (L_{BT}) as a function of focal stand element basal area. L_{BT} biomass increases rapidly with increases in stand density, eventually exceeding 1 Mg/ha per year.

This approach is similar to Aber and Melillo (1982), who estimated L_{BT} as min(1, BA/40) (producing up to 1 Mg/ha per year of twig litter). Derived from twig production estimates gathered from a number of northern forested ecosystems (Hurd, 1971; Gosz et al., 1972; Pastor and Bockheim, 1984; Morrison, 1991), Eq. (51) allows for L_{BT} to range from 0 to >1 Mg/ha per year at higher local densities (Fig. 23). Coarse root litter production was calculated by multiplying L_{BT} with a constant (currently 1.33333) that proportions the mass of coarse root litter to branch litter. Individual dead juvenile (i.e. all stems <10 cm DBH) woody biomass was calculated by subtracting the fine biomass from the total weight of the juvenile tree.

Herb and shrub (HS) litter production is estimated by multiplying the HSCI by constants for herb and shrub LAI, HS specific leaf weight, and a HS shoot-to-root ratio (currently = 1.5). Highest HS litter production occurs in open conditions because the herb/shrub CI is maximum (HSCI = 1) at this stage.

5.2.5.3. Net primary production (NPP). Waring and Schlesinger (1985) considered NPP as:

$$\mathrm{NPP} = \Delta B + \mathrm{ADP} + C \quad (52)$$

where ΔB is the annual change in biomass, ADP is annual detrital production, and C is annual consumption of biomass by other organisms. *NORTHWDS* explicitly tracks two of these components. In the heavily forested northern Lake States, ΔB is primarily a function of the annual diameter increment and leaf and fine root mass growth of the trees (although herb and shrub biomass increment can also be important). Since *NORTHWDS* recalculates stand biomass (both above- and belowground) every cycle, changes in this component are easily monitored. ADP is also calculated every cycle since these parts are incorporated in the biogeochemistry submodels. The only part of Eq. (52) *NORTHWDS* does not account for quantitatively is the consumption of biomass by other organisms, which is usually only a small fraction of NPP in most temperate forest communities (Waring and Schlesinger, 1985).

5.2.6. Regeneration and juvenile dynamics

5.2.6.1. NORTHWDS regeneration strategy. Although reproduction is one of the most critical components of forest dynamics, multitudes of interacting factors make predicting regeneration extremely difficult (Shugart, 1984). *NORTHWDS* uses a compromise approach between simple ingrowth and complex seed-based regeneration models. Rather than monitoring fresh-from-seed germinants, *NORTHWDS* tracks "established propagules" (seedlings predicted to survive at least one 5-year cycle after germination). Each mature (i.e. reproducing) tree is assigned an EP production level based on its fraction of maximum optimal crown surface area (Eq. (21)). For *NORTHWDS*, maximum crown size is assumed to occur when an individual of the largest diameter possible for that species grows under optimal conditions. This strategy assumes that crown surface area is the best approximation of photosynthate production, which in turn translates to the amount of carbon available for reproduction. Seed production appears to be more related to crown volume than the variable most models use (DBH) (Burns and Honkala, 1990a,b), although DBH remains influential because larger individuals usually produce more crown than do smaller ones. Predicted EP output also represents an average over the 5-year *NORTHWDS* cycle, so variance in annual production due to masting is not simulated.

Many hardwoods also regenerate using various asexual strategies (e.g. suckering, sprouting), which can be their primary reproductive mechanism (e.g. *Populus* spp.). Layering as a mechanism for reproduction is not currently included, and none of the conifers native to the Lake States region exhibit other

Table 7
Species groups and coefficients for asexually reproducing species in *NORTHWDS*

Group	Species codes	c_3	c_4	c_5
1	POPBAL, POPGRA, POPTRE	−0.050	1.050	0.500
2	ACERUB, BETPAP	0.000	0.200	−0.400
3	ACESAC, TILAME, ULMAME, BETALL, PRUSER	0.000	0.027	−0.500
4	OSTVIR, PRUPEN, QUERUB	0.000	0.050	−0.001

forms of vegetative reproduction. $EP_{asexual}$ depends upon relative diameter and species:

$$EP_{asexual} = \left[c_3 + c_4 \left(\frac{DBH}{DBH_{max}}\right)^{c_5}\right] VEGMAX \quad (53)$$

where VEGMAX and DBH_{max} are the maximum species-specific $EP_{asexual}$ production and DBH, respectively, DBH is current tree DBH, and c_3, c_4, and c_5 are species group-specific coefficients. Currently, 13 hardwood species capable of asexual EP production have been pooled into one of four classes (Table 7) designed to differentiate between their developmental stage (relative DBH) and their ability to produce vegetative propagules. These species groups have been designed to allow for the differences in asexual reproduction success (Fig. 9b), as some species are more capable of asexual reproduction when young (e.g. sugar maple).

In *NORTHWDS*, each species with stored propagules contributes to a species-specific pool. The numbers of stored propagules contributed is determined similarly to established propagules, with the production capacity based on relative crown surface area. *NORTHWDS* SP pools are adjusted using the following decay model:

$$SP_{t+1} = SP_t + SP_{new} - SP_t[\exp(k_{SP} \times t)] \quad (54)$$

where the number of stored propagules in the next cycle (SP_{t+1}) is a function of the current pools size (SP_t), the input of new SPs (SP_{new}), and species-specific loss coefficients (k_{SP}) (Fig. 24). *Populus* pools decreased slowest, followed by pin cherry. Seeds stored in jack pine and black spruce cones die quickly, with most lost after 15 years (Chai and Hansen, 1952; Greene et al., 1999).

5.2.6.2. Limits to regeneration. To prevent the establishment of propagules on sites inconsistent with the environmental tolerances of some species, a series of "hard" regeneration limits based on site quality and propagule light availability were instituted. These absolute limits affect only propagules and do not influence other juvenile classes. At their extreme, hard regeneration limits prevent species establishment, but each also has an optimal range for which these limits are negligible.

Light is one of the primary limiting factors in the establishment of seedlings, but establishment may not be a monotonically increasing function of available light. Tubbs (1977) classified a number of Midwestern species as to their relative height growth performance under different light levels. Not surprisingly, the species with the lowest shade tolerance preferred the highest amount of light. However, shade tolerant species grew best under some shade rather than full sun, in part due to differences in wood accumulation between exposed and sheltered individuals. If it is assumed that relatively high growth suggests a low likeli-

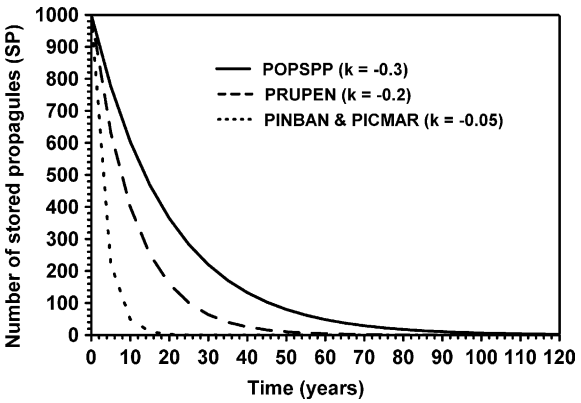

Fig. 24. Loss rates of stored propagules by species (see Table 2 for species codes). For demonstration purposes, this decline assumes that the initial 1000 stored propagules are not added to (only subtracted from).

hood of mortality (e.g. Buchman et al., 1983; Ribbens et al., 1994), then it is possible to base survivorship curves on this principle. To establish a light-based hard regeneration limit (HRL_{LIGHT}), a β-function was fit based on species shade tolerance (ST):

$$HRL_{LIGHT} = 1.21(LIGHT - \zeta)^{0.25}(\tau - LIGHT)^{0.25} \quad (55)$$

where LIGHT is forest floor insolation, $\zeta = 0.15(1 - ST/10)$, and $\tau = 1.40 + \zeta$ (Fig. 25a).

A similar effort was made to limit propagule establishment with site quality. Based on the species-based site quality responses, this limit (HRL_{SQ}) likewise incorporated a β-function:

$$HRL_{SQ} = 0.362(\rho - 0.25)^{2.1}(2.5 - \rho)^{4.0} \quad (56)$$

where ρ is the species-specific stand element site quality relative to maximum species site index ($\rho = SI_{actual}/SI_{max}$). ρ ranges from 0 to 1, with decreasing EP mortality corresponding to increasing ρ values (Fig. 25b). Note that no EPs survive ρ values $\leq$0.25 and only 50% survive ρ values of ~0.60, thus preventing nutrient or moisture demanding species from occupying unfavorable sites.

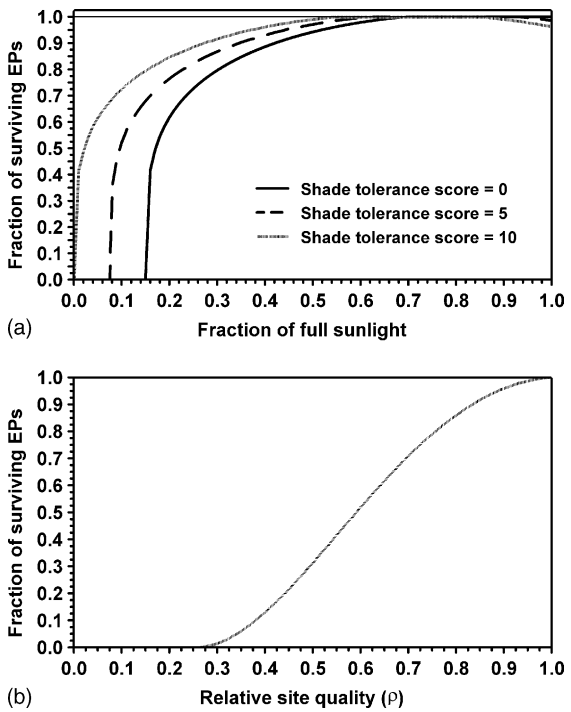

Fig. 25. Hard regeneration limits related to light availability (a) and relative site quality (b), which help restrict species establishment in unfavorable sites.

Heat sum also helps determine EP success. The hard regeneration limit associated with heat sum (HRL_{HSUM}) is calculated as:

$$HRL_{HSUM} = 1.52(GDD_i^*)^{0.3}(1 - GDD_i^*)^{0.3} \quad (57)$$

where

$$GDD_i^* = \frac{GDD_i - MINGDD_i}{MAXGDD_i - MINGDD_i} \quad (58)$$

Relative GDD favorability (GDD^*) is determined for species i following minimums (MINGDD) and maximums (MAXGDD) adapted from Botkin (1992). Fig. 26 provides typical response curves for species across the range of GDD^* values. Note that heat sum is also a component in determining site quality; however, this was deemed insufficient to fully account for temperature's role in determining establishment success, so HRL_{HSUM} was added.

To implement the hard regeneration limits, Eqs. (55)–(57) generate scalars (ranging from 0 to 1) that are multiplied against the number of pooled EPs in size class EP1 for each species and simulated stand element:

$$EP1 = NINT(EP1 \times HRL_{LIGHT} \times HRL_{SQ} \times HRL_{HSUM}) \quad (59)$$

5.2.6.3. Propagule dispersal patterns. Several approaches to predict propagule dispersal have been developed, ranging from micrometeorological models

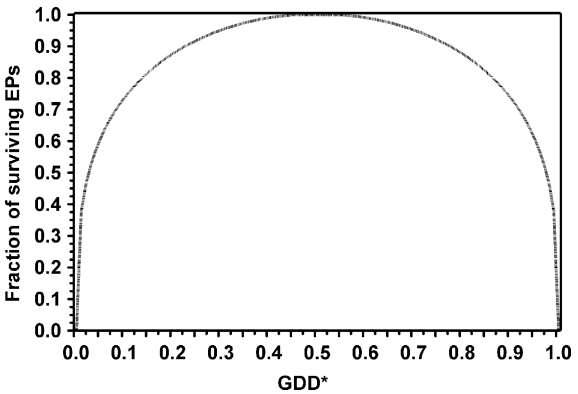

Fig. 26. Hard regeneration limit as a function of adjusted heat sum (GDD^*).

of seed dispersal (Greene and Johnson, 1989) to the registration of established seedlings from spatially isolated individuals (Johnson, 1988). Some northern forest models have invested considerable effort into determining the probability of seedling distribution at short intervals from parent trees (e.g. Ribbens et al., 1994) while others simply add propagules from a filtered list of possibilities (e.g. Botkin, 1993). Since *NORTHWDS* lacks the fine scale structure of models like *SORTIE*, a dispersal approach was developed that retains some level of dispersal pattern and intensity (Fig. 27). Most information on dispersal distance was adapted from Burns and Honkala (1990a,b). Species with large, heavy, or poorly dispersed propagules

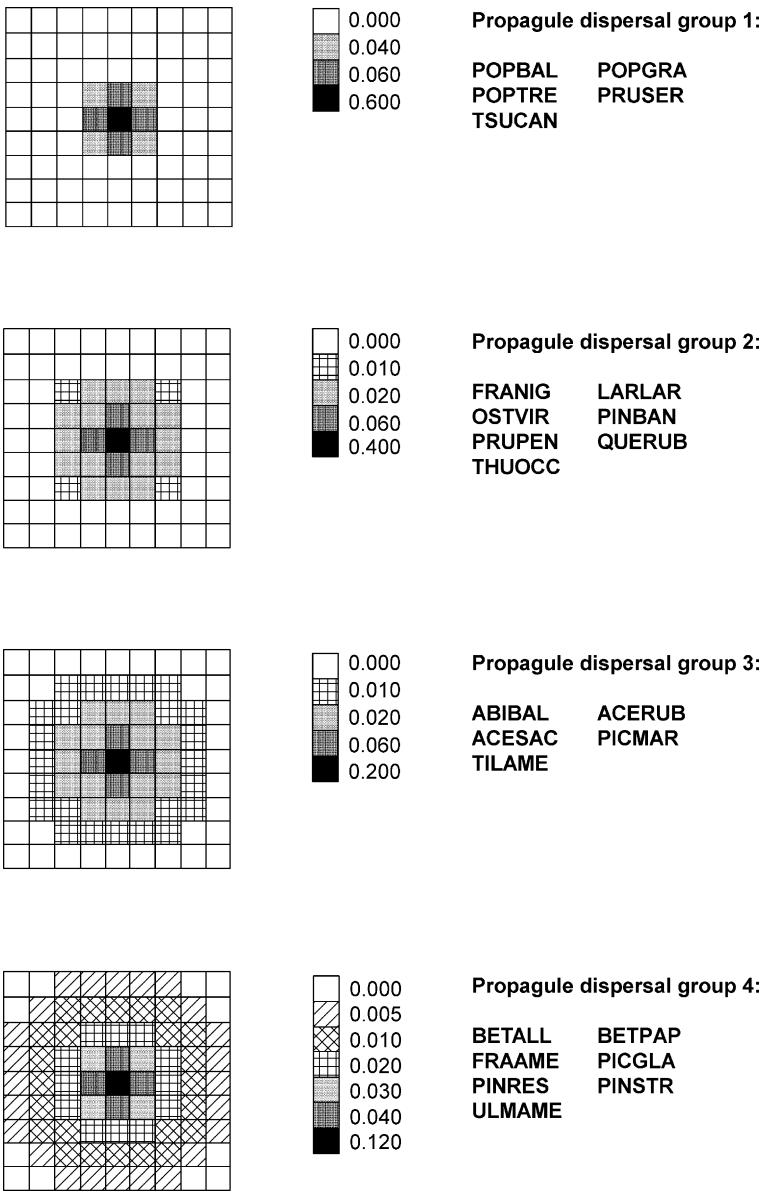

Fig. 27. Propagule dispersal patterns by species group included in *NORTHWDS* (see Table 2 for species codes). Stand element recruitment probabilities are summed over the dispersal area to account for all propagules.

are assigned to dispersal group 1, those with highly mobile propagules are placed in dispersal group 4, while intermediate species are assigned to group 2 or 3. In every case, the focal stand element (the pixel in which the dispersing trees are located) receives the largest portion of propagules, with decreasing deposition at increasing distance. This general pattern has been found in most studies of dispersal, although some variation between species and local environmental conditions are apparent (Johnson, 1988; Ribbens et al., 1994). Maximum dispersal distance is currently limited to that possible in a 9×9 pixel local neighborhood (roughly equivalent to 120 m). While it is hard to predict most recruitment trends without complicated, site-specific models, effective recruitment distances rarely exceeds 120 m from the parent tree (Burns and Honkala, 1990a,b; Ribbens et al., 1994). Long distance dispersal by animals, wind, or water is not currently simulated by *NORTHWDS*. Because reproduction in *NORTHWDS* is spatially explicit, the simulated area is wrapped upon a torus to eliminate the discrete edge of the simulation field.

5.2.6.4. Juvenile upgrowth. Juvenile upgrowth is treated separately from mature growth. The fraction of a size class moving up one or two juvenile size classes depends on the shade tolerance of the species (ST), the level of forest floor available light (LIGHT, from LAI), relative site quality (ρ), sapling size weight (D_{wt}, defined later), and white-tailed deer herbivory (BS_i, BP_i, BIV, defined later):

$$\mathrm{JUV_{UP}} = \frac{4}{(1/\mathrm{LIGHT}) + (1/\rho) + [1/(1 - \sqrt[3]{\mathrm{BS}_i \times \mathrm{BP}_i \times \mathrm{BIV}})] + (1/D_{wt})} \times \left(\frac{20 - \mathrm{ST}}{20}\right) \quad (60)$$

When individuals are juvenile size class 4 or smaller, the fraction of stems moving up two sizes (JUV_2) equals $JUV_{UP}^2/2$, and the fraction advancing only one size class (JUV_1) equals $JUV_{UP}/2$ (it is also possible for juveniles to stay in the same size class, i.e. $JUV_0 = 1 - (JUV_{UP}^2/2) - (JUV_{UP}/2)$). If the individuals are in juvenile size class EP4, then they can only move up one size class (into the smallest mature size class). Upgrowth (Fig. 28) rises with increasing light availability, more favorable site quality, lower deer browsing, and is differentially sensitive to juvenile size (the bigger the juvenile, the more rapidly it will grow) and shade tolerance (shade intolerant species grow faster than shade tolerants).

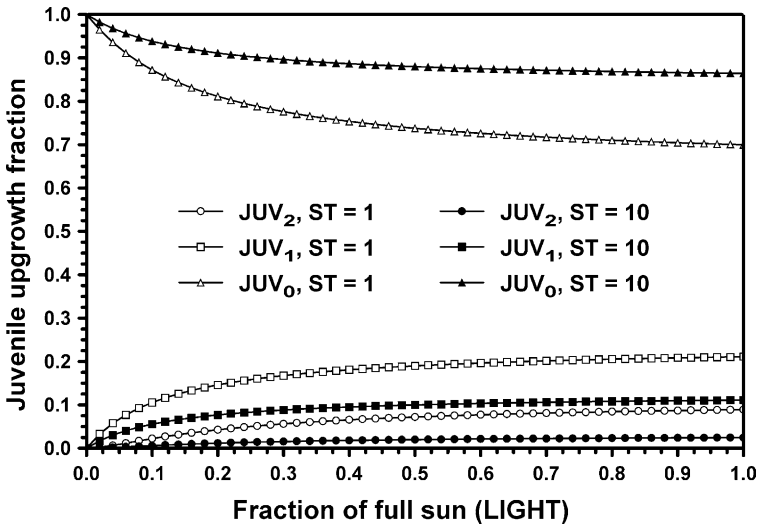

Fig. 28. Juvenile upgrowth for the smallest EP class (EP1) by light availability (assuming moderate site quality and deer browsing) for a very shade intolerant species (ST = 1) and a very shade tolerant species (ST = 10).

5.2.6.5. Juvenile mortality. Many factors contribute to juvenile mortality. The first level of mortality is a function of the hard regeneration limits and only affects the smallest EP class (stored propagule losses were discussed earlier). The hard regeneration limits are multiplied by the number of individuals in EP1 to eliminate a fraction of this size class. Primary juvenile mortality is determined by three factors: light availability (JM_{LIGHT}), herb and shrub competition (JM_{HS}), and deer browsing (JM_{DEER}). To arrive at juvenile mortality (JM), the following function is calculated:

$$JM = 1 - \frac{3}{(1/JM_{LIGHT}) + (1/JM_{HS}) + (1/JM_{DEER})} \quad (61)$$

Juvenile survivorship related to light availability (JM_{LIGHT}) was adapted from Pacala et al. (1995) who fit the following mortality curve to seedling data:

$$JM_{LIGHT} = b_{38} + \frac{b_{39}}{LIGHT^{b_{40}}} \quad (62)$$

where b_{38}–b_{40} are species-specific coefficients. As a general rule, shade tolerant species have considerably higher low light survivorship than shade intolerant species (Pacala et al., 1995). Herb and shrub-based juvenile mortality is also linked to shade tolerance and light availability (see section on HSCI). Mortality resulting from herb and shrub competition (JM_{HS}) is determined from:

$$JM_{HS} = 1 - \left[\frac{ST}{10} \times \ln\left(\frac{100 \times HSCI}{8}\right) D_{wt}\right] \quad (63)$$

where HSCI is the herb shrub competition index (defined in the next section) and juvenile size class survival coefficients (D_{wt}) are as follows: EP1 = 0.1, EP2 = 0.2, EP3 = 0.4, EP4 = 0.6, and EP5 = 0.8. These coefficients are used as a multiplier to other survivorship functions, and have the effect of increasing survival or upgrowth with larger juvenile size classes. Shade intolerant species are assumed to be less affected by competition than shade tolerant trees within the herb and shrub layer. This pattern of response was hypothesized because the general nature of shade intolerant species (widely dispersing propagules) presumably puts them in competition with herbs, shrubs, and graminoids more frequently, and thus this trend allows for disturbed or open sites (e.g. old fields) to be more aggressively colonized by shade intolerant species.

Juvenile survivorship fraction is also related to white-tailed deer browsing (JM_{DEER}):

$$JM_{DEER} = 1 - BIV(\sqrt{BP_i \times BS_i}) D_{wt} \quad (64)$$

where the species-specific browsing sensitivity (BS_i) is weighted equally with the estimated white-tailed deer forage preferences (BP_i) and the browsing intensity value (defined later) for that stand element (BIV). Both BS_i and BP_i are relative scores where some species are more responsive than others (ranked on a scale from 0 (not sensitive or preferred) to 1 (extremely sensitive or preferred)). Rankings were adapted for *NORTHWDS* from a variety of sources (e.g. Beals et al., 1960; Stiteler and Shaw, 1966; Burns and Honkala, 1990a,b; Canham et al., 1994) and are admittedly subjective. However, their assumed sensitivity is consistent with their susceptibility to deer browsing. This general approach to differential deer browsing impacts has also been featured in some gap models (e.g. Seagle and Liang, 2001).

Timber harvesting is another major source of juvenile mortality in the current version of *NORTHWDS*. The vulnerability of juvenile size classes to mortality during harvesting was deemed important enough to include a survivorship probability in the parameter files when harvests are implemented. These are fixed values that predict the fraction of juveniles of each size class capable of surviving the harvests by ownership and cover type code.

5.2.7. Interactions amongst trees, herbs, and shrubs

Often overlooked, graminoids, herbs, shrubs, and other non-tree vegetation can have substantial impacts on the dynamics of forested ecosystems. The herb and shrub (HS) layer affects stand development in ways other than just increasing species and structural richness, including influencing the success of overstory trees and site biogeochemistry. The impact of the HS layer is interlaced throughout *NORTHWDS*, both as a process and as an indicator of certain environmental conditions (e.g. the degree of insolation).

5.2.7.1. Impacts of the HS layer on tree regeneration. One of the most important roles HS vegetation has on forest development is its influence on the regeneration

of trees. As with all vascular plants, the HS layer occupies a portion of the physical environment and thus competes with the trees for limited resources. While the massive size of mature trees relative to the HS layer provides for strongly asymmetrical competition, this is not true for seedlings and saplings. At this level, the HS layer proves a sometimes overwhelmingly effective competitor and can have a substantial role in determining seedling success and other forest dynamics (e.g. Buttrick, 1921; Hough, 1937; Tappeiner and Alm, 1975; Zavitkovski, 1976; Maguire and Forman, 1983). Extensive understory vegetation has even been shown to reduce growth in relatively large trees (Wilde et al., 1968), although this type of interaction is not currently incorporated in *NORTHWDS*.

HS cover is positively correlated with the light environment of the forest floor. Numerous studies indicate the rapid expansion of the HS layer following the opening of the canopy (Anderson et al., 1969; Siccama and Bormann, 1970; Zavitkovski, 1976; Wallace and Freedman, 1986; Balogh and Grigal, 1988; Goldblum, 1997; Lieffers et al., 1999). Many models have addressed the release of resources in a forest to favor both the growth of existing trees and the accelerated establishment of new propagules, but few have recognized its impact on the HS layer. *NORTHWDS* assumes that HS competition (stated in terms of a herb/shrub competition index (HSCI) ranging from 0 (no competition) to 1 (maximal competition)) is a function of forest floor light availability, with more HS cover (and hence more interaction with juvenile trees) as the light level (LIGHT) increases:

$$\mathrm{HSCI} = 0.9997^{[(100\times\mathrm{LIGHT})-100]^2} \quad (65)$$

This model of the HS layer response to light availability (Fig. 29a) was suggested by several studies of non-tree species (Anderson et al., 1969; Wallace and Freedman, 1986; Balogh and Grigal, 1988). Juvenile mortality functions (Fig. 29b) related to HS cover competition can be found in the section on juvenile tree dynamics. The HS layer is not assumed to have any impact on mature trees, although shading by mature stems decreases HS cover.

5.2.7.2. The HS layer and site biogeochemistry. Other work has indicated the importance of the understory on site biogeochemistry, especially for early successional stands (e.g. Tappeiner and Alm, 1975; Zavitkovski, 1976). The HS layer can contribute a significant volume of litter (and extract substantial quantities of nutrients) under the right conditions, contributed solely to the fine litter pool.

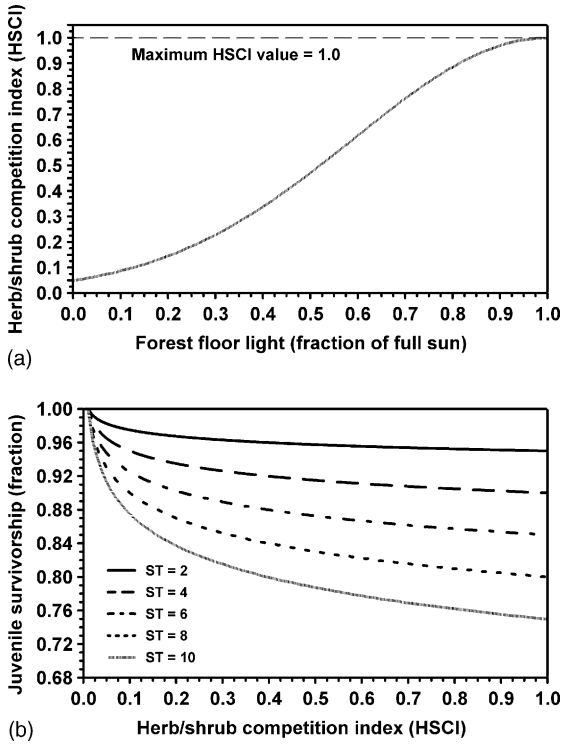

Fig. 29. Herb and shrub competition influences on stand dynamics. Herb and shrub cover responds positively to the amount of forest-floor available light (a), reaching a maximum under full sun. Juvenile survivorship by shade tolerance (b) declines with increasing HSCI (more so for shade tolerant species).

A sparse HS layer under a continuous closed forest canopy probably has little effect on site biogeochemistry (with the possible exception of N-fixers). However, this stratum becomes increasingly important as the canopy opens. Under clearcut conditions, the HS layer becomes a major factor in N cycling until the developing stand overtops and reclaims the site (Crow et al., 1991). Given an open canopy, *NORTHWDS* predicts a HS layer LAI of $4\,m^2/m^2$, with an assumed specific leaf weight of $0.075\,kg/m^2$. Henry (1973) sampled over 80 species of grasses, forbs, and shrubs for their foliar N content. An average value of approximately 1.75% was derived from

Henry's work and adopted as the *NORTHWDS* HS N content.

5.2.8. Deer browsing and northern forest development

White-tailed deer are influential browsers of juvenile trees throughout their range (Arbogast and Heinselman, 1950; Bramble and Goddard, 1953; Graham, 1954a; Stoeckeler et al., 1957; Curtis and Rushmore, 1958; Beals et al., 1960; Stiteler and Shaw, 1966; Tierson et al., 1966; Cooperrider and Behrend, 1980; Tilghman, 1989; Waller and Alverson, 1997; Frelich, 2002; Horsley et al., 2003). Deer prefer herbaceous forage during the late spring, summer, and early fall, but they switch to woody browse during the late fall to early spring period (Bramble and Goddard, 1953). The foliage, branch tips, and growing leaders of juvenile trees are the most accessible to deer, although the high lignin content and low nutrient levels of this source require elevated consumption of this browse. Since deer rarely kill individual trees through their consumption (*NORTHWDS* juvenile tree mortality from deer browsing is discussed in Section 5.2.6.5), browsing would not be much of a problem if the tree species consumed were all equally palatable or tolerant of herbivory. However, some species respond poorly to the loss of their growing tips and foliage, resulting in different ecological consequences through juvenile mortality, growth reductions, and alteration of interspecific dynamics. Though deer browsing has been recognized as a critical determining factor in many forested ecosystems, few simulators have incorporated it as an integral component. Most (e.g. Dyer and Shugart, 1992; Mladenoff and Stearns, 1993; Seagle and Liang, 2001) couple deer browsing as an external control on regeneration growth and survivorship. *NORTHWDS* integrates both regeneration effects and deer population dynamics (as a function of stand type favorability).

5.2.8.1. Implementing deer browsing in NORTHWDS. Both growth reductions and browsing-induced mortality have been included in *NORTHWDS* juvenile tree subroutines. These impacts are assumed to only influence juveniles since larger trees are beyond the reach of the deer. Growth reductions are achieved by limiting the ability of juvenile size classes to grow from one class to another (see Stoeckeler et al., 1957; Frelich, 2002). Overall habitat favorability is inferred from site cover type. As forests mature or are perturbed away from their current condition, their relative favorability changes and may influence deer population dynamics. This, in turn, helps to shape the biotic environment juvenile trees experience, which is significant because of the variable response of the tree species to browsing. In effect, deer help control the structure and composition of the forest environment they live in, which eventually influences its ability to sustain deer populations.

Cover type code classification. The browsing intensity value (BIV) is not strictly a function of individual species but rather the general suitability of the vegetation on a given stand element for attracting white-tailed deer. To understand the derivation of BIV, it is necessary to first describe cover type classification in *NORTHWDS*. *NORTHWDS* designates a cover type code (CTC) for every stand element based on an importance value calculated for major species groups. This importance value (IV_i):

$$IV_i = \frac{1}{2}(CV_R + BA_R) \quad (66)$$

where CV_R and BA_R are relative bole volume and basal area of species *i*, was used to segregate stand elements into one of 14 possible types (Table 8). This pathway is ordered to assign stands into a logical organization that emphasizes regional tree composition patterns. There also is a degree of "fuzziness" in this classification since apart from majority dominance of the species (or suite of species) delimiting any given cover type, exact threshold values are not required. For example, a stand classified as "moderately tolerant northern hardwoods" (CTC 3) could be composed purely of red maple, or a mixture of red maple, yellow birch, and white ash, or American elm, white ash, and yellow birch, etc. Presence of nontypal species does not preclude the assignment of a given cover type. In the extreme case when the stand element composition is sufficiently eclectic that no single group suggests a classification, a "mixed" stand option is provided (CTC 11). This permutation is common in the northern Lake States as diverse assemblages can result from natural disturbances, topoedaphic variability, population dynamics, and/or forestry practices.

The final categories (CTC 12–14) were included because there are instances when the lack of tree cover precludes cover type determination. After failing to

Table 8
Cover type code (CTC) classification key

1. If $TSUCAN_{IV} \geq 0.5$ then CTC = 1
1. Else ...
  2. If $ACESAC_{IV} + TILAME_{IV} + OSTVIR_{IV} \geq 0.5$ then CTC = 2
  2. Else ...
    3. If $BETALL_{IV} + FRAAME_{IV} + ULMAME_{IV} + ACERUB_{IV} \geq 0.5$ then CTC = 3
    3. Else ...
      4. If $POPGRA_{IV} + POPTRE_{IV} + BETPAP_{IV} + PRUSER_{IV} + PRUPEN_{IV} \geq 0.5$ then CTC = 4
      4. Else ...
        5. If $QUERUB_{IV} \geq 0.5$ then CTC = 5
        5. Else ...
          6. If $FRANIG_{IV} + POPBAL_{IV} \geq 0.5$ then CTC = 6
          6. Else ...
            7. If $ABIBAL_{IV} + PICGLA_{IV} \geq 0.5$ then CTC = 7
            7. Else ...
              8. If $THUOCC_{IV} + PICMAR_{IV} + LARLAR_{IV} \geq 0.5$ then CTC = 8
              8. Else ...
                9. If $PINRES_{IV} + PINSTR_{IV} \geq 0.5$ then CTC = 9
                9. Else ...
                  10. If $PINBAN_{IV} \geq 0.5$ then CTC = 10
                  10. Else ...
                    11. If sum of all species > 0 then CTC = 11
                    11. Else ...
                      12. If drainage index (DI) ≤ 80 then CTC = 12
                      12. Else ...
                        13. If $80 < DI < 100$ then CTC = 13
                        13. Else ...
                          14. If DI = 100 then CTC = 14

Cumulative relative importance value thresholds are used to delineate cover types, and hence any given stand element can change CTC from one cycle to the next, depending on the dominance of the species.

classify under the first eight categories, the first break comes at site DI values. If the site has a DI < 80, the stand element is assumed to be either a field or a clearcut. Sites with $80 \leq DI < 100$ are assumed to be open wetlands, although some clearcut areas or fields may be this moist and could be inaccurately classified as an open wetland. However, such a misclassification should prove temporary as CTCs are continually recalculated, and sites favorable for forest should eventually reforest and be given a forest cover type. If a site has a DI = 100, it is assigned an "open water" class. CTCs are also used by other portions of *NORTHWDS*, e.g. timber harvest assignment.

Translating CTC into deer population densities. Once a CTC has been assigned to a stand element, a white-tailed deer density is inferred from this code. These values have been adapted (Table 9) from systems developed by McCaffery (1996) and Doepker et al. (1996) that assign deer densities based on the habitat favorability of each CTC. It should be noted that the deer density values are expert systems based on the experience of the original researchers, and some values had to be inferred for several cover types not specified in their work. However, their systems fit well with the observations of others (e.g. Christensen, 1962). As can be see in Table 9, seral stands (e.g. successional hardwoods, open (potential forest)) were assigned the highest densities, followed by the other forest cover types, and finally by non-forested wetlands. From these density levels, the following equation reflects a BIV for each stand element (BIV_{SE}):

$$BIV_{SE} = 1 - \exp[-131.4\delta(1 + HSCI)] \quad (67)$$

where δ is the number of deer per stand element and HSCI is the herb and shrub competition index (see section on HCSI). The HSCI factor in Eq. (67) was included to allow for better simulation of successional stands of each cover type (Fig. 30), which are more favorable deer habitat than mature, closed

Table 9
CTC possibilities in *NORTHWDS* (deer densities by cover type adapted from McCaffery, 1996 and Doepker et al., 1996)

CTC	Cover type description	Dominant tree species codes	Deer/km^2	Deer per stand element
1	Eastern hemlock	TSUCAN	6.9	0.00621
2	Very tolerant northern hardwoods	ACESAC, TILAME, OSTVIR	3.9	0.00351
3	Moderately tolerant northern hardwoods	BETALL, FRAAME, ULMAME, ACERUB	5.0	0.00450
4	Intolerant hardwoods	POPGRA, POPTRE, BETPAP, PRUSER, PRUPEN	12.3	0.01107
5	Oak	QUERUB	12.3	0.01107
6	Swamp hardwoods	FRANIG, POPBAL	3.9	0.00351
7	Spruce/fir	ABIBAL, PICGLA	6.9	0.00621
8	Swamp conifers	THUOCC, PICMAR, LARLAR	3.9	0.00351
9	Mixed pines	PINRES, PINSTR	6.9	0.00621
10	Jack pine	PINBAN	5.0	0.00450
11	Mixed species	All possible	7.7	0.00693
12	Open (potential forest)	Few to none	12.3	0.01107
13	Open (wetland)	Few to none	1.9	0.00171
14	Open (water)	None	0.0	0.00000

canopy forests of that same CTC (Gysel, 1966; Doepker et al., 1996; McCaffery, 1996), largely because of better herb and shrub forage in seral stands.

BIV_{SE} are further modified to reflect multiscale vegetation patterns that determine the influence of the surrounding stand elements on population levels. While deer densities are initially estimated at the stand element level, habitat favorability of the surrounding countryside contributes to the browsing experienced (BIV) at any particular stand element:

$$BIV = (0.3BIV_{SE} + 0.4BIV_{25} + 0.3BIV_{361})\omega \quad (68)$$

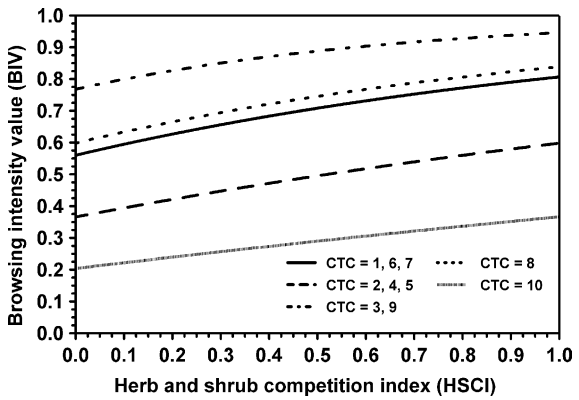

Fig. 30. White-tailed deer browsing intensity value as a function of HSCI. Since HSCI depends on stand openness, forests recovering from disturbance will have higher coverage of herbs, shrubs, and graminoids, which in turn improves the feeding conditions for deer and thus increases their density. See Tables 8 and 9 for cover type code (CTC) descriptions and their relationship to deer density.

where $\omega = 0$ if CTC $= 14$, and 1 otherwise (this prevents open water from being assigned a browsing level). Note that under this formulation, local browse pressure (BIV_{SE}) receives a weight of 0.3, while a larger 5×5 local neighborhood average BIV (BIV_{25}) is weighted 0.4 and the 19×19 stand average BIV (BIV_{361}) is assigned a weight of 0.3. Eq. (68) modifies the browsing level for each stand element by the composition of the forest at different scales so that an isolated stand of favorable habitat in a matrix of unfavorable habitat will be browsed at a lower level than that anticipated for the same stand in favorable deer habitat. Conversely, a patch of unfavorable habitat in a matrix of good habitat will be browsed more heavily than expected.

5.2.9. *Integrating catastrophic wind disturbance*

Windthrow has long been recognized as a significant factor in the development of the forests of North America (e.g. Curtis, 1943; Stoeckeler and Arbogast, 1955; Lorimer, 1977). Catastrophic wind events are the primary natural disturbance agent across much of the northern Lake States (Canham and Loucks, 1984; Frelich and Lorimer, 1991; Frelich, 2002), but more frequent, small-scale wind disturbances that partially remove the canopy have a more pervasive impact on a landscape. Wind disturbance alters northern forested landscapes by removing vulnerable individuals, especially if that particular area has not been disturbed recently. Areas not affected accumulate trees with an elevated risk for windthrow (e.g. diseased or decayed

stems) that can be widely impacted when a storm with even moderate winds strikes the region.

5.2.9.1. Separating windthrow in NORTHWDS. *NORTHWDS* separates wind damage into two mortality levels: chronic and acute. Chronic mortality events are experienced by each stand element during every 5-year cycle, resulting in the death of individual vulnerable trees. Acute events can be best described as relatively rare but severe events that cause spatially extensive mortality. Both mortality types are possible during any cycle on any stand element, although the odds of acute mortality events are significantly lower.

Determining tree vulnerability to chronic windthrow. *NORTHWDS* uses both site and vegetative factors to influence the susceptibility of individual trees to windthrow. To predict the likelihood of failure under chronic wind events, a simple wind hazard rating (WHR) system was developed with the information available to *NORTHWDS*. The integrated WHR value is calculated for each size class in the stand table, and represents the combination of tree, local stand conditions, and topoedaphic factors:

$$\mathrm{WHR} = \mathrm{WH_{TP}} + \mathrm{WH_{DS}} + \mathrm{WH_{RD}} + \mathrm{WH_{SD}} + \mathrm{WH_{DBH}} + \mathrm{WH_{SPP}} \quad (69)$$

where $\mathrm{WH_{TP}}$ is a calculated topographic position variable that includes average relative stand height, $\mathrm{WH_{DS}}$ is a drainage score factor, $\mathrm{WH_{RD}}$ is related to the depth to any root-restricting layer, $\mathrm{WH_{SD}}$ is associated with stand density (in terms of basal area), $\mathrm{WH_{DBH}}$ is tree diameter factor, and $\mathrm{WH_{SPP}}$ is a species-specific risk value. With the exception of $\mathrm{WH_{SPP}}$, all factors received equal weighting (the first five receive a value up to 0.12 on a scale from 0 to 1; $\mathrm{WH_{SPP}}$ has a maximum value of 0.10). Chronic windthrow occurs when a randomly drawn number $<\mathrm{WHR} \times \prod r_i$, where $i =$ 1–5 and r is a unique real number (1 per year).

Topographic position. The topographic position variable is calculated for a local neighborhood of stand elements and represents the relative exposure of the focal stand element to high winds. Relative exposure is determined by comparing the combined (ground elevation + tree height) elevation of the focal pixel to its neighborhood: a tally is kept of the neighbors that are lower than the focal element. In equation form, this trend is modeled as:

$$\mathrm{WH_{TP}} = 0.12(\text{fraction of lower pixels}) \quad (70)$$

A neighbor is classified as lower if the ground elevation plus average tree height of the focal stand element is at least 3 m higher than the sum of elevation + mean tree height of the neighboring pixel. A focal pixel the same height (or lower) as all of its neighbors has no increased risk of windthrow, while one that rises above most or all of its neighbors experiences greater wind damage. Using a combination of ground elevation and tree height to determine exposure provides both a better representation of the physical surface and allows for added damage along abrupt forest edges (especially those stands isolated by harvest).

Drainage index. Drainage index has been identified as a significant factor in windthrow vulnerability separate from root restriction (see next section). Water acts as a lubricant and reduces the friction between the soil and roots, allowing for less resistance to the torque applied by the aboveground biomass when acted upon by wind (Schaetzl et al., 1989; Mitchell, 1995). To address this behavior, a DS-based modifier was included:

$$\mathrm{WH_{DS}} = 0.12\,\mathrm{DS} \quad (71)$$

Very dry soils (low DS values) experience less loss to windthrow, while wet areas have substantially greater damage (e.g. Behre, 1921; Stoeckeler and Arbogast, 1955) (keeping in mind that increased windthrow in wetlands also arises from shallow rooting habits).

Root restriction. Vertical root restriction contributes to windthrow as it limits an individual's ability to anchor itself to the site. A number of environmental factors can inhibit root penetration, including high water tables, fragipans, bedrock, permafrost, etc., and are usually noticeable from the pit-and-mound topography that results. The inconsistency in depth to an obstructing layer and the plasticity in tree rooting response makes a categorical approach to weight the impacts of root restriction most appropriate. To achieve this, greatest impact from root restriction occurs when the obstruction is from 0 to 30 cm ($\mathrm{WH_{RD}} = 0.12$), followed by 30–60 cm ($\mathrm{WH_{RD}} = 0.06$), then 60–100 cm ($\mathrm{WH_{RD}} = 0.03$). Root restrictions below 100 cm are assumed to be insignificant.

Stand density. Stand density has been shown to affect windthrow (Eyre and Longwood, 1951; Stoeckeler and Arbogast, 1955; Valinger and Fridman, 1997) although not in entirely consistent patterns. Trees rapidly transitioning from dense to more open stand conditions (e.g. after a thinning) often experience accelerated windthrow while those growing in isolation develop significant windfirmness in response to the constant buffeting. *NORTHWDS* assumes that trees under less dense conditions are more vulnerable to windthrow (WH_{SD}):

$$WH_{SD} = \left(\frac{60 - LBA}{60}\right)^3 \times 0.12 \quad (72)$$

where LBA is local basal area of the focal stand element (in m^2/ha). For instances when LBA exceeds 60 m^2/ha, local stand density is considered to contribute little to windthrow risk.

Individual size and species differences. While average stand height has already been factored into WH_{TP}, an additional factor is based on individual size (in this case, DBH) since a number of researchers have detected differences in windthrow risk by size (e.g. Duerr and Stoddard, 1938; Henry and Swan, 1974; Brewer and Merritt, 1977; Foster and Boose, 1992; Valinger and Fridman, 1997). Under the assumptions of *NORTHWDS*, windthrow vulnerability responds modally to increasing tree size:

$$WH_{DBH} = 17.8\left[\left(\frac{DBH}{DBH_{max}}\right)^{5.0} \times \left(1.5 - \frac{DBH}{DBH_{max}}\right)^{5.0}\right] \times 0.12 \quad (73)$$

where DBH_{max} has been pre-defined for each species. This response curve produces the highest risk of windthrow when $DBH/DBH_{max} = 0.75$ (Fig. 31). While larger trees have thicker stems more resistant to bending, they experience other forces that tend to lessen their resistance to wind. First, they usually support larger crowns, which intercept more wind and add to the forces acting on the bole and roots (Schaetzl et al., 1989; Everham and Brokaw, 1996). Second, the stiffness inherent in the larger bole provides less flexibility under high winds than a thin stem does. Finally, a tree with a large bole is probably older than one with a small stem, increasing the likelihood of heartrot, root damage, or other factors that contribute to individual vulnerability (Stephens, 1956; Everham and Brokaw, 1996). Nevertheless, the *NORTHWDS* response curve is modal with the very largest trees experience a somewhat lower windthrow risk (Fig. 31). Trees reaching this size are assumed to have developed ample root systems that allow them to survive severe winds. It is also common for very large and old trees to have reduced crowns, lessening their vulnerability to high winds.

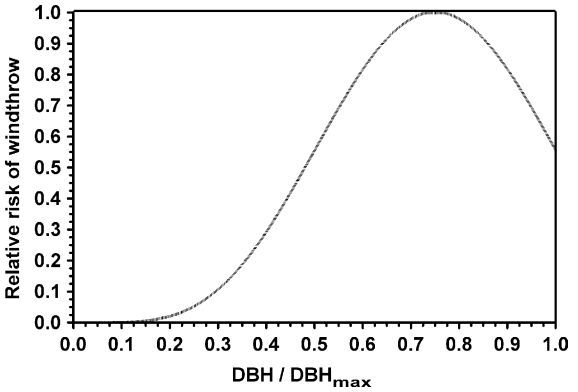

Fig. 31. Chronic windthrow risk as a function of relative tree size. The modal response curve produces the highest windthrow when $DBH/DBH_{max} = 0.75$.

The other tree-based factor influencing windthrow is species-specific differences in wind resistance. These differences may arise from variation in decay pattern, stem resiliency, rooting habit, or crown architecture (or some combination thereof), but the net result is that some species experience windthrow less frequently than others. Sugar maple, for example, appears more wind resistant than some associates (e.g. yellow birch, balsam fir, eastern hemlock, white spruce) in the northern forest landscape (Behre, 1921; Eyre and Longwood, 1951; Stoeckeler and Arbogast, 1955; Brewer and Merritt, 1977; Webb, 1989). Since little more than anecdotal reports of relative wind resistance are available, one of three species-based wind resistance scores ($WH_{SPP} = 0.01$, 0.05, or 0.10, with the higher values indicating greater vulnerability) are assigned to each species (Table 10).

Modeling acute windthrow events. Acute windthrow represents the most severe (yet least predictable) mode

Table 10
Species-specific wind resistance scores (WH_{SPP}) used by *NORTHWDS*

WH_{SPP}	Species code
0.01	PINRES, ACESAC, BETALL, FRAAME, OSTVIR, TILAME, ULMAME
0.05	LARLAR, PINSTR, THUOCC, TSUCAN, ACERUB, BETPAP, FRANIG, POPBAL, POPGRA, PRUPEN, PRUSER, QUERUB
0.10	ABIBAL, PICGLA, PICMAR, PINBAN, POPTRE

of windthrow and are applied as discrete mortality incidents with statistical frequencies, spatial patterns, and intensities. These properties are controlled by a series of variables within *NORTHWDS* to achieve the desired distributions and can be adjusted as necessary. First, the number of catastrophic wind events across the simulated forest during the current cycle is determined, with few events per cycle being more common than numerous ones. Each wind event is then assigned a number of stand elements to be affected. Although most events tend to be small, they could conceivably extend over the entire simulated area. Finally, a disturbance intensity value is derived for each event (ranging from 0.1 to 1.0), translating to the fraction of stems killed by the disturbance (0.1 = 10% mortality, 1.0 = 100% mortality). This intensity is applied more or less equally (within ±10% of the its value) across the affected region, although there is flexibility in how trees respond to acute disturbance as both WH_{DBH} and WH_{SPP} help determine which are lost.

5.2.9.2. Windthrow's contribution to regeneration. Many of the hardwood species in the Lake States region have the capacity to resprout from stumps or roots after the main stem has been killed. This response is modeled by *NORTHWDS* for trees removed by timber harvesting and those lost to windthrow since both disturbances involve the death of the aboveground stem. However, *NORTHWDS* does not distinguish between trees that have been broken by wind or cut from those that have been uprooted, as all are assumed to be equally capable of asexual reproduction through sprouting (see section on vegetative propagation).

5.2.9.3. Catastrophic disturbances other than windthrow. Technically, the acute windthrow component is also part of the landscape model, but was included in this paper because of its relationship to the chronic windthrow submodel and the desire to use windthrow as a means to demonstrate the potential of *NORTHWDS*. Other large-scale natural disturbances (e.g. fire, insect outbreaks, drought) and timber harvesting are integrated to the *NLM* level of the hierarchy.

5.3. Operational example

To highlight *NORTHWDS*' ability to conduct long-term ecosystem simulation, an example using different windthrow regimes is considered. In effect, this demonstration is a sensitivity analysis of the impact of wind disturbance on model outcomes, given a deterministic set of initial conditions and a stochastic implementation of the perturbations. Values of the parameters used for these simulations can be found in Table 11.

5.3.1. Study area description

NORTHWDS was parameterized for the forests of the northern Lake States. Thus, the study area was assembled from an FIA plot in Forest County, Wisconsin deemed typical of hardwood-dominated forests in this region. Rather than sampling a large and variable area to provide the input information, a 36 ha stand was "synthesized" from a characteristic cross-section of vegetation and site conditions by aggregating 400 stand elements containing exactly the same initial site and vegetative conditions. Though greatly simplified compared to natural forest landscapes, this ensured consistency in starting conditions across the study area, allowing for greater appreciation of the influence of different windthrow treatments.

5.3.1.1. Vegetation. An early seral structure was designed into this synthetic stand. The overstory vegetation (Fig. 32a) was dominated by quaking and bigtooth aspen, with lesser amounts of yellow birch, red maple, sugar maple, eastern white pine, white spruce, and balsam fir. Stand density (24.1 m^2/ha of basal area) and stocking (1011 trees per hectare) were consistent with a maturing northern hardwood stand. With the exception of a few scattered large eastern white pines, most trees were from 10 to 25 cm in DBH and approximately 30 years old (although some minor age variation would be present).

Table 11
NORTHWDS coefficients for three of the species highlighted in this paper

Parameter	Quaking aspen	Yellow birch	Sugar maple
FIA species code	746	371	318
Maximum DBH (cm)	98.6	203.7	188.4
Shade tolerance score (0–10)	0.7	6.3	9.7
b_1 (PRI coefficient)	4.847405	3.11963	3.521235
b_2 (PRI coefficient)	−0.5068604	−0.784164	−0.79872
b_3 (PRI coefficient)	0.965699	0.981528	0.992414
b_4 (crown width coefficient)	0.917086	1.297467	2.119784
b_5 (crown width coefficient)	0.42657	0.697197	0.346366
b_6 (crown width coefficient)	0.772969	0.670675	0.813395
b_7 (crown width coefficient)	−0.034042	−0.023695	−0.017616
b_8 (height coefficient)	6.4301	7.1852	5.3416
b_9 (height coefficient)	0.23545	0.28384	0.23044
b_{10} (height coefficient)	1.338	1.4417	1.1529
b_{11} (height coefficient)	0.4737	0.38884	0.54194
b_{12} (height coefficient)	0.73385	0.82157	0.8344
b_{13} (crown length coefficient)	3.83	4.18	3.4
b_{14} (crown length coefficient)	0.0024	0.0025	0.0066
b_{15} (crown length coefficient)	9.99	1.41	2.87
b_{16} (crown length coefficient)	0.009	0.512	0.434
b_{17} (competition index exponent)	1.4	1.4	1.5
b_{18} (drainage index coefficient)	−0.640157	−1.63645	−0.462746
b_{19} (drainage index coefficient)	0.0823112	0.106585	0.0496033
b_{20} (drainage index coefficient)	−0.0012155	−0.00119	−0.0003
b_{21} (drainage index coefficient)	0.0000045	0.0000024	−0.0000021
b_{22} (EP production coefficient)	1.00	1.00	1.00
b_{23} (SP decay constant)	−0.300	0.000	0.000
b_{24} (mortality coefficient)	0.985	0.99	0.985
b_{25} (mortality coeffiicent)	0.3772	2.203	2.4852
b_{26} (mortality coefficient)	34.55	19.11	60.76
b_{27} (mortality coefficient)	1.089	0.8298	1.205
b_{28} (mortality coefficient)	0.09314	1.517	0.8503
b_{29} (mortality coefficient)	3.419	2.169	1.01
b_{30} (mortality coefficient)	0.5346	0.7958	0.2394
b_{31} (biomass coefficient)	0.0527	0.0872	0.1676
b_{32} (biomass coefficient)	2.5084	2.587	2.3646
b_{33} (bole volume coefficient)	157.7	4118000.0	500.4
b_{34} (bole volume coefficient)	0.21361	0.2914	0.00742
b_{35} (bole volume coefficient)	0.03154	0.00021	0.02825
b_{36} (bole volume coefficient)	2.717	2.301	2.758
b_{37} (fine root biomass coefficient)	30	30	30
b_{38} (low light seedling mortality coefficient)	1.0662	0.001	0.003
b_{39} (low light seedling mortality coefficient)	−1.0552	0.0037	0.0008
b_{40} (low light seedling mortality coefficient)	−0.5	0.7159	0.8789
Maximum species site index (m at 50 years)	26	24	23
Low N tolerance score	2	2	2
Maximum number of EPs	60	200	300
Maximum number of vegetative EPs	500	20	15
Maximum number of SPs	3000	0	0
SP loss coefficient	−0.3	0	0
Propagule dispersal pattern	1	4	3
Maximum leaf area index	2.9	6.5	8.4
Foliar light extinction coefficient	0.3	0.45	0.5
Minimum species GDD	600	2000	2000

Table 11 (*Continued*)

Parameter	Quaking aspen	Yellow birch	Sugar maple
Maximum species GDD	5600	5300	6300
Fine litter decomposition coefficient	0.4	0.8	0.5
Coarse litter decomposition coefficient	0.25	0.25	0.25
CWD decomposition coefficient	0.08	0.09	0.09
Fine litter N content (0–1)	0.0168	0.0188	0.0132
Fine litter N retranslocation rate	0.5	0.5	0.5
Maximum reproductive mass (Mg per tree)	0.01	0.01	0.01
Coarse litter to fine litter ratio	0.93	0.87	0.9
Air-dry weight of wood (Mg/m^3)	0.38	0.62	0.63
Browse sensitivity coefficient	0.5	0.5	0.25
Browse preference coefficient	0.05	0.5	0.05

This stand was also constructed to reflect the beginnings of the shift from early to later succession species. The abundance of more shade tolerant taxa, especially in the smaller size classes, suggests the eventual replacement of aspen, barring any major catastrophic disturbance. The understory size classes (Fig. 32b) had a few intolerant aspen and black cherry, and were better stocked with balsam fir, red maple, sugar maple, yellow birch, and eastern hophornbeam. The smallest established propagule class (EP1) was composed entirely of balsam fir, white spruce, red maple, and sugar maple.

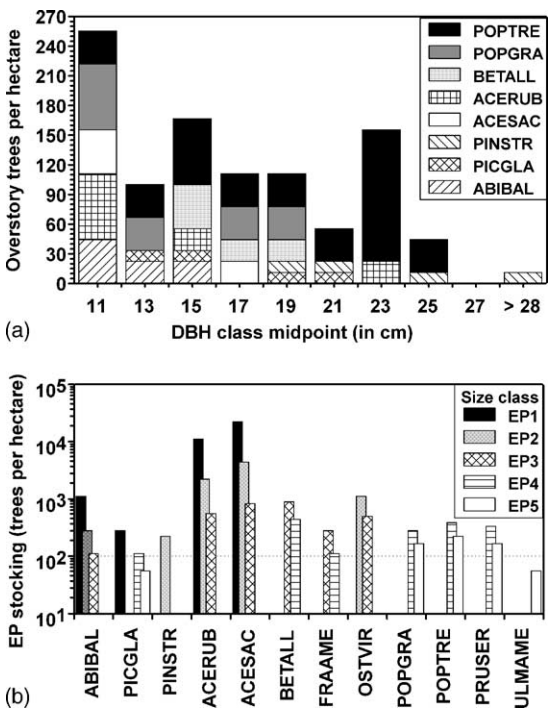

Fig. 32. Initial species composition and size class distribution for the overstory (a) and understory (b) of the 36 ha synthetic stand.

5.3.1.2. Site conditions. Site conditions assumed for the synthetic stand were designed to be consistent with the glacial moraines common to the northern Lake States. Climatically, this region averages 80–90 cm of precipitation annually, with average January and July temperatures assumed to be −11.6 and 18.7 °C, respectively. The somewhat acidic (pH = 5.5) and spodic soils were sandy, with a prominent silt and clay fractions (65% sand, 25% silt, and 10% clay) and limited coarse fragment content. These forested soils are relatively fertile, with good levels of nutrients (e.g. 120 kg/ha of available N) and moisture (drainage score (DS) = 70), and a root-limiting fragipan at 0.5 m.

White-tailed deer browsing was held at a constant level typical of contemporary herd sizes, and was initially constant across the synthetic study area. Since deer browsing tracks stand composition, shifts from one cover type to another may trigger different levels of browsing during succession. For example, the conversion from an intolerant hardwood cover type to the very shade tolerants would reduce deer density from over 12 to <4 deer/km^2.

5.3.2. Scenario building

Since the most fundamental *NORTHWDS* components are the same as those in *NIRM*, the scenarios tested for this paper will concentrate on a higher level process: wind disturbance. Ecosystem response to different patterns of windthrow considerably influences vegetation development (Everham and Brokaw,

1996; Frelich, 2002), so realistic portrayal of this factor should facilitate our understanding of *NORTHWDS* behavior. As with many large-scale phenomena, systematically studying long-term wind disturbance impacts on forest development is virtually impossible to implement in the field. Simulation of these perturbations provides a degree of control unavailable to field studies.

Four different windthrow environments were modeled for this exercise: no windthrow simulated (NONE); chronic windthrow only (CHRONIC); acute windthrow only (ACUTE); and both chronic and acute windthrow regimes (BOTH). Given a sufficiently large landscape, any of these scenarios are possible, although the most characteristic windthrow regime affecting the forest of the northern Lake States would be the BOTH scenario. In the no windthrow scenario, trees are allowed to grow free of any type of damaging wind event. While highly unlikely over a multi-century period, this undisturbed condition provides an extreme point along the spectrum of possibilities. The CHRONIC only scenario considered the small-scale loss of trees to frequent but low intensity wind events (see earlier discussion), where mortality is a function of site conditions, tree size and species, and stand density. Unlike chronic windthrow, the ACUTE only scenario depends on a series of distributions related to event intensity, frequency, and spatial extent. Even though the ACUTE scenario was more probable than NONE, the likelihood of either scenario for any given stand for centuries is small. The scenario most consistent with upland forests of the study region was BOTH, with co-occurring chronic and acute windthrow.

5.3.3. Data analysis

Because multiple *NORTHWDS* subroutines contain stochastic elements, 10 replicates of each windthrow "treatment" were generated using identical initial conditions. Each scenario replicate was run for 60 cycles (300 years) over the 36 ha synthetic stand, and consumed 38–57 min of processing time on a 550 MHz Pentium^{TM} III computer with 384 MB of RAM. Statistical analysis were conducted across each synthetic stand (i.e. results are the average across the 400 stand elements) as opposed to comparing an individual stand element because aggregate stand behavior under the windthrow regimes was desired. This reduced the cycle-to-cycle variation experienced at the stand element-level, but better reflected overall stand dynamics.

Two measures of stand condition (overstory tree richness and aboveground live tree biomass) were determined for each scenario and compared using Tukey's honestly significant difference (HSD) test at an $\alpha = 0.05$. Species compositional differences for the synthetic stands under each scenario were also examined to highlight shifts in composition as a function of successional trends. Because stocking varied by species in the initial stand, no significance tests between taxa were developed. However, qualitative comparisons by species are provided.

5.4. Results and discussion of NORTHWDS simulations

The results of these simulations strongly suggest the need for a mesoscale simulation capacity in a hierarchical model of forest dynamics. An individual tree model like *NIRM* is incapable of forecasting aggregate and emergent community patterns, for it lacks the larger scale dynamics (e.g. disturbance, deer browsing, neighborhood effects) found in the *NORTHWDS* model. Yet individual tree behavior is consistent between the levels, all else being equal. Larger landscape process like perturbation have critical roles in determining fine scale pattern and process, but may miss fine-scale neighborhood effects.

5.4.1. Predicted acute windthrow patterns

Fig. 33 provides histograms of the acute wind disturbance frequencies simulated for both scenarios in this effort that considered this windthrow pattern (ACUTE and BOTH). Consistent with observations of severe windthrow in eastern forests, acute windthrow scenarios were designed to have frequent, low-intensity, small-scale events with rare large-scale, intense episodes of wind damage. For example, Frelich and Lorimer (1991) estimated that intense (>50% canopy removal) disturbance events had a rotation from roughly 2500 to over 7000 years in the Upper Peninsula of Michigan. The vast majority of windthrow events occur on a very small scale (Canham and Loucks, 1984; Frelich, 2002). As apparent in Fig. 34, a large, severe windthrow striking a particular 36 ha area was an unusual event.

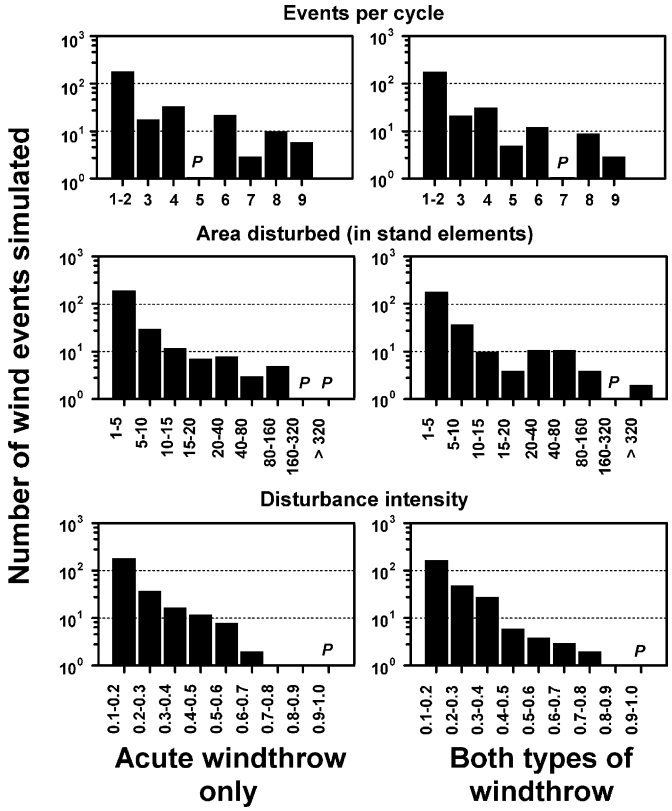

Fig. 33. Distribution of the number of acute windthrow events per cycle, area disturbed by event, and event intensity simulated for the ACUTE and BOTH scenarios. Blanks spots marked with a "*P*" designate bins with one observation that were not apparent given the scaling.

On average, there were between 1.3 and 1.5 acute windthrow events per 5-year cycle on the synthetic stand for each acute scenario, and rarely up to nine events occurred (Table 12). In other words, during a 300-year period, between 78 and 90 acute windthrow events of various sizes would be expected (on average) over the 36 ha study area. If one multiplies the average number of acute wind events (78–90 events) by the average area of damage (0.882–1.161 ha) by the average intensity of the events (0.205–0.212 (fraction of trees lost per event)) and divides by the number of years (300) and area (36 ha) simulated, an estimate of canopy turnover can be generated. Using the distributions assumed for this paper, this estimate would range from 0.13 to 0.21% annual tree loss due exclusively to acute windthrow events. Frelich and Lorimer (1991) estimated annual canopy mortality due to fire and wind disturbance in the Upper Peninsula of Michigan of 0.57–0.69% in old-growth northern hardwood-dominated stands, which is appreciably higher than our estimates. However, Frelich and Lorimer's methodology would not have separated acute and chronic windthrow losses, nor did our estimate include any mortality due to fire. There may also be a "dilution" effect in our estimates, which considered a well-stocked early seral stand rather than a less dense old-growth forest. The loss of 1–2% of the canopy every decade due to severe windthrow events is consistent with estimates from other studies of eastern forests (e.g. Eyre and Longwood, 1951; Lorimer, 1977; Brewer and Merritt, 1977; Canham and Loucks, 1984).

5.4.2. Aggregate stand behavior

5.4.2.1. Overstory tree species richness. Overstory tree richness displayed subtle but significant differences between windthrow scenarios (Fig. 35). All

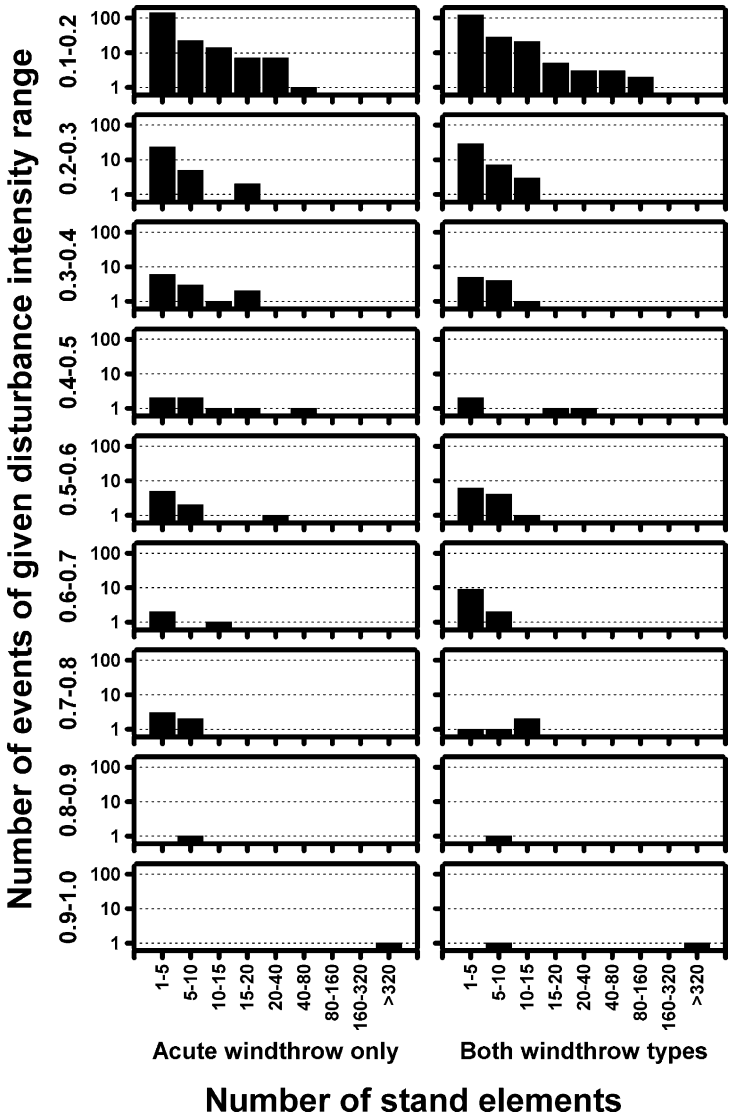

Fig. 34. Distribution of area disturbed by disturbance intensity for the ACUTE and BOTH scenarios. The abundance of events in small, low intensity categories parallels numerous other studies, but note that it is possible to have large, severe wind disturbances.

scenarios increased in overstory diversity immediately after simulation inception because some taxa were only represented by understory individuals that quickly achieved overstory status. Over time, the less shade tolerant species (e.g. aspen) began disappearing from the stand and were replaced in the canopy by shade tolerant species like sugar maple. As simulated in this study, the catastrophic windthrow events were not sufficiently devastating to ensure long-term abundance of very intolerant species. This pattern is consistent with observations of presettlement and modern forests in the northern Lake States. Taxa like aspen and paper birch were noticeably less common in virgin forests (Frelich, 1995), but became much more abundant after the extensive logging, failed agriculture, and burning that accompanied Euroamerican settlement (Frelich, 2002). On good sites, barring severe canopy disturbance and heavy white-tailed deer

Table 12
Predicted acute windthrow disturbance frequencies, areas, and intensities for the ACUTE and BOTH scenarios

Parameter	Acute windthrow only (ACUTE)	Both acute and chronic (BOTH)
Events per cycle		
Minimum	1	1
Maximum	9	9
Average	1.5	1.3
S.D.	1.8	1.6
Area of events (number of 0.09 ha stand elements)		
Minimum	1	1
Maximum	400	400
Average	9.8	12.9
S.D.	31.2	41.9
Intensity of events (fraction of trees killed by an acute windthrow event, minimum = 0.1, maximum = 1.0)		
Minimum	0.101	0.101
Maximum	1.000	1.000
Average	0.205	0.212
S.D.	0.122	0.123

browsing, stands would progressively move towards sugar maple and eastern hemlock, with a considerable component of yellow birch. However, these scenarios were run with contemporary levels of deer browsing, which are pronounced enough to limit the browse-sensitive species.

Chronic windthrow assumptions embedded within *NORTHWDS* appear considerably more effective in altering tree species richness than the infrequent and limited acute windthrow events (Fig. 35). Chronic windthrow serves to remove large shade intolerant trees from the overstory while failing to open the canopy enough to permit their re-establishment, accelerating the conversion towards shade tolerant species. Only rarely will a particularly large and severe acute windthrow event release enough resources for shade intolerants to recolonize many sites (Frelich, 2002). Moderately tolerant and very shade tolerant species are capable of exploiting these limited gaps, and can increase their representation at the expense of shade intolerant taxa. Thus, the greater richness experienced early in the simulations is understandable. The transition to higher richness for the chronically disturbed stands approximately 150 years after scenario initiation coincides with the loss of the last shade intolerant canopy dominants and the increasing presence of more moderately tolerant species such as red maple.

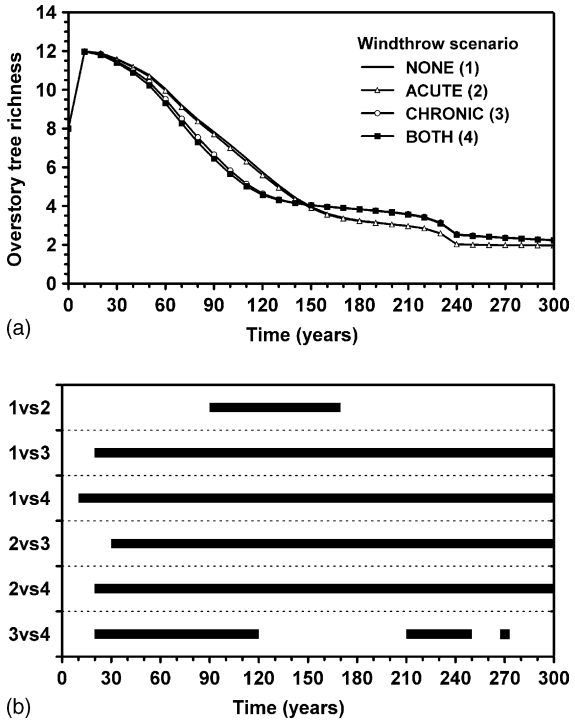

Fig. 35. Effects of different windthrow scenarios on overstory tree species richness for the synthetic study area. All scenarios increased tree richness immediately after simulation inception as understory individuals grew into the overstory, then gradually declined over time towards a species-poor condition (a). Significant ($P < 0.05$, Tukey's HSD test) differences over time between the scenarios are indicated by solid bars (b).

5.4.2.2. Aboveground live tree biomass. As with tree species richness, aboveground live tree biomass response can be partitioned into two primary scenario categories: chronically-impacted stands versus no chronic windthrow. The relative vulnerability of large individuals to chronic windthrow, especially on sites with limited rooting potential, is largely responsible for the noticeable difference between the NONE and ACUTE scenarios and the CHRONIC and BOTH scenarios. Each scenario rapidly accumulated biomass during the first 50–70 years, reaching a maximum by stand age ≈100 years, before declining slightly to long-term averages of 260–300 Mg/ha (Fig. 36a). This range is consistent with observations of remnant old-growth northern hardwood stands in the northern Lake States (e.g. Dunn et al., 1983; Mroz et al., 1985;

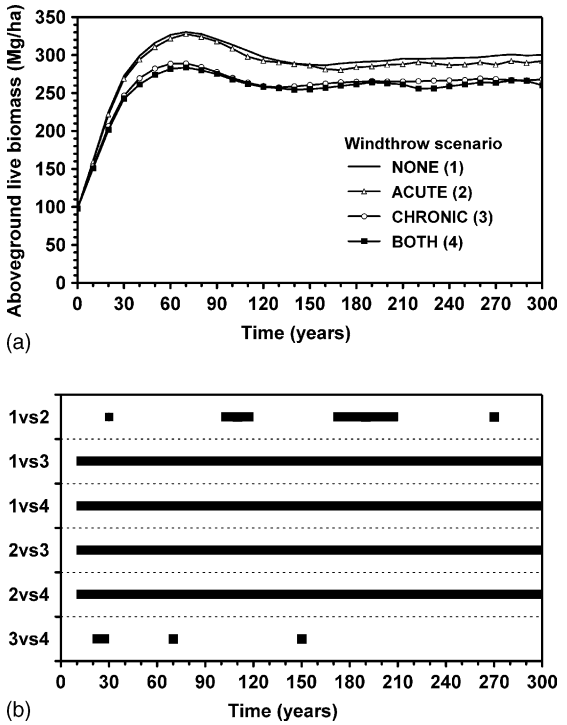

Fig. 36. Impact of different windthrow scenarios on aboveground live tree biomass (in Mg) for the synthetic study area. Biomass increased rapidly (a) as the stand matured, reach a maximum approximately 70 years after the beginning of the simulation (stand age ≈ 100 years old). Biomass then decreased slightly under all scenarios, but remained relatively high. Note how much more chronic windthrow was predicted to decrease total stand aboveground live tree biomass, although significant differences occasionally appeared for all scenarios (b).

Albert and Barnes, 1987; Rutkowski and Stottlemyer, 1993; Fisk et al., 2002).

5.4.3. Species composition trends

5.4.3.1. Shade intolerant species. The synthetic stand used for this demonstration was initiated with conditions that would obviously track expected successional trends if the model performed consistent with expectations for the region. Aspen followed expected trends, with an initial small increase in their portion of the stand's basal area, followed by a rapid decline over the next 50 years. Given that the stand was approximately 30 years old when the simulation began, this placed the pronounced decline of aspen at a stand age of approximately 50 years, with very little remaining by 90 years (Fig. 37a and b). Shields and Bockheim (1981) reported maximum aspen basal area at stand age of 50–60 years, followed by a decline to virtually no aspen by 120 years (see also Zehngraff, 1949). Traces of aspen were still found >100 years after the simulation began, probably arising from the rare intense disturbance that sufficiently released this shade intolerant species.

Windthrow scenarios had relatively minor impacts on aspen abundance. The NONE and ACUTE scenarios slightly decreased quaking aspen basal area as a function of stand age (Fig. 37a), but had no noticeably impact on bigtooth aspen (Fig. 37b). The inclusion of chronic windthrow accelerated the decline of aspen through the removal of more exposed mature aspen, but these differences disappeared over time as aspen stocking declined. Windthrow appears to slightly reduce aspen stocking, but as implemented in this demonstration, never reached sufficient extent or intensity to reinitiate widespread aspen coverage, given the size of the simulated forest. This parallels aspen's historical presence in the northern Lake States, where the extensive aspen forests were largely the product of large-scale timber harvesting and fire (Zehngraff, 1949; Stoeckeler and Macon, 1956), not catastrophic windthrow (Frelich, 2002).

5.4.3.2. Moderately shade tolerant species. Both red maple and yellow birch fared better initially under the NONE and ACUTE scenarios (Fig. 37c and d), although red maple's success increased somewhat about 100 years after the beginning of the simulation. This transition coincided with the rapid decline of the aspen overstory, releasing resources to the lower canopy levels. Yellow birch's inability to respond similarly, however, probably reflects an interaction with deer browsing. Unlike red maple, yellow birch reacts poorly to deer browsing of juvenile twigs and buds (Graham, 1954a, 1958; Stoeckeler et al., 1957; Anderson and Katz, 1993). Heavy deer browsing helped to limit advanced yellow birch regeneration, with few yellow birch saplings surviving to respond to any canopy gap formation.

Regardless of their response to deer browsing, neither red maple nor yellow birch markedly increased their long-term abundance in the stand. As with aspen, windthrow does not appear to suffi-

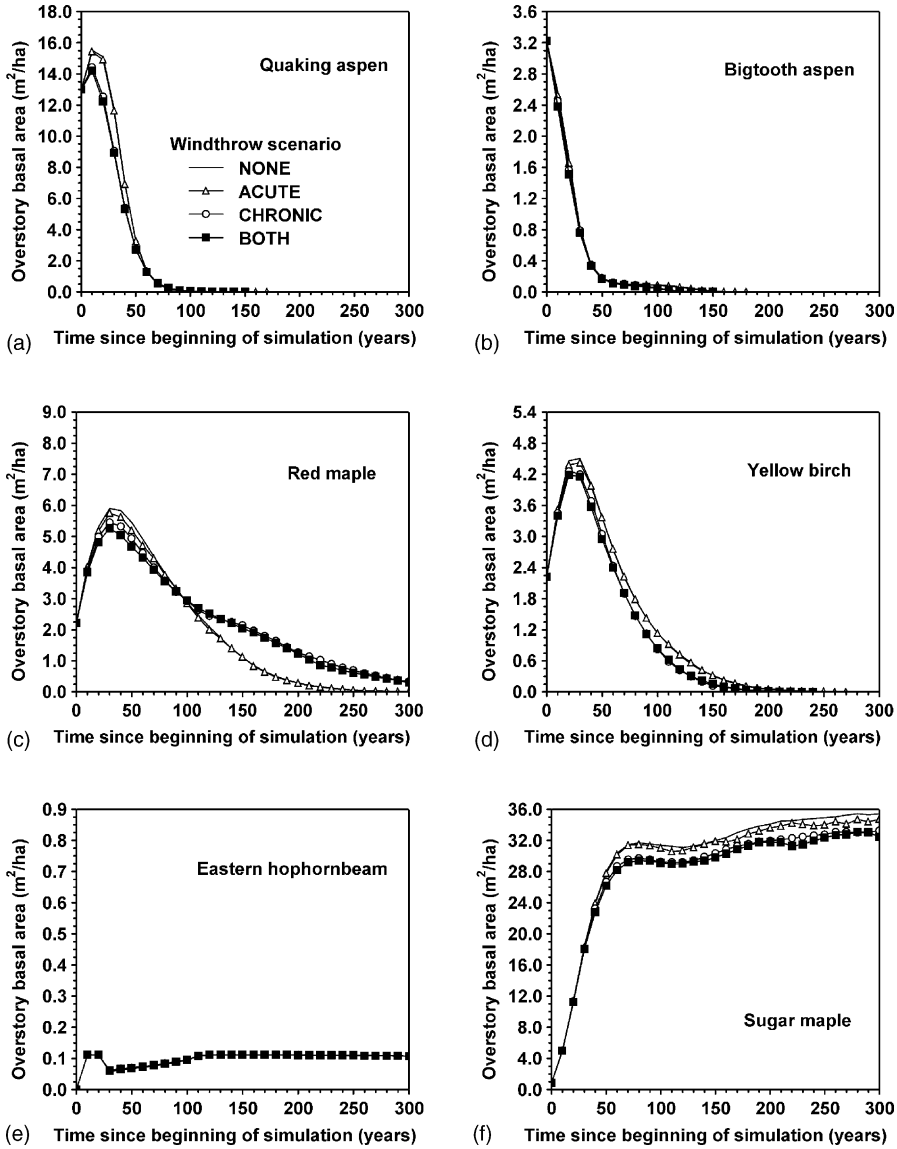

Fig. 37. Species success under the different windthrow scenarios. Early successional species like quaking (a) and bigtooth (b) aspen experienced initial success, followed by a steep decline, while the mid-tolerant red maple (c) and yellow birch (d) peaked slightly later. The very shade and browse tolerant eastern hophornbeam (e) and sugar maple (f) ultimately dominated the stand.

ciently contribute to elevated mid-tolerant success because of limited canopy release. Multiple severe windthrow disturbances, coupled with lower deer browsing and perhaps greater exposure of mineral soil may increase the presence of mid-tolerant species on good northern hardwood sites (see also Frelich, 2002).

5.4.3.3. Very shade tolerant species. Unlike less tolerant species, two of the most shade tolerant taxa experienced moderate to very good success under all simulated windthrow scenarios. Both eastern hophornbeam (Fig. 37e) and sugar maple (Fig. 37f) progressively increased their importance in the stand until they eventually dominated the stand. As reported ear-

lier, stand richness declined from a peak of 12 species soon after simulation initiation to roughly two species (usually eastern hophornbeam and sugar maple) by the end of the simulation period. This dominance arises from key autecological attributes of these species. First, they are both considered extremely shade tolerant, and are capable of surviving long periods in the understory until released (Burns and Honkala, 1990b). Eastern hophornbeam's limited stature necessitates its ability to tolerate high shading, as it lacks sugar maple's ability to grow into a tall canopy. Second, both are considered tolerant of deer browsing and less preferable as browse species than taxa like eastern hemlock or yellow birch (Stoeckeler et al., 1957; Alverson et al., 1988; Anderson and Katz, 1993).

The ability to persist, even under heavy browsing, in the understory until released has important ramifications for regional successional trends. Other experiments (both field- and model-based) have suggested that browse-sensitive species will continue to lose prominence in northern Lake States landscapes (Frelich and Lorimer, 1985; Alverson et al., 1988; Anderson and Katz, 1993; see also Seagle and Liang, 2001), even if other conditions favor their continued persistence. Observations of the increasing importance of sugar maple and similarly behaving species in this region given current deer densities and disturbance regimes (especially uneven-aged harvesting) may produce significantly simplified overstory assemblages (Crow et al., 2002). These simulations suggest that this trend may be insensitive at least to windthrow disturbance patterns, and may also extend to other disturbance regimes (e.g. timber harvesting or fire) that are being considered for restoration of presettlement vegetation patterns (Morton et al., 1991; Vora, 1994; Crow et al., 2002).

5.5. Context and utility of NORTHWDS

Achieving a balance between model detail and predictive utility are often viewed as one of the major challenges to effective ecosystem simulation. Traditional gap models (e.g. Botkin et al., 1972; Shugart and West, 1977; Solomon, 1986) have been criticized for their lack of physiological and ecological functionality, especially related to key simplifications and lack of spatial context (Pacala et al., 1996; Gustafson et al., 2000). Other individual-based models have attempted to address these concerns by developing a very detailed, fine-scale kernel (e.g. an individual tree), and then making stands, forests, and even landscapes by adding more and more individuals to an often spatial platform (e.g. Pacala et al., 1993; Bossel, 1996; Luan et al., 1996).

So what is the application space of *NORTHWDS*? Given that its most efficient operating context is in the realm of tens to hundreds of hectares and that its finest grain is a 0.09 ha pixel containing a stand list, *NORTHWDS* is notably coarser in many aspects compared to other individual-based models like *SORTIE* (Pacala et al., 1993, 1996) or *FOREST* (Ek and Monserud, 1974) yet is considerably more extensible than most gap models, especially with spatially-related ecosystem attributes. *NORTHWDS* is capable of forest-wide or even small landscape simulation, although its internal design and mechanisms are not conducive to large scale simulations characteristic of models like *LANDIS* (Mladenoff et al., 1996; He et al., 2002). However, because of the nature of its tree lists, *NORTHWDS* contains more detail in stand attributes (e.g. size class structure) than many landscape simulators that track cohorts or patches of a given type. As with virtually all process-based models, *NORTHWDS* lacks some of the precision of locally-developed empirical models (e.g. Adams and Ek, 1974; Lin et al., 1996) but the incorporation of mechanism permits considerably greater hypothesis testing and scenario building capacities.

Although *NORTHWDS* borrows heavily from several existing models, it differs from these efforts in how it is structured (primarily in its relationships between other hierarchical levels) and some parts of the implementation of traditional components (e.g. tree initiation, growth, and mortality, see individual sections). One of the key differentiating aspects of *NORTHWDS* is the emphasis on homogeneity of detail. Many models invest considerable effort in describing a very limited number of processes to great detail, and minimize other important dynamics. For instance, some (e.g. *FOREST*, *SORTIE*, *FORDYN*; Luan et al., 1996) provide detailed crown structure and dynamics, capitalizing on the biological principle that tree growth is strongly correlated to light availability. In their implementation of this relationship, however, they require considerable spatial and relational information between the individuals being simulated, making the outcomes highly dependent on initial conditions and

most have far less detail on moisture or nutrient gradients. *NORTHWDS* avoids this variability in detail by tracking individual trees no more precisely than their presence in a given stand element, and subjecting growth to similarly detailed environmental modifiers refined to a specific location.

NORTHWDS was also developed with the intention of providing a research-grade tool to forest managers in a package that is easily approachable and parameterizable. Vanclay (2003) echoed the sentiments of many when he questioned why few models are useful for both research and management applications. Even though it is unlikely that a process-based forest model will ever provide the level of precision of empirically fitted growth and yield models, it is possible to develop simulators capable of reasonable input values, predictions of productivity, and ecological mechanisms that can provide results in terms common to management (Sievänen and Burk, 1990). Computer-savvy forest managers are increasingly capable and willing to use process-based models, especially if they can be convinced that some sacrifice of precision is worth the flexibility gained. *NORTHWDS* offers many such attributes—the ability to incorporate deer browsing, for example, in silvicultural planning is becoming a more critical issue in eastern North American forests (Horsley et al., 2003). Even something as basic as *NORTHWDS*' predictive ability into multi-species, multi-cohort forests of uncertain composition is a distinct advantage over the single-species, single-cohort stands commonly applied.

6. Conclusions

Computer simulation modeling permits researchers to investigate ecological phenomena that do not otherwise lend themselves to traditional experimental manipulation. Modeling also allows the development and testing of hypotheses, permits the exact replication of study areas (or at least initial conditions), tolerates large spatiotemporal scales, and contributes to our understanding of complex systems. We have blended the qualities of connectivity, complexity, and context in a hierarchically structured modeling system (*NIHMS*) that allows the user to engage in multiscale ecological analysis. The intent of this modeling system is to emulate forest dynamics from individual trees to landscapes. The larger spatial and longer temporal scales provided in the mesoscale model provide contextual information used in the individual tree-based (microscale) model.

Although *NIHMS* was developed to simulate temperate forest dynamics, the general approach has broader applications because its hierarchical organization assumes biophysical interdependence. The ability to simulate at different scales using an internally consistent model provides both continuity of assumptions and clarity of process. Internal continuity also avoids problems that may be encountered when coupling unrelated models developed for distinct application spaces that may or may not be scale compatible. We also recognize that some components and processes are more closely connected than others. When abstracting such a reality with computer simulators, by necessity the strongest interactions receive the most attention and form the core of every model. Fortunately, this parsimony lends predictability to a model system, which is more ecologically informative that efforts focused solely on empirical fitting exercises (Zeide, 1991; Allen and Hoekstra, 1992).

The ability to use a low-order, high resolution model (like *NIRM*) within a complex hierarchical system like *NIHMS* to determine the responsiveness of controllable environmental conditions increases the confidence in model outcomes while allowing for adjustments to model behavior. The case studies provided in this paper demonstrated that *NIRM* has the capability of predicted individual tree response to its biophysical environment in a manner consistent with ecological expectations. While the scenarios examined were simple and did not involve complicated and interactive environmental gradients, the predictions of *NIRM* did reveal dynamic and logical responses to competitive, nutrient, and moisture gradients consistent with the expected behavior of the species tested. *NIRM* proves a useful tool in both concrete (e.g. testing diameter increment response to stand density manipulation) and abstract (e.g. sensitivity analysis of at a critical level of hierarchical structure) applications, but as with any model created for a specific use, its application must be constrained within the scale-based limits of its development.

NORTHWDS behavior was tested under a series of windthrow-related scenarios to indicate its relative sensitivity to this regionally important natural pertur-

bation. The resulting patterns in structure, composition, and succession in response to these scenarios were consistent with other studies of forest dynamics in hardwood-dominated stands of the northern Lake States region. Not only were the patterns similar, but their magnitude and timing also met expectations. Hence, we feel that the behavior of the *NORTHWDS* is consistent with expectations of forest change in this region. The structured approach ingrained in this mesoscale level of a larger hierarchical model system provides a good opportunity to increase our understanding of forest dynamics given its uncertainty across multiple scales. Because of its interfacing role, this middle ground is a fundamental part of the modeling system but perhaps the most difficult to characterize (O'Neill et al., 1986; Shugart et al., 1992). The *NORTHWDS* mesoscale model helps define the relations between successive levels in the hierarchical structure while providing a new tool for forest researchers and managers.

Acknowledgements

Many people and organizations helped make this paper possible: Burton Barnes, John Bissonette, Hope Bragg, Jim Guldin, Jim Long, Terry Sharik, and the USDA Forest Service, Southern and North Central Research Stations. We are especially grateful for the contributions of the Ecology Center and Department of Forest Resources, Utah State University and the USDA Forest Service, North Central Research Station. Alan Ek, Eric Gustafson, Dave Lytle, Dave Mladenoff, Jim Manolis, and two anonymous referees provided helpful review comments on an earlier draft of this manuscript.

References

Aber, J.D., Melillo, J.M., 1982. FORTNITE: a computer model of organic matter and nitrogen dynamics in forest ecosystems. University of Wisconsin College of Agriculture and Life Sciences Research Bulletein R3130.

Aber, J.D., Botkin, D.B., Melillo, J.M., 1979. Predicting the effects of different harvesting regimes on productivity and yield in northern hardwoods. Can. J. For. Res. 9, 10–14.

Adams, D.M., Ek, A.R., 1974. Optimizing the management of uneven-aged forest stands. Can. J. For. Res. 4, 274–287.

Albert, D.A., Barnes, B.V., 1987. Effects of clearcutting on the vegetation and soil of a sugar maple-dominated ecosystem, western Upper Michigan. For. Ecol. Manage. 18, 283–298.

Allen, T.F.H., 1998. The landscape "level" is dead: persuading the family to take it off the respirator. In: Peterson, D.L., Parker, V.T. (Eds.), Ecological Scale: Theory and Applications. Columbia University Press, New York, pp. 35–54.

Allen, T.F.H., Hoekstra, T.W., 1992. Toward a Unified Ecology. Columbia University Press, New York, 384 pp.

Alverson, W.S., Waller, D.M., Solheim, S.L., 1988. Forests too deer: edge effects in northern Wisconsin. Conserv. Biol. 2, 348–358.

Anderson, R.C., Katz, A.J., 1993. Recovery of browse-sensitive tree species following release from white-tailed deer *Odocoileus virginianus* Zimm. browsing pressure. Biol. Conserv. 63, 203–208.

Anderson, R.C., Loucks, O.L., Swain, A.M., 1969. Herbaceous response to canopy cover, light intensity, and throughfall precipitation in coniferous forests. Ecology 50, 255–263.

Arbogast, C., Heinselman, M.L., 1950. Damage to natural reproduction by deer browsing. USDA Forest Service Technical Note LS-332.

Auger, P., 1986. Dynamics in hierarchically organized systems: a general model applied to ecology, biology, and economics. Syst. Res. 3, 41–50.

Balogh, J.C., Grigal, D.F., 1988. Tall shrub dynamics in northern Minnesota aspen and conifer forests. USDA Forest Service Research Paper NC-283.

Beals, E.W., Cottam, G., Vogl, R.J., 1960. Influence of deer on vegetation of the Apostle Islands, Wisconsin. J. Wildl. Manage. 24, 68–80.

Beerling, D.J., Woodward, F.I., 2001. Vegetation and the Terrestrial Carbon Cycle: Modelling the First 400 Million Years. Cambridge University Press, Cambridge, UK, 405 pp.

Behre, C.E., 1921. A study of windfall in the Adirondacks. J. For. 19, 632–637.

Belcher, D.M., Holdaway, M.R., Brand, G.J., 1982. A description of STEMS—the stand and tree evaluation and modeling system. USDA Forest Service General Technical Report NC-79.

Bockheim, J.G., Jepsen, E.A., Heisey, D.M., 1991. Nutrient dynamics in decomposing leaf litter of four tree species on a sandy soil in northwestern Wisconsin. Can. J. For. Res. 21, 803–812.

Bonan, G.B., Sirois, L., 1992. Air temperature, tree growth, and the northern and southern range limits to *Picea mariana*. J. Veg. Sci. 3, 495–506.

Bormann, F.H., Likens, G.E., 1994. Pattern and Process in a Forested Ecosystem, 2nd ed. Springer-Verlag, New York.

Bormann, F.H., Likens, G.E., Melillo, J.M., 1977. Nitrogen budget for an aggrading northern hardwood forest ecosystem. Science 196, 981–983.

Bossel, H., 1996. TREEDYN3 forest simulation model. Ecol. Model. 90, 187–227.

Botkin, D.B., 1992. Manual for JABOWA-II. Oxford University Press, New York.

Botkin, D.B., 1993. Forest Dynamics: an Ecological Model. Oxford University Press, New York.

Botkin, D.B., Janak, J.F., Wallis, J.R., 1972. Some ecological consequences of a computer model of forest growth. J. Ecol. 60, 849–872.

Bragg, D.C., 1999. Multi-scalar spatial modeling of northern forest dynamics: foundations, theories, and applications. Ph.D. dissertation, Department of Forest Resources, Utah State University, Logan, UT, 532 pp.

Bragg, D.C., 2001a. Potential relative increment (PRI): a new method to empirically derive optimal tree diameter growth. Ecol. Model. 137, 77–92.

Bragg, D.C., 2001b. A local basal area adjustment for crown with prediction. North. J. Appl. For. 18, 22–28.

Bramble, W.C., Goddard, M.K., 1953. Seasonal browsing of woody plants by white-tailed deer in the ridge and valley section of central Pennsylvania. J. For. 51, 815–819.

Brewer, R., Merritt, P.G., 1977. Wind throw and tree replacement in a climax beech-maple forest. Oikos 30, 149–152.

Buchman, R.G., 1983. Survival predictions for major Lake States tree species. USDA Forest Service Research Paper NC-233.

Buchman, R.G., Lentz, E.L., 1984. More Lake States tree survival predictions. USDA Forest Service Research Note NC-312.

Buchman, R.G., Pederson, S.P., Walters, N.R., 1983. A tree survival model with applications to species of the Great Lakes region. Can. J. For. Res. 13, 601–608.

Bugmann, H.K.M., Yan, X., Sykes, M.T., Martin, P., Linder, M., Desanker, P.V., Cumming, S.G., 1996. A comparison of forest gap models: model structure and behavior. Clim. Change 34, 289–313.

Burns, R.M., Honkala, B.H. (Technical Coordinators), 1990a. Silvics of North America, Vol. 1: Conifers. USDA Forest Service Agriculture Handbook 654.

Burns, R.M., Honkala, B.H. (Technical Coordinators), 1990b. Silvics of North America, Vol. 2: Hardwoods. USDA Forest Service Agriculture Handbook 654.

Buttrick, P.L., 1921. A study of regeneration on certain cut-over hardwood lands in northern Michigan. J. For. 19, 872–876.

Canham, C.D., Loucks, O.L., 1984. Catastrophic windthrow in the presettlement forests of Wisconsin. Ecology 65, 803–809.

Canham, C.D., McAninch, J.B., Wood, D.M., 1994. Effects of the frequency, timing, and intensity of simulating browsing on growth and mortality of tree seedlings. Can. J. For. Res. 24, 817–825.

Caspersen, J.P., Silander, J.A., Canham, C.D., Pacala, S.W., 1999. Modeling the competitive dynamics and distribution of tree species along moisture gradients. In: Mlandenoff, D.J., Baker, W.L. (Eds.), Spatial Modeling of Forest Landscape Change: Approaches and Applications. Cambridge University Press, New York, pp. 14–41.

Chai, T.S., Hansen, H.L., 1952. Characteristics of black spruce seed from cones of different ages. Minnesota Forest Note #2, 2 pp.

Chamberlin, T.C., 1965. The method of multiple working hypotheses. Science 148, 754–759.

Christensen, E.M., 1962. Classification of the winter habitats of the white-tailed deer in northern Wisconsin based on forest ordination. Ecology 43, 134–135.

Clutter, J.L., Fortson, J.C., Pienaar, L.V., Brister, G.H., Bailey, R.L., 1983. Timber Management: a Quantitative Approach. Wiley, New York.

Cooperrider, A.Y., Behrend, D.F., 1980. Simulation of forest dynamics and deer browse production. J. For. 78, 85–88.

Crow, T.R., Mroz, G.D., Gale, M.R., 1991. Regrowth and nutrient accumulations following whole-tree harvesting of a maple-oak forest. Can. J. For. Res. 21, 1305–1315.

Crow, T.R., Buckley, D.S., Nauertz, E.A., Zasada, J.C., 2002. Effects of management on the composition and structure of northern hardwood forests in Michigan. For. Sci. 48, 129–145.

Cullinan, V.I., Simmons, M.A., Thomas, J.M., 1997. A Bayesian test of hierarchy theory: scaling up variability in plant cover from field to remotely sensed data. Landscape Ecol. 12, 273–285.

Curtis, J.D., 1943. Some observations on wind damage. J. For. 41, 877–882.

Curtis, R.O., Rushmore, F.M., 1958. Some effects of stand density and deer browsing on reproduction in an Adirondack hardwood stand. J. For. 56, 116–121.

Dale, M.E., 1962. An easy way to calculate crown-surface area. J. For. 60, 826–827.

Deleuze, C., Hervé, J., Colin, F., Ribeyrolles, L., 1996. Modelling crown shape of *Picea abies*: spacing effects. Can. J. For. Res. 26, 1957–1966.

Doepker, R.V., Beyer, D.E., Donovan, M., 1996. Deer population trends in Michigan's Upper Peninsula. In: Mroz, G.D., Martin, J. (Eds.), Proceedings of Hemlock Ecology and Management Conference. Department of Forestry, University of Wisconsin, Madison, WI, pp. 99–108.

Duerr, W.A., Stoddard, C.H., 1938. Results of a commercial selective cutting in northern hemlock-hardwoods. J. For. 36, 1224–1230.

Dunn, C.P., Guntenspergen, G.R., Dorney, J.R., 1983. Catastrophic wind disturbance in an old-growth hemlock-hardwood forest, Wisconsin. Can. J. Bot. 61, 211–217.

Dyer, M.I., Shugart, H.H., 1992. Multi-level interactions arising from herbivory: a simulation analysis of deciduous forests utilizing FORET. Ecol. Appl. 2, 376–386.

Ek, A.R., Monserud, R.A., 1974. FOREST: a computer model for simulating the growth and reproduction of mixed species forest stands. University of Wisconsin College of Agricural and Life Sciences Report R2635.

Ek, A.R., Birdsall, E.T., Spears, R.J., 1984. A simple model for estimating total and merchantable tree heights. USDA Forest Service Research Note NC-309.

Everham, E.M., Brokaw, N.V.L., 1996. Forest damage and recovery from catastrophic wind. Bot. Rev. 62, 113–185.

Eyre, F.H., Longwood, F.R., 1951. Reducing mortality in old-growth northern hardwoods through partial cutting. USDA Forest Service Research Paper LS-24.

Feibleman, J.K., 1954. Theory of integrative levels. Br. J. Philos. Sci. 5, 59–66.

Fisk, M.C., Zak, D.R., Crow, T.R., 2002. Nitrogen storage and cycling in old- and second-growth northern hardwood forests. Ecology 83, 73–87.

Fleming, R.A., 1996. Better derivations and an improvement for the specific increment equations of tree growth. Can. J. For. Res. 26, 624–626.

Foster, D.R., Boose, E.R., 1992. Patterns of forest damage resulting from catastrophic wind in central New England, USA. J. Ecol. 80, 79–98.

Frelich, L.E., 1995. Old forests in the Lake States today and before European settlement. Nat. Areas J. 15, 157–167.

Frelich, L.E., 2002. Forest Dynamics and Disturbance Regimes: Studies from Temperate Evergreen-Deciduous Forests. Cambridge University Press, Cambridge, UK, 266 pp.

Frelich, L.E., Lorimer, C.G., 1985. Current and predicted long-term effects of deer browsing on hemlock forests in Michigan. Biol. Conserv. 34, 99–120.

Frelich, L.E., Lorimer, C.G., 1991. Natural disturbance regimes in hemlock-hardwood forests of the upper Great Lakes region. Ecol. Monogr. 61, 145–164.

Goldblum, D., 1997. The effects of treefall gaps on understory vegetation in New York State. J. Veg. Sci. 8, 125–132.

Goodall, D.W., 1974. The hierarchical approach to model building. In: Proceedings of First International Congress of Ecology, The Hague, The Netherlands, pp. 244–249.

Gosz, J.R., Likens, G.E., Bormann, F.H., 1972. Nutrient content of litter fall on the Hubbard Brook Experimental Forest, New Hampshire. Ecology 53, 769–784.

Graham, S.A., 1954a. Changes in northern Michigan forests from browsing by deer. Trans. N. Am. Wildl. Conf. 19, 526–533.

Graham, S.A., 1954b. Scoring tolerance of forest trees. Michigan For. 4, 1–2.

Graham, S.A., 1958. Results of deer exclosure experiments in the Ottawa National Forest. Trans. N. Am. Wildl. Conf. 23, 478–490.

Graney, D.L., 1987. Ten-year growth of red and white oak crop trees following thinning and fertilization in the Boston Mountains of Arkansas. In: Procrrdings of Fourth Biennial Southern Silvicultural Research Conference. USDA Forest Service General Technical Report SE-42, pp. 445–450.

Greene, D.F., Johnson, E.A., 1989. A model of wind dispersal of winged or plumed seeds. Ecology 70, 339–347.

Greene, D.F., Zasada, J.C., Sirois, L., Kneeshaw, D., Morin, H., Charron, I., Simand, M.-J., 1999. A review of the regeneration dynamics of North American boreal forest tree species. Can. J. For. Res. 29, 824–839.

Groffman, P.M., Tiedje, J.M., 1989a. Denitrification in north temperate forest soils: spatial and temporal patterns at the landscape and seasonal scales. Soil Biol. Biogeochem. 21, 613–620.

Groffman, P.M., Tiedje, J.M., 1989b. Denitrification in north temperate forest soils: relationships between denitrification and environmental factors at the landscape scale. Soil Biol. Biogeochem. 21, 621–626.

Groffman, P.M., Gold, A.J., Simmons, R.C., 1992. Nitrate dynamics in riparian forests: microbial studies. J. Environ. Quality 21, 666–671.

Gustafson, E.J., Shifley, S.R., Mladenoff, D.J., Nimerfro, K.K., He, H.S., 2000. Spatial simulation of forest succession and timber harvesting using LANDIS. Can. J. For. Res. 30, 32–43.

Guttenberg, S., 1953. Loblolly crown length—clue to vigor. USDA Forest Service Southern Forest Note #88, 1 pp.

Gysel, L.W., 1966. Ecology of a red pine (*Pinus resinosa*) plantation in Michigan. Ecology 47, 465–472.

Hahn, J.T., Carmean, W.H., 1982. Lake States site index curves formulated. USDA Forest Service General Technical Report NC-88, 5 pp.

Hamilton, D.A., 1986. A logistic model of mortality in thinned and unthinned mixed conifer stands of northern Idaho. For. Sci. 32, 989–1000.

Hansen, M.H., Frieswyk, T., Glover, J.F., Kelly, J.F., 1992. The eastwide forest inventory data base: users manual. USDA Forest Service General Technical Report NC-151, 48 pp.

Harlow, W.M., Harrar, E.S., White, F.M., 1979. Textbook of Dendrology, 6th ed. McGraw-Hill Book Company, New York, 510 pp.

Hawkes, C., 2000. Woody plant mortality algorithms: description, problems and progress. Ecol. Model. 126, 225–248.

He, H.S., Larsen, D.R., Mladenoff, D.J., 2002. Exploring component-based approaches in forest landscape modeling. Environ. Model. Software 17, 519–529.

Henry, D.C., 1973. Foliar nutrient concentrations of some Minnesota forest species. Minnesota Forest Research Note #241, 4 pp.

Henry, J.D., Swan, J.M.A., 1974. Reconstructing forest history from live and dead plant material—an approach to the study of forest succession in southwest New Hampshire. Ecology 55, 772–783.

Hoffman, F., 1995. FAGUS, a model for growth and development of beech. Ecol. Model. 83, 327–348.

Holdaway, M.R., 1986. Modeling tree crown ratio. For. Chron. 62, 451–455.

Hole, F.D., 1978. An approach to landscape analysis with emphasis on soils. Geoderma 21, 1–23.

Horsley, S.B., Stout, S.L., DeCalesta, D.S., 2003. White-tailed deer impact on the vegetation dynamics of a northern hardwood forest. Ecol. Appl. 13, 98–118.

Hough, A.F., 1937. A study of natural tree reproduction in the beech-birch-maple-hemlock type. J. For. 35, 376–378.

Hurd, R.M., 1971. Annual tree-litter production by successional forest stands, Juneau, Alaska. Ecology 52, 881–884.

Huston, M., 1979. A general hypothesis of species diversity. Am. Nat. 113, 81–101.

Isebrands, J.G., Rauscher, H.M., Crow, T.R., Dickmann, D.J., 1990. Whole-tree growth process models based on structural–functional relationships. In: Dixon, R.K., Heldahl, R.S., Ruark, G.A., Warren, W.G. (Eds.), Process Modeling of Forest Growth Responses to Environmental Stress. Timber Press, Portland, OR, pp. 96–112.

Jantsch, E., 1979. The Self-Organizing Universe: Scientific and Human Implications of the Emerging Paradigm of Evolution. Pergamon Press, New York, 321 pp.

Johnson, W.C., 1988. Estimating dispersibility of *Acer*, *Fraxinus*, and *Tilia* in fragmented landscapes from patterns of seedling establishment. Landscape Ecol. 1, 175–187.

Jurik, T.W., 1986. Temporal and spatial patterns of specific leaf weight in successional northern hardwood species. Am. J. Bot. 73, 1083–1092.

Kimmins, J.P., Mailly, D., Seely, B., 1999. Modelling forest ecosystem net primary production: the hybrid simulation approach used in FORECAST. Ecol. Model. 122, 195–224.

Klijn, F., Udo de Haes, H.A., 1994. A hierarchical approach to ecosystems and its implications for ecological land classification. Landscape Ecol. 9, 89–104.

Kobe, R.S., Pacala, S.W., Silander, J.A., Canham, C.D., 1995. Juvenile tree survivorship as a component of shade tolerance. Ecol. Appl. 5, 517–532.

Larocque, G.R., Marshall, P.L., 1994. Crown development in red pine stands. I. Absolute and relative growth measures. Can. J. For. Res. 24, 762–774.

Ledig, F.T., Korbobo, D.R., 1983. Adaptation of sugar maple populations along altitudinal gradients: photosynthesis, respiration, and specific leaf weights. Am. J. Bot. 70, 256–265.

Lieffers, V.J., Messier, C., Stadt, K.J., Gendron, F., Comeau, P.G., 1999. Predicting and managing light in the understory of boreal forests. Can. J. For. Res. 29, 796–811.

Lin, C.R., Buongiorno, J., Vasievich, M., 1996. A multi-species, density-dependent matrix growth model to predict tree diversity and income in northern hardwood stands. Ecol. Model. 91, 193–211.

Liu, J., Ashton, P.S., 1998. FORMOSAIC: an individual-based spatially explicit model for simulating forest dynamics in landscape mosaics. Ecol. Model. 106, 177–200.

Long, J.N., Daniel, T.W., 1990. Assessment of growing stock in uneven-aged stands. West. J. Appl. For. 5, 93–96.

Lorimer, C.G., 1977. The presettlement forest and natural disturbance cycle of northeastern Maine. Ecology 58, 139–148.

Luan, J., Muetzelfeldt, R.I., Grace, J., 1996. Hierarchical approach to forest ecosystem simulation. Ecol. Model. 86, 37–50.

Maguire, D.A., Forman, R.T.T., 1983. Herb cover effects on tree seedling patterns in a mature hemlock-hardwood forest. Ecology 64, 1367–1380.

Mäkelä, A., 2003. Process-based modelling of tree and stand growth: towards a hierarchical treatment of multiscale processes. Can. J. For. Res. 33, 398–409.

Marks, P.L., 1974. The role pin cherry (*Prunus pensylvanica*) in the maintenance of stability in northern hardwood ecosystems. Ecol. Monogr. 44, 73–88.

McCaffery, K.R., 1996. History of deer populations in northern Wisconsin. In: Mroz, G.D., Martin, J. (Eds.), Proceedings of Hemlock Ecology and Management Conference. Department of Forestry, University of Wisconsin, Madison, WI, pp. 109–114.

Minchin, P.R., 1987. Simulation of multidimensional community patterns: towards a comprehensive model. Vegetatio 71, 145–156.

Mitchell, S.J., 1995. The windthrow triangle: a relative windthrow hazard assessment procedure for forest managers. For. Chron. 71, 446–450.

Mitchell, H.L., Chandler, R.F., 1939. The nitrogen nutrition and growth of certain deciduous trees of northeastern United States. Black Rock Forest Bulletin #11, 94 pp.

Mitchell, M.J., Foster, N.W., Shepard, J.P., Morrison, I.K., 1992. Nutrient cycling in Huntington Forest and Turkey Lakes deciduous stands: nitrogen and sulfur. Can. J. For. Res. 22, 457–464.

Mladenoff, D.J., Stearns, F., 1993. Eastern hemlock regeneration and deer browsing in the northern Great Lakes region: a re-examination and model simulation. Conserv. Biol. 7, 889–900.

Mladenoff, D.J., Host, G.E., Boeder, J., Crow, T.R., 1996. LANDIS: a spatial model of forest landscape disturbance, succession, and management. In: Goodchild, M.F., Steyaert, L.T., Parks, B.O. (Eds.), GIS and Environmental Modeling: Progress and Research Issues. GIS World Books, Fort Collins, CO.

Morrison, I.K., 1991. Addition of organic matter and elements to the forest floor of an old-growth *Acer saccharum* forest in the annual litter fall. Can. J. For. Res. 21, 462–468.

Morton, D., The New Perspectives Team, 1991. Maintaining old growth in northern hardwood ecosystems. In: Procrrdings of 1991 SAF National Conservation. Society of American Foresters, Bethesda, MD, pp. 527–528.

Mroz, G.D., Gale, M.R., Jurgensen, M.F., Frederick, D.J., Clark, A., 1985. Composition, structure, and aboveground biomass of two old-growth northern hardwood stands in Upper Michigan. Can. J. For. Res. 15, 78–82.

O'Neill, R.V., King, A.W., 1998. Homage to St. Michael or, why are there so many books on scale? In: Peterson, D.L., Parker, V.T. (Eds.), Ecological Scale: Theory and Applications. Columbia University Press, New York, pp. 3–15.

O'Neill, R.V., DeAngelis, D.L., Waide, J.B., Allen, T.F.H., 1986. A hierarchical concept of ecosystems. Monogr. Pop. Biol. 23, 1–272.

O'Neill, R.V., Johnson, A.R., King, A.W., 1989. A hierarchical framework for the analysis of scale. Landscape Ecol. 3, 193–205.

Overton, W.S., 1972. Toward a general model structure for a forest ecosystem. In: Franklin, J.F., Dempster, L.J., Waring, R.H. (Eds.), Research on Coniferous Forest Ecosystems: First Year Progress in the Coniferous Forest Biome, US/IBP. USDA Forest Service Pacific Northwest Forest and Range Experimental Station, Portland, OR, pp. 37–47.

Overton, W.S., 1975. The ecosystem modeling approach in the coniferous forest biome. In: Patten, B.C. (Ed.), Systems Analysis and Simulation in Ecology, vol. III. Academic Press, New York, pp. 117–138.

Overton, W.S., Lavender, D.P., Hermann, R.K., 1973. Estimation of biomass and nutrient capital in stands of old-growth Douglas-fir. In: IUFRO Biomass Studies. University of Maine, Orono, ME, pp. 91–103.

Pacala, S.W., Canham, C.D., Silander, J.A., 1993. Forest models defined by field measurements: I. The design of a northeastern forest simulator. Can. J. For. Res. 23, 1980–1988.

Pacala, S.W., Canham, C.D., Silander, J.A., Kobe, R.K., 1995. Sapling growth as a function of resources in a north temperate forest. Can. J. For. Res. 24, 2172–2183.

Pacala, S.W., Canham, C.D., Saponara, J., Silander, J.A., Kobe, R.K., Ribbens, E., 1996. Forest models defined by field measurements: estimation, error analysis and dynamics. Ecol. Monogr. 66, 1–43.

Panshin, A.J., de Zeeuw, C., 1970. Textbook of Wood Technology, 3rd ed. McGraw-Hill Book Company, New York, 705 pp.

Pastor, J., Bockheim, J.G., 1984. Distribution and cycling of nutrients in an aspen-mixed-hardwood-spodosol ecosystem in northern Wisconsin. Ecology 65, 339–353.

Pastor, J., Post, W.M., 1986. Influence of climate, soil moisture, and succession on forest carbon and nitrogen cycles. Biogeochemistry 2, 3–27.

Pattee, H.H. (Ed.), 1973. Hierarchy Theory, the Challenge of Complex Systems. George Braziller, New York, 155 pp.

Pearson, G.A., 1930. Light and moisture in forestry. Ecology 11, 145–160.

Perala, D.A., Alban, D.H., 1982. Rates of forest floor decomposition and nutrient turnover in aspen, pine, and spruce stands on two different soils. USDA Forest Service Research Paper NC-227.

Platt, J.R., 1964. Strong inference. Science 146, 347–354.

Prentice, I.C., Sykes, M.T., Cramer, W., 1991. The possible dynamic response of northern forests to global warming. Global Ecol. Biogeol. Lett. 1, 129–135.

Pritchett, W.L., Fisher, R.F., 1987. Properties and Management of Forest Soils, 2nd ed. Wiley, New York, 494 pp.

Raile, G.K., Smith, W.B., Weist, C.A., 1982. A net volume equation for Michigan's Upper and Lower Peninsulas. USDA Forest Service General Technical Report NC-80.

Rasse, D.P., François, L., Aubinet, M., Kowalski, A.S., Vande Walle, I., Laitat, E., Gérard, J.-C., 2001. Modelling short-term CO_2 fluxes and long-term tree growth in temperate forests with ASPECTS. Ecol. Model. 141, 35–52.

Raulier, F., Ung, C., Ouellet, D., 1996. Influence of social status on crown geometry and volume increment in regular and irregular black spruce stands. Can. J. For. Res. 26, 1742–1753.

Ribbens, E., Silander, J.A., Pacala, S.W., 1994. Seedling recruitment in forests: calibrating models to predict patterns of tree seedling dispersion. Ecology 75, 1794–1806.

Roberts, D.W., 1987. A dynamical systems perspective on vegetation theory. Vegetatio 69, 27–33.

Roberts, D.W., 1996a. Modelling forest dynamics with vital attributes and fuzzy systems theory. Ecol. Model. 90, 161–173.

Roberts, D.W., 1996b. Landscape vegetation modelling with vital attributes and fuzzy systems theory. Ecol. Model. 90, 175–184.

Robinson, A.P., Ek, A.R., 2000. The consequences of hierarchy for modeling in forest ecosystems. Can. J. For. Res. 30, 1837–1846.

Roe, E.I., 1963. Seed stored in cones of some jack pine stands, northern Minnesota. USDA Forest Service Research Paper LS-1.

Roskoski, J.P., 1980. Nitrogen fixation in hardwood forests of the northeastern United States. Plant and Soil 54, 33–44.

Running, S.W., Coughlan, J.C., 1988. A general model of forest ecosystem processes for regional applications. I. Hydrologic balance, canopy gas exchange and primary production processes. Ecol. Model. 42, 125–154.

Rutkowski, D.R., Stottlemyer, R., 1993. Composition, biomass and nutrient distribution in mature northern hardwood and boreal forest stands, Michigan. Am. Midl. Nat. 130, 13–30.

Sander, I.L., 1990. Northern red oak—*Quercus rubra* L. In: Burns, R.M., Honkala, B.H. (Technical Coordinators), Silvics of North America: Vol. 2. Hardwoods. USDA Agriculture Handbook 654, pp. 727–733.

Sartz, R.S., Knighton, M.D., 1978. Soil water depletion after four years of forest regrowth in southwestern Wisconsin. USDA Forest Service Research Note NC-230.

Schaetzl, R.J., 1986. Soilscape analysis of contrasting glacial terrains in Wisconsin. Ann. Assoc. Am. Geogr. 76, 414–425.

Schaetzl, R.J., Johnson, D.L., Burns, S.F., Small, T.W., 1989. Tree uprooting: review of terminology, process, and environmental implications. Can. J. For. Res. 19, 1–11.

Schenk, H.J., 1996. Modeling the effects of temperature on growth and persistence of tree species: a critical review of tree population models. Ecol. Model. 92, 1–32.

Schlesinger, R.C., 1990. White ash—*Fraxinus americana* L. In: Burns, R.M., Honkala, B.H. (Technical Coordinators), Silvics of North America: Vol. 2. Hardwoods. USDA Agriculture Handbook 654, pp. 333–338.

Seagle, S.W., Liang, S.-Y., 2001. Application of a forest gap model for prediction of browsing effects on riparian forest succession. Ecol. Model. 144, 213–229.

Shields, W.J., Bockheim, J.G., 1981. Deterioration of trembling aspen clones in the Great Lakes region. Can. J. For. Res. 11, 530–537.

Shugart, H.H., 1984. A Theory of Forest Dynamics. Springer-Verlag, New York.

Shugart, H.H., West, D.C., 1977. Development of an Appalachian deciduous forest succession model and its application to assessment of impact of the chestnut blight. J. Environ. Manage. 5, 161–180.

Shugart, H.H., Crow, T.R., Hett, J.M., 1973. Forest succession models: a rationale and methodology for modeling forest succession over large regions. For. Sci. 19, 203–212.

Shugart, H.H., Smith, T.M., Post, W.M., 1992. The potential for application of individual-based simulation models for assessing the effects of global change. Ann. Rev. Ecol. Syst. 23, 15–38.

Siccama, T.G., Bormann, F.H., 1970. The Hubbard Brook ecosystem study: productivity, nutrients, and phytosociology of the herbaceous layer. Ecol. Monogr. 40, 389–402.

Sievänen, R., Burk, T.E., 1990. Process-based models and forest management. Silva Carelica 15, 241–246.

Simon, H.A., 1962. The architecture of complexity. Proc. Am. Philos. Soc. 106, 467–482.

Smith, W.B., 1985. Factors and equations to estimate forest biomass in the North Central region. USDA Forest Service Research Paper NC-268.

Smith, W.B., Brand, G.J., 1983. Allometric biomass equations for 98 species of herbs, shrubs, and small trees. USDA Forest Service Research Note NC-299.

Solomon, A.M., 1986. Transient response of forests to CO_2-induced climate change: simulation experiments in eastern North America. Oecologia 68, 567–579.

Stephens, E.P., 1956. The uprooting of trees: a forest process. Soil Sci. Soc. Am. Proc. 20, 113–116.

Stiteler, W.M., Shaw, S.P., 1966. Use of woody browse by whitetail deer in heavily forested areas of northeastern United States. Trans. N. Am. Wildl. Conf. 31, 205–212.

Stoeckeler, J.H., Arbogast, C., 1955. Forest management lessons from a 1949 windstorm in northern Wisconsin and Upper Michigan. USDA Forest Service Lake States Forest Experimental Station Paper #34.

Stoeckeler, J.H., Macon, J.W., 1956. Regeneration of aspen cutover areas in northern Wisconsin. J. For. 54, 13–16.

Stoeckeler, J.H., Strothmann, R.O., Krefting, L.W., 1957. Effect of deer browsing on reproduction in the northern hardwood-hemlock type in northeastern Wisconsin. J. Wildl. Manage. 21, 75–80.

Tappeiner, J.C., Alm, A.A., 1975. Undergrowth vegetation effects on the nutrient content of litterfall and soils in red pine and birch stands in northern Minnesota. Ecology 56, 1193–1200.

Ter-Mikaelian, M.T., Korzukhin, M.D., 1997. Biomass equations for sixty-five North American tree species. For. Ecol. Manage. 97, 1–24.

Tierson, W.C., Patric, E.F., Behrend, D.F., 1966. Influence of white-tailed deer on the logged northern hardwood forest. J. For. 64, 801–805.

Tilghman, N.G., 1989. Impacts of white-tailed deer on forest regeneration in northwestern Pennsylvania. J. Wildl. Manage. 53, 524–532.

Tsoumis, G., 1991. Science and Technology of Wood: Structure, Properties, Utilization. Van Nostrand Reinhold, New York.

Tubbs, C.H., 1977. Natural regeneration of northern hardwoods in the northern Great Lakes Region. USDA Forest Service Research Paper NC-150.

Urban, D.L., O'Neill, R.V., Shugart, H.H., 1987. Landscape ecology. Bioscience 37, 119–127.

Urban, D.L., Harmon, M.E., Halpern, C.B., 1993. Potential response of Pacific Northwestern forests to climatic change, effects of stand age and initial composition. Clim. Change 23, 247–266.

Valinger, E., Fridman, J., 1997. Modeling probability of snow and wind damage in Scots pine stands using tree characteristics. For. Ecol. Manage. 97, 215–222.

Vanclay, J.K., 2003. Realizing opportunities in forest growth modelling. Can. J. For. Res. 33, 536–541.

Viereck, L.A., Johnston, W.F., 1990. Black spruce—*Picea mariana* (Mill.) B.S.P. In: Burns, R.M., Honkala, B.H. (Technical Coordinators), Silvics of North America: Vol. 1. Conifers. USDA Agriculture Handbook 654, pp. 227–237.

Voit, E.O., Sands, P.J., 1996a. Modeling forest growth. I. Canonical approach. Ecol. Model. 86, 51–71.

Voit, E.O., Sands, P.J., 1996b. Modeling forest growth. II. Biomass partitioning in Scots pine. Ecol. Model. 86, 73–89.

Vora, R.S., 1994. Integrating old-growth forest into managed landscapes: a northern Great Lakes perspective. Nat. Areas J. 14, 113–123.

Wallace, E.S., Freedman, B., 1986. Forest floor dynamics in a chronosequence of hardwood stands in central Nova Scotia. Can. J. For. Res. 16, 293–302.

Waller, D.M., Alverson, W.S., 1997. The white-tailed deer: a keystone herbivore. Wildl. Soc. Bull. 25, 217–226.

Waring, R.H., 1987. Characteristics of trees predisposed to die. Bioscience 37, 569–574.

Waring, R.H., Schlesinger, W.H., 1985. Forest Ecosystems: Concepts and Management. Academic Press, San Diego, CA, 340 pp.

Webb, S.L., 1989. Contrasting windstorm consequences in two forests, Itasca State Park, Minnesota. Ecology 70, 1167–1180.

Weinberg, G.M., 1975. An Introduction to General Systems Thinking. Wiley, New York, 320 pp.

Wilde, S.A., Shaw, B.H., Fedkenheuer, A.W., 1968. Weeds as a factor depressing forest growth. Weed Res. 8, 196–204.

Williams, M., 1996. A three-dimensional model of forest development and competition. Ecol. Model. 89, 73–98.

Woodward, F.I., 1993. Leaf responses to environment and extrapolation to larger scales. In: Solomon, A.M., Shugart, H.H. (Eds.), Vegetation Dynamics and Global Change. Chapman and Hall, New York, pp. 71–100.

Wu, J., David, J.L., 2002. A spatially explicit hierarchical approach to modeling complex ecological systems: theory and applications. Ecol. Model. 153, 7–26.

Wu, H., Rykiel, E.J., Hutton, T., Walker, J., 1994. An integrated rate methodology (IRM) for multi-factor growth rate modelling. Ecol. Model. 73, 97–116.

Wykoff, W.R., Crookston, N.L., Stage, A.R., 1982. User's guide to the stand prognosis model. USDA Forest Service General Technical Report INT-133.

Zavitkovski, J., 1976. Ground vegetation biomass, production, and efficiency of energy utilization in some northern Wisconsin forest ecosystems. Ecology 57, 694–706.

Zehngraff, P.J., 1949. Aspen as a forest crop in the Lake States. J. For. 47, 555–565.

Zeide, B., 1989. Accuracy of equations describing diameter growth. Can. J. For. Res. 19, 1283–1286.

Zeide, B., 1991. Quality as a characteristic of ecological models. Ecol. Model. 55, 161–174.

Zeide, B., 1993. Analysis of growth equations. For. Sci. 39, 594–616.

Zeide, B., 2003. The U-approach to forest modeling. Can. J. For. Res. 33, 480–489.